



# Stratégies de MIMO coopératif pour les réseaux de capteurs sans fil contraints en énergie

Tuan-Duc Nguyen

## ► To cite this version:

Tuan-Duc Nguyen. Stratégies de MIMO coopératif pour les réseaux de capteurs sans fil contraints en énergie. Traitement du signal et de l'image [eess.SP]. Université Rennes 1, 2009. Français. NNT : . tel-00438589v2

**HAL Id: tel-00438589**

**<https://theses.hal.science/tel-00438589v2>**

Submitted on 11 Jan 2010

**HAL** is a multi-disciplinary open access archive for the deposit and dissemination of scientific research documents, whether they are published or not. The documents may come from teaching and research institutions in France or abroad, or from public or private research centers.

L'archive ouverte pluridisciplinaire **HAL**, est destinée au dépôt et à la diffusion de documents scientifiques de niveau recherche, publiés ou non, émanant des établissements d'enseignement et de recherche français ou étrangers, des laboratoires publics ou privés.



**THÈSE / UNIVERSITÉ DE RENNES 1**  
*sous le sceau de l'Université Européenne de Bretagne*

pour le grade de  
**DOCTEUR DE L'UNIVERSITÉ DE RENNES 1**  
*Mention : Traitement du Signal et Télécommunications*  
**Ecole doctorale MATISSE**

présentée par  
**Tuan-Duc NGUYEN**

préparée à l'IRISA (UMR 6074)  
Institut de Recherche en Informatique et Systèmes Aléatoires  
École Nationale Supérieure de Sciences Appliquées et de  
Technologie (ENSSAT)

---

**Cooperative MIMO  
Strategies for  
Energy Constrained  
Wireless Sensor Networks**

**Thèse soutenue à l'ENSSAT Lannion  
le 15 mai 2009**

devant le jury composé de :

**Emmanuel BOUTILLON**

Professeur à l'Université de Bretagne Sud / président

**Jean-Francois DIOURIS**

Professeur à l'École Polytechnique de l'Université de  
Nantes / rapporteur

**Jean-Marie GORCE**

Professeur à l'INSA de Lyon / rapporteur

**Mischa DOHLER**

Chercheur au Centre Tecnològic de Telecomunica-  
cions de Barcelona / examinateur

**Olivier SENTIEYS**

Professeur à l'Université de Rennes 1 /  
directeur de thèse

**Olivier BERDER**

Maître de Conférences à l'Université de Rennes 1 /  
co-directeur de thèse

# Contents

<b>Acronyms</b>	<b>iv</b>
<b>Notations</b>	<b>vi</b>
<b>Introduction</b>	<b>1</b>
<b>1 Diversity and MIMO Techniques</b>	<b>9</b>
1.1 Introduction . . . . .	9
1.2 Diversity Techniques . . . . .	10
1.2.1 Time Diversity . . . . .	10
1.2.2 Frequency Diversity . . . . .	10
1.2.3 Spatial Diversity . . . . .	11
1.2.4 Antenna Diversity . . . . .	11
1.3 Combination Techniques . . . . .	12
1.3.1 Maximum Ratio Combining . . . . .	12
1.3.2 Selection Combining . . . . .	14
1.3.3 Hybrid Combining Technique . . . . .	15
1.4 MIMO Techniques . . . . .	16
1.4.1 MIMO Channel Model . . . . .	17
1.4.2 MIMO Channel Capacity . . . . .	18
1.5 Space Time Coding . . . . .	22
1.5.1 Space-Time Block Codes . . . . .	23
1.5.2 Quasi-Orthogonal Space-Time Block Codes (QSTBC) . . . . .	29
1.5.3 Space Time Trellis Codes . . . . .	31
1.6 Spatial Multiplexing . . . . .	35
1.7 Conclusion . . . . .	39
<b>2 Cooperative techniques in Wireless Sensor Networks</b>	<b>41</b>
2.1 Introduction . . . . .	41
2.2 Multi-Hop Technique . . . . .	42

2.3	Relay Cooperation Techniques . . . . .	44
2.3.1	Amplify and Forward . . . . .	46
2.3.2	Decode and Forward . . . . .	47
2.3.3	Re-encode and Forward . . . . .	48
2.4	Parallel Relay Networks . . . . .	49
2.5	Cooperative MIMO Techniques . . . . .	50
2.5.1	Local Data Exchange . . . . .	51
2.5.2	Cooperative MIMO Transmission . . . . .	52
2.5.3	Cooperative Reception . . . . .	52
2.5.4	Multi-hop Cooperative MIMO Technique . . . . .	53
2.6	Cooperative MIMO Transmission in the CAPTIV Project . . . . .	54
2.6.1	CAPTIV Project Overview . . . . .	54
2.6.2	Description of the CAPTIV System . . . . .	55
2.6.3	Proposed Cooperative Transmission Schemes in CAPTIV . . . . .	56
2.7	Conclusion . . . . .	59
<b>3</b>	<b>Energy Efficiency of Cooperative MIMO Techniques</b>	<b>61</b>
3.1	Introduction . . . . .	61
3.2	Application of STBC to Wireless Sensor Networks . . . . .	62
3.3	Energy Consumption Model . . . . .	64
3.3.1	Energy Consumption of Non Cooperative Systems . . . . .	64
3.3.2	Multi-Hop SISO System . . . . .	66
3.4	Cooperative MIMO System . . . . .	68
3.5	Energy Efficiency of Cooperative MIMO Systems . . . . .	70
3.5.1	Cooperative MISO vs. SISO Techniques . . . . .	70
3.5.2	Cooperative MIMO vs. Cooperative MISO Techniques . . . . .	70
3.5.3	Cooperative MISO vs. Multi-hop SISO Techniques . . . . .	72
3.5.4	Cooperative MIMO vs. Multi-hop Cooperative MIMO Techniques . . . . .	73
3.5.5	Influence of the distance between cooperative nodes . . . . .	74
3.5.6	Impacts of the Error Rate Requirement and the Power Path Loss Factor . . . . .	74
3.5.7	Energy Consumption of the Coding Systems . . . . .	76
3.6	Conclusion . . . . .	77
<b>4</b>	<b>Effect of Transmission Synchronization Errors and Cooperative Reception Techniques</b>	<b>79</b>
4.1	Introduction . . . . .	79
4.2	Effect of Transmission Synchronization Error . . . . .	80
4.2.1	Cooperative Transmission Synchronization Error . . . . .	81

4.2.2	Channel Estimation Error . . . . .	85
4.3	Effect of Cooperative Reception Techniques . . . . .	87
4.3.1	Proposed Strategies for Cooperative Reception . . . . .	87
4.3.2	Proposed Cooperative Reception Techniques Performance . . . . .	89
4.4	Cooperative MIMO Energy Consumption . . . . .	90
4.5	Conclusion . . . . .	95
<b>5</b>	<b>MSOC Combination for Un-synchronized Cooperative MIMO Transmissions</b>	<b>96</b>
5.1	Introduction . . . . .	96
5.2	Effect of Transmission Synchronization Error on the performance of the max-SNR OSTBC . . . . .	97
5.3	Multiple Sampling Orthogonal Combination Technique . . . . .	99
5.3.1	Synchronization Technique . . . . .	100
5.3.2	Space-time Combination Technique . . . . .	101
5.3.3	Performance of the MSOC Technique . . . . .	103
5.4	Energy consumption of MSOC Technique . . . . .	106
5.5	Conclusion and Discussion . . . . .	107
<b>6</b>	<b>Cooperative MIMO and Relay Association Strategy</b>	<b>109</b>
6.1	Introduction . . . . .	109
6.2	Cooperative MIMO and Relay Techniques Performance Comparison . . . .	110
6.2.1	Case of Two Cooperation Transmission Nodes . . . . .	111
6.2.2	Case of Multiple Cooperation Transmission Nodes . . . . .	112
6.2.3	Effect of Transmission Synchronization Error . . . . .	113
6.2.4	Effects of Power Path-loss Factor and Error Control Coding . . . . .	114
6.3	Cooperative MISO and Relay Techniques Energy Consumption Comparison	115
6.3.1	Energy Consumption Analysis . . . . .	116
6.3.2	Transmission Delay Comparison . . . . .	121
6.4	Cooperative MISO and Relay Association Strategies . . . . .	122
6.4.1	Association Schemes . . . . .	123
6.4.2	Performance and Energy Consumption of the Association Scheme .	124
6.5	Conclusion . . . . .	124
<b>7</b>	<b>Conclusion and Future Works</b>	<b>127</b>
	<b>Bibliography</b>	<b>133</b>
	<b>Bibliography</b>	<b>133</b>

# Acronyms

A-F	Amplify-and-Forward
AWGN	Additive White Gaussian Noise
BER	Bit Error Rate
BPSK	Binary Phase Shift Keying
CAPTIV	Consumption And cooPerative strategies for Transmissions between Infrastructure and Vehicles
C-F	Combine-and-Forward
CONV	Convolutional Code
CSI	Channel State Information
D-BLAST	Diagonal Bell Laboratories Layered Space-Time Architecture
D-F	Decode-and-Forward
DFE	Decision Feedback Equalization
ECC	Error Control Coding
EGC	Equal Gain Combining
F-C	Forward-and-Combine
FER	Frame Error Rate
ISI	Inter Symbol Interference
LOS	Line of Sight
LLC	Logical Link Control
ML	Maximum Likelihood
MAC	Medium Access Control
MIMO	Multi-Input Multi-Output
MISO	Multiple-Input-Single-Output
MMSE	Minimum Mean Square Error
M-PSK	M-ary Phase Shift Keying
M-QAM	M-ary Quadrature Amplitude Modulation
MRC	Maximum Ratio Combining
MSOC	Multiple Sampling Orthogonal Combination
nLOS	non Line of Sight
OFDM	Orthogonal Frequency Division Multiplexing

OSTBC	Orthogonal Space-Time Block Code
PAN	Personal Area Network
pdf	Probability Density Function
PHY	Physical Layer
PSK	Phase Shift Keying
QOSTBC	Quasi Orthogonal Space-Time Block Code
RF	Radio Frequency
R-F	Re-encode and Forward
SC	Selection Combining
SIMO	Single-Input-Multiple-Output
SINR	Signal to Interference and Noise Ratio
SISO	Single-Input-Single-Output
SM	Spatial Multiplexing
SNR	Signal to Noise Ratio
STBC	Space-Time Block Code
STTC	Space-Time Trellis Code
S-T	Space-time
TCM	Trellis Code Modulation
V-BLAST	Vertical Bell Laboratories Layered Space-Time Architecture
WSN	Wireless Sensor Networks
ZF	Zero Forcing

# Notations

$N$	Transmit antennas number
$M$	Receive antennas number
$A$	Average Signal-to-Noise Ratio
$C_{T,n}$	Cooperative transmit node $n$
$C_{R,m}$	Cooperative receive node $m$
$C$	Channel capacity
$c$	Transmit code
$\mathbf{c}$	Transmit code vector
$\mathbf{C}$	Space-time code matrix
$s$	Transmit symbol
$\alpha$	Channel coefficient
$\mathbf{H}$	Channel matrix
$r$	Received signal
$\mathbf{r}$	Received signal vector
$p(t)$	Raised cosine pulse shape
$\gamma$	Received SNR
$\sigma$	Variance of AWGN noise
$d$	Transmission distance
$d_m$	Local transmission distance
$d_{hop}$	Distance of one hop
$d_1$	Source-relay distance
$E$	Energy
$E_b$	Energy per bit
$E_s$	Energy per symbol
$G$	Gain
$G_d$	Diversity Gain
$K$	Power path loss factor
$K_c$	Power amplification factor
$K_R$	Power gain factor at relay node
$N_b$	Number of transmit bits



$N_{sb}$	Number of bits/symbol for quantization
$N_0$	Power density of AWGN noise
$P_e$	Error Probability
$P$	Power
$P_{out}$	Outage Probability
$Pr$	Preamble sequence
$\eta$	Additive noise
S	Source node
D	Destination node
R	Relay node
$R_b$	Data transmission rate
$T_s$	Symbol duration
$\delta$	Transmission synchronization error
$\Delta T_{syn}$	Synchronization error range
$B$	Signal bandwidth
$B_c$	Coherence bandwidth
$T_c$	Coherence time

# List of Figures

1	Structure of one wireless sensor node . . . . .	2
2	Layered decomposition of wireless sensor networks . . . . .	3
3	Cooperative MIMO transmission in WSN . . . . .	4
1.1	Principle of temporal diversity and frequency diversity . . . . .	11
1.2	Principle of the Maximum Ratio Combining Technique . . . . .	13
1.3	Principle of the Selection Combining Technique . . . . .	14
1.4	Principle of the Hybrid Combining Technique . . . . .	15
1.5	SNR gain of different combining methods . . . . .	16
1.6	MIMO model with $N$ transmit antennas and $M$ receive antennas. . . . .	17
1.7	The ergodic channel capacity of MIMO channel . . . . .	20
1.8	Outage probability with $C_{out} = 2$ bits/(s Hz), $M$ receive antennas, one transmit antenna . . . . .	21
1.9	Outage probability with $C_{out} = 2$ bits/(s Hz), one receive antenna, $N$ trans- mit antennas . . . . .	22
1.10	Alamouti encoding scheme . . . . .	23
1.11	STBC decoding scheme . . . . .	25
1.12	BER performance of the QPSK Alamouti Codes, $N = 2$ , $M = 1, 2$ . . . . .	25
1.13	Bit error performance for OSTBC of 3 bits/channel use on $N \times 1$ channels with i.i.d Rayleigh fading. . . . .	29
1.14	Bit error performance for OSTBC of 2 bits/channel use on $N \times 1$ channels with i.i.d Rayleigh fading. . . . .	30
1.15	Bit error probability plotted against SNR for different space-time block codes at 2 bits/(s Hz); four transmit antennas, one receive antenna. . . . .	32
1.16	Two four state STTC, two transmit antennas, 2 bits/s/Hz using 4-PSK modulation. . . . .	33
1.17	A four-state STTC; 2 bits/(s Hz) using two receive antennas . . . . .	34
1.18	Spatial Multiplexing Transmission Technique . . . . .	35
1.19	Sphere Decoding Technique. . . . .	36
1.20	VBLAST decoder block diagram. . . . .	39

1.21	Bit error probability plotted against SNR for spatial multiplexing using QPSK, 4 bits/s/Hz; two transmit and receive antennas. . . . .	40
2.1	Multi-hop transmission model with $n$ hops. . . . .	43
2.2	Multi-hop transmission model with $n$ hops. . . . .	43
2.3	Three terminal relay diversity scheme. . . . .	44
2.4	Amplify-and-Forward (a) and Decode-and-Forward (b) techniques in relay networks . . . . .	46
2.5	Performance of Amplify-and-Forward and Decode-and-Forward relay techniques . . . . .	48
2.6	Coded cooperation or Re-encode-and-Forward technique in relay networks .	48
2.7	Transmission scheme in a parallel relay network with $N - 1$ relay nodes. .	49
2.8	Cooperative MIMO transmission scheme from S to D with $N - 1$ cooperative transmission nodes ( $C_{T,1}, C_{T,2}..C_{T,N-1}$ ) and $M - 1$ cooperative reception nodes ( $C_{R,1}, C_{R,2}..C_{R,M-1}$ ). . . . .	51
2.9	Cooperative reception techniques in cooperative MIMO networks. . . . .	52
2.10	Multi-hop cooperative MIMO transmission. . . . .	53
2.11	Infrastructure-to-Infrastructure and Infrastructure-to-Vehicle wireless communications in the CAPTIV, Intelligent Transport System Project. . . . .	54
2.12	Multi-hop SISO transmission between infrastructure and vehicle. . . . .	57
2.13	Relay transmission between infrastructure and vehicle . . . . .	57
2.14	Cooperative MISO transmission between infrastructure and vehicle . . . . .	58
2.15	Cooperative MIMO transmission between infrastructure and vehicle . . . . .	58
2.16	Cooperative MIMO transmission between infrastructure and infrastructure	59
2.17	Multi-hop cooperative MIMO transmission between infrastructure and vehicle	59
3.1	BER and FER performance of STBC for various number of transmit and receive antennas ( $N$ and $M$ ) over a Rayleigh fading channel. . . . .	62
3.2	Transmitter and receiver blocks with $N$ transmit and $M$ receive antennas. .	64
3.3	Transmission energy ( $E_{pa}$ ) and circuit energy ( $E_c$ ) repartitions of a SISO system for transmission distances $d = 10m$ and $d = 100m$ . . . . .	66
3.4	Energy consumption in function of the distance of SISO and non-cooperative MIMO systems with 2, 3 and 4 transmit antennas. . . . .	67
3.5	Multi-hop transmission scheme with $n$ -hop SISO transmissions from $S$ to $D$ . 67	
3.6	Energy consumption in function of transmission distances of SISO and multi hop SISO systems, $FER = 10^{-3}$ requirement, Rayleigh block fading channel with power path-loss factor $K = 2$ . . . . .	68

3.7	Transmission energy ( $E_{pa}$ ), circuit energy ( $E_c$ ) and cooperative energy ( $E_{coop}$ ) repartitions of the SISO and the cooperative MISO systems for the transmission distance $d = 100m$ . . . . .	70
3.8	Energy consumption in function of transmission distances of cooperative MISO and SISO systems, $N = 2, 3$ and 4 cooperative transmit nodes, $FER = 10^{-3}$ requirement, Rayleigh block fading channel with power path-loss factor $K = 2$ . . . . .	71
3.9	Energy consumption of cooperative MIMO and cooperative MISO systems, $N = 2, 3, 4$ and $M = 2$ cooperative transmit and receive nodes, $FER = 10^{-3}$ requirement, Rayleigh block fading channel with power path-loss factor $K = 2$ . . . . .	71
3.10	Optimal $N - M$ transmit and receive antennas set selection as a function of transmission distance, $FER = 10^{-3}$ requirement, Rayleigh block fading channel with power path-loss factor $K = 2$ . . . . .	72
3.11	Energy consumption lower bound of cooperative MIMO systems, $FER = 10^{-3}$ requirement, Rayleigh block fading channel with power path-loss factor $K = 2$ . . . . .	72
3.12	Energy consumption in function of transmission distances of cooperative MISO, SISO and multi-hop SISO systems, $FER = 10^{-3}$ requirement, Rayleigh block fading channel with power path-loss factor $K = 2$ . . . . .	73
3.13	Energy consumption in function of transmission distances of cooperative MIMO and multi-hop MIMO 2 – 2 systems, $FER = 10^{-3}$ requirement, Rayleigh block fading channel with power path-loss factor $K = 2$ . . . . .	74
3.14	Energy consumption of the cooperative MISO 2 – 1 with different cooperative transmission distances $d_m = 5, 10$ and $20m$ , $FER = 10^{-3}$ requirement, Rayleigh block fading channel with power path-loss factor $K = 2$ . . . . .	75
3.15	Energy consumption in function of transmission distances of cooperative MISO and SISO systems, $N = 2, 3, 4$ cooperative transmit nodes, $FER = 10^{-2}$ requirement, Rayleigh block fading channel with power path-loss factor $K = 2$ . . . . .	75
3.16	Energy consumption in function of transmission distances of cooperative MIMO and multi-hop MIMO 2 – 2 systems, $FER = 10^{-2}$ requirement, Rayleigh block fading channel with power path-loss factor $K = 3$ . . . . .	76
3.17	FER performance of STBC in concatenation with CONV [7 4 3] codes over a Rayleigh block fading channel. . . . .	77
3.18	Energy consumption in function of transmission distances of cooperative MISO and SISO systems, CONV [7 4 3], $FER = 10^{-3}$ requirement, Rayleigh block fading channel with power path-loss factor $K = 2$ . . . . .	78

4.1	Un-synchronized cooperative MISO transmission. . . . .	81
4.2	ISI of un-synchronized sequence with the synchronization error $\delta$ . . . . .	83
4.3	Effect of the transmission synchronization error on the performance of cooperative MISO systems with two transmit nodes $N = 2$ , Alamouti STBC over a Rayleigh fading channel. . . . .	84
4.4	Effect of transmission synchronization error on the performance of cooperative MISO systems with four transmit nodes $N = 4$ , Tarokh STBC over a Rayleigh fading channel. . . . .	84
4.5	Effect of transmission synchronization and channel estimation errors on the performance of cooperative MISO systems with two and four transmit nodes $N = 2$ and $N = 4$ , Alamouti and Tarokh STBCs over a Rayleigh fading channel. . . . .	86
4.6	Forward-and-Combine cooperative reception technique principle. . . . .	87
4.7	Combine-and-Forward cooperative reception technique principle. . . . .	89
4.8	Performance of the proposed cooperative reception techniques, Alamouti STBC over a Rayleigh fading channel, transmission synchronization error $\Delta T_{syn} = 0.25T_s$ . . . . .	90
4.9	Total energy consumption of cooperative MISO vs. SISO and multi-hop SISO systems, $FER = 10^{-3}$ requirement, power path-loss factor $K = 2$ . . .	91
4.10	Total energy consumption of cooperative MISO vs. SISO and multi-hop SISO systems, $FER = 10^{-2}$ requirement, power path-loss factor $K = 2$ . . .	92
4.11	Total energy consumption of cooperative MIMO with different reception techniques vs. cooperative MISO, $\Delta T_{syn} = 0.25T_s$ , $FER = 10^{-3}$ requirement, power path-loss factor $K = 2$ . . . . .	93
4.12	Optimal $N - M$ transmit and receive antennas set selection as a function of transmission distance, $FER = 10^{-3}$ requirement, Rayleigh fading channel with power path-loss factor $K = 2$ . . . . .	94
4.13	Energy consumption lower bound of cooperative MIMO systems, $FER = 10^{-3}$ requirement, Rayleigh fading channel with power path-loss factor $K = 2$ . . . . .	94
5.1	Effect of transmission synchronization error on the performance of cooperative MISO systems with four transmit nodes $N = 4$ , using Tarokh and max-SNR STBC over a Rayleigh fading channel. . . . .	99
5.2	Signal synchronization process of the MSOC combination technique . . . .	100
5.3	MSOC space-time combination technique . . . . .	101
5.4	FER of MSOC technique vs. traditional combination technique with two transmission nodes, QPSK modulation over a Rayleigh channel . . . . .	104

5.5	FER of MSOC technique vs. traditional combination technique with three transmission nodes, QPSK modulation over a Rayleigh channel . . . . .	105
5.6	FER of MSOC technique vs. traditional combination technique with four transmission nodes, QPSK modulation over a Rayleigh channel . . . . .	105
5.7	Energy consumption of new combination and traditional combination, $N=2$ , $M=1$ , $FER = 10^{-3}$ . . . . .	106
5.8	Energy consumption of new combination and traditional combination, $N=3$ and 4, $M=1$ , $FER = 10^{-2}$ . . . . .	107
6.1	FER of relay technique vs. cooperative MIMO technique with two transmission nodes, non-coded QPSK modulation over a Rayleigh channel, 120 bits/frame, source-relay distance $d_1 = d/3$ , and power path-loss factor $K=2$ . . . . .	111
6.2	FER of relay techniques with different source-relay distances, non-coded QPSK modulation over a Rayleigh channel, 120 bits/frame and the power path-loss factor $K=2$ . . . . .	112
6.3	FER performance of relay techniques vs. cooperative MIMO techniques with three and four transmission nodes, non-coded QPSK modulation over a Rayleigh channel, source-relay distance $d_1 = d/3$ . . . . .	113
6.4	Performance of relay technique vs. cooperative MIMO technique with transmission synchronization error $\Delta T_{syn} = 0.25T_s$ and $0.5T_s$ , source-relay distance $d_1 = d/3$ . . . . .	114
6.5	FER performance of relay technique vs. cooperative MIMO technique, non-coded QPSK modulation over a Rayleigh channel, power path-loss factor $K = 3$ , source-relay distance $d_1 = d/3$ . . . . .	115
6.6	FER of relay technique vs. cooperative MIMO technique, with convolution Codes [4, 15, 17], QPSK modulation over a Rayleigh channel, power path-loss factor $K = 2$ , source-relay distance $d_1 = d/3$ . . . . .	116
6.7	Energy Consumption of relay technique vs. cooperative MIMO technique with two transmission nodes, power path-loss factor $K = 2$ , source-relay distance $d_1 = d/3$ . . . . .	119
6.8	Energy consumption of relay technique vs. cooperative MIMO technique with two and three transmission nodes, power path-loss factor $K = 2$ , source-relay distance $d_1 = 1/3d$ . . . . .	120
6.9	Energy consumption of relay technique vs. cooperative MISO technique with two transmission nodes $N = 2$ , power path-loss factor $K = 3$ , error rate $FER = 10^{-2}$ and source-relay distance $d_1 = d/3$ . . . . .	120

6.10	Energy consumption of relay technique vs. cooperative MISO technique with two transmission nodes $N = 2$ , power path-loss factor $K = 3$ , error rate $FER = 10^{-2}$ , transmission synchronization error range $\Delta T_{syn} = 0.5T_s$ and source-relay distance $d_1 = d/3$ . . . . .	121
6.11	Delay Comparison of Relay technique vs. Cooperative MISO technique with different number of cooperative (or relay) nodes. . . . .	122
6.12	Association scheme of cooperative MIMO and relay techniques . . . . .	123
6.13	FER performance of the association strategy vs. relay technique vs. cooperative MIMO technique, number of transmission nodes $N = 3$ , non-coded QPSK modulation over a Rayleigh channel, power path-loss factor $K = 2$ , source-relay distance $d_1 = d/3$ . . . . .	125
6.14	Energy Consumption of the Association Strategy vs. Relay technique vs. Cooperative MIMO technique, number of transmission nodes $N = 3$ , non-coded QPSK modulation over a Rayleigh channel, power path-loss factor $K = 3$ , source-relay distance $d_1 = 1/3d$ . . . . .	125
6.15	Transmission delay comparison of the Association Strategy vs. Relay technique vs. Cooperative MIMO technique, with the number of cooperative (or relay) nodes = 1,2 and 3. . . . .	126

# List of Tables

3.1	$SNR$ requirement of STBC for $BER = 10^{-5}$ , non-coding QPSK modulation, Rayleigh block fading channel . . . . .	63
3.2	$SNR$ requirement of STBC for $FER = 10^{-3}$ , non-coding QPSK modulation, Rayleigh block fading channel, 120 bits per frame . . . . .	63
3.3	System parameters for the energy consumption evaluation. . . . .	66
4.1	$SNR$ requirement of cooperative MIMO system for $FER = 10^{-3}$ , transmission synchronization error $\Delta T_{syn} = 0.25T_s$ , Forward-and-Combine cooperative reception with $K_c = \sqrt{4}$ , Rayleigh fading channel . . . . .	93



# Introduction

Wireless sensor networks (WSN) allow many wireless devices to communicate and cooperate on the monitoring of environmental conditions, the detection of hazardous events, the tracking of enemy targets, the support of robotic vehicles, etc. These wireless nodes are distributed and have a sensor to collect information on entities of interest. They can be deployed on the ground, in the air, inside building, on bodies, and in vehicles to detect events of interests and monitor environmental parameters. The development of WSN was originally motivated by military applications such as battlefield surveillance. However, WSN are now used in many industrial and civilian applications, some of them are listed below:

- **Environment Monitoring:** Sensor networks can be deployed to monitor environmental parameters such as temperature in a large region.
- **Patients Monitoring:** Body-area wireless sensor networks are proposed to monitor vital signs of patients, which can enable 24-hours real-time monitoring without compromising the convenience of patients.
- **Security Applications:** Networks of video, acoustic, and other sensors can be used to track suspected targets or bio-sensors can be deployed along the national borders to detect the smuggling of bio-weapons by terrorists.
- **Intelligent Transport Systems (ITS):** Image sensors and other types of sensors have been used at road-way infrastructure to monitor traffic conditions. The information collected by the sensors is transmitted and automatically processed by a network center, which will perform traffic control functions related to signaling and responding to accidents, traffic jam... A more advanced concept proposes to embed wireless sensors in vehicles and road infrastructures, like in the CAPTIV project, which funded this thesis work, where vehicles can not only receive the signaling from the infrastructure along the road but also exchange some information with other vehicles (such as parking guidance and information systems, weather information, and so on). The concepts developed in this work will sometimes be applied to this context in order to evaluate the performance.

## Energy constrained design in WSN

Unlike wireless broadband networks which allow mobile people to communicate with high-speed data transmission, WSN place put emphasis on communication between low-cost sensor devices to collect information and transmit it to a data sink within an acceptable delay. WSN are expected to be low-cost, reliable, expandable, and easy to deploy. In addition, these networks have hard energy constraints since each node is powered by a small battery that may not be rechargeable or renewable for a long time (or all the lifetime for some applications). Therefore, reducing energy consumption in order to increase network lifetime is the most important design consideration for WSN.

Typical components of a WSN node are shown in Fig. 1, and include a sensor, the radio part, the energy source (generator, battery, DC converter), processors and memories. The radio part is usually composed of baseband processor, transceiver, filter, RF amplifier, antennas... Processors are required to be low-cost and low consumption, leading to a limited calculation capacity. The generator in WSN (solar cell or battery) is usually limited to a small physical size.

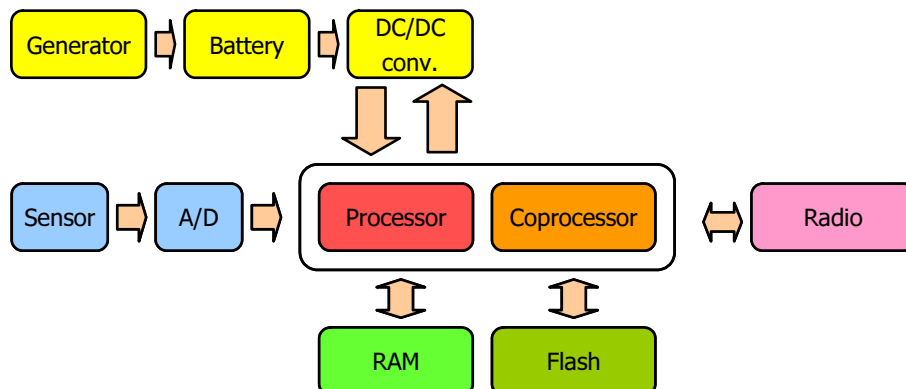


Figure 1: Structure of one wireless sensor node

With evolving technologies, each hardware part of the sensor node becomes more and more efficient. Batteries and processors are now designed to be as compact and powerful as possible. A co-processor (e.g. a low power FPGA) can be added for signal processing tasks, as error control coding or cooperative schemes that are developed in this thesis.

On the other hand, WSN would require a cross-layer design [34, 20] in order to efficiently reduce the energy consumption [18], enhance the performance under the constraint of calculation complexity. The important layers of a WSN, illustrated in Fig. 2, are the physical (PHY), medium access control (MAC), network (NTW) and application (APL) layers.

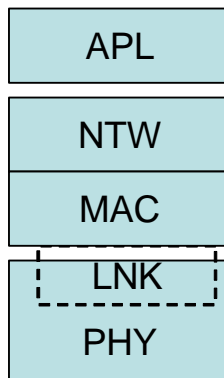


Figure 2: Layered decomposition of wireless sensor networks

- PHY layer ensures the data transmission over a complicated wireless medium with the minimum error rate. The link layer (LNK), also referred to as the physical layer in WSN, controls the reliability of a point-to-point wireless link. PHY layer is desired to be robust to noise and interference under the constraint of the low complexity.
- MAC layer controls how different users share the given medium and ensures reliable packet transmissions by allocating different users through either deterministic access or random access, minimizing the collisions and guaranteeing the fairness access scheme.
- NTW layer establishes and maintains end-to-end connections in the network. Its main functions are neighbor discovery, clustering, routing, and dynamic resource allocation with respect to the energy consumption and some quality of service (QoS) in terms of throughput, delays. . .
- APL layer ensures the data generating, data gathering, information processing, devices controlling. . . and is desired having a low complexity and a flexible configuration to the underlying NTW, MAC and PHY layers.

As the physical layer affects all higher layers in the protocol stack, it plays an important role in the energy constrained design of WSN. The energy consumption of the physical layer consists of two components: the transmission energy consumption (depending on the transmission distance, required signal strength, power path loss factor, antennas characteristic and all coefficients of transmission channel) and the circuit energy consumption (depending on the consumption of RF blocks and baseband signal processor). The question is then: how much signal processing can be added to decrease the transmission energy with reasonable complexity algorithms, such that the global energy consumption is really minimized?

For short range transmissions where the wireless nodes are densely distributed (the average distance between nodes is usually below 10 m), the circuit energy consumption is comparable to or even greater than the transmission energy. However, for medium and long range transmission (typically from hundred meters in long transmission WSN application like in ITS applications, in environment monitoring, ...), the transmission energy consumption is the dominant part in the total energy consumption.

The work of this thesis is mainly focusing on signal processing and efficient transmission techniques to reduce the total energy consumption in medium to long range transmission WSN. The overall energy consumption including both transmission and circuit energy consumption is considered in order to find the optimal transmission scheme.

## Cooperative MIMO strategies for WSN

The temporal and spatial diversity of multiple antenna techniques are very attractive due to their simplicity and their performance for wireless transmission over fading channels. Multi-antenna systems have been studied intensively in recent years due to their potential to dramatically increase the system performance in fading channels. Space time codes can exploit the diversity gain at both transmission and reception to increase the system performance or to reduce transmission energy for the same transmission reliability and the same throughput requirement. This energy efficiency of MIMO techniques is particularly useful for WSN where the energy consumption is the most important design criterion.

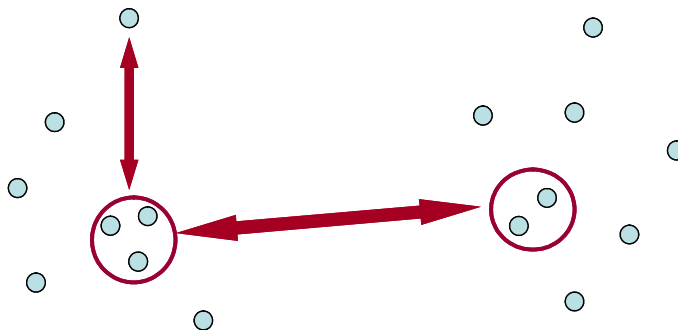


Figure 3: Cooperative MIMO transmission in WSN

Since a wireless sensor node can typically support one antenna due to the limited size and cost, the direct application of multi-antenna technique to distributed WSN is impractical. However, wireless sensor nodes can cooperate in transmission and reception in order to deploy a MIMO transmission (like in Fig. 3). This cooperation technique is referred to as a cooperative MIMO transmission which allows space time diversity gain to reduce the transmission energy consumption and the total energy consumption. Cooperative MIMO

techniques have been recently studied in [24], [61], [59], [49], [63], and have shown their efficiency in term of energy consumption [16] [50].

## Thesis contributions

In this thesis, some strategies using cooperative MIMO techniques are proposed for Wireless Sensor Networks (WSN). Cooperative MIMO techniques, allowing the application of space-time coding technique in order to reduce the energy consumption in WSN, are presented. The performance and the energy consumption advantages of cooperative MIMO technique are investigated, in comparison with the Single-Input Single-Output (SISO), multi-hop SISO techniques. The energy efficiency of cooperative MIMO techniques for WSN is proved and a multi-hop cooperative MIMO scheme for resource constrained WSNs is also proposed. Based on the total energy consumption, an optimal transmit-receive antennas number is selected as a function of the transmission distance [a][b][c].

Differing from a traditional MIMO system, the performance of cooperative MIMO techniques in wireless distributed networks is degraded by the effect of an un-synchronized transmission at the transmission side and cooperative reception noises at the reception side, which affects this energy efficiency [d]. The drawbacks of cooperative MIMO techniques are investigated. Two new cooperative reception techniques based on the relay principle and a new efficient space-time combination technique [e][f] are then proposed in order to increase the performance and the energy efficiency of cooperative MIMO systems.

Relay has been known as a simple cooperative technique that can exploit the space-time diversity transmission in distributed network. The performance and energy consumption comparisons between cooperative MIMO and relay techniques are performed and an association strategy is also proposed to exploit simultaneously the advantages of the two cooperative techniques.

## Structure of the thesis

### • Chapter 1: Diversity and MIMO Techniques

The combination of transmit and receive diversity techniques, known as MIMO techniques, not only achieves the reliability in wireless communications due to the diversity gain, but also efficiently increases the channel capacity and the data transmission rate. In this chapter, the principles of different types of diversity techniques and the performance of combination techniques are firstly presented. Then, the capacity and diversity gain of MIMO systems are referred. The principles and advantages of three MIMO techniques: Space Time Block Code (STBC), Space Time Trellis Code (STTC) and Spatial Multiplexing (SM), are also presented.

- **Chapter 2: Cooperative Techniques in Wireless Sensor Networks**

In wireless distributed networks where multiple antennas can not be integrated into one node, cooperative techniques help to reduce the transmission energy consumption in different manners. In this chapter, the energy efficiency advantages of the multi-hop transmission, the cooperative relay techniques and the recently developed cooperative MIMO techniques are presented. At the end of chapter, some details on the CAPTIV project, funding this thesis work, are presented and cooperative strategies for energy efficient communications between road sign infrastructure and mobile vehicles in CAPTIV are also proposed.

- **Chapter 3: Energy Efficiency of Cooperative MIMO Techniques**

The advantage of an orthogonal STBC transmission over a SISO transmission and the application to cooperative MIMO networks are presented. The reference energy consumption model of a radio frequency (RF) system is given, allowing an energy consumption comparison with SISO, non-cooperative MIMO and SISO multi-hop systems. The energy efficiency of the cooperative MIMO technique over the SISO and multi-hop SISO technique for medium and long transmission distance is proved, and an optimization of the number of cooperative transmitters and receivers can then be selected to design the most energy-efficient cooperative MIMO scheme with respect to the transmission distance.

- **Chapter 4: Effect of Transmission Synchronization Errors and Cooperative Reception Techniques**

Since the wireless nodes are physically separated in cooperative MIMO systems, the imperfect time synchronization between cooperative nodes clocks leads to an unsynchronized MIMO transmission. The effect of this un-synchronization is that inter-symbol interference appears and the space-time sequences from different nodes are no longer orthogonal. At the reception side, each cooperative node has to forward its received signal through a wireless channel to the destination node for space-time signal combination which leads to additional noise in the final received signal.

In this chapter, the performance of cooperative MISO systems using STBC is analyzed in the presence of transmission synchronization error and the performance of different cooperative reception techniques is investigated. The performance of cooperative MIMO system decreases and affects the energy efficiency advantage of cooperative MIMO system over SISO system.

- **Chapter 5: Multiple Sampling Orthogonal Combination for an Unsynchronized Cooperative MIMO Transmission**

The performance of cooperative MISO systems is decreased when the transmission is un-synchronized. For small range of transmission synchronization errors, the performance degradation is negligible. However, for large range of errors, the performance decreases quickly and the degradation becomes significant. A new efficient space-time combination technique based on a low complexity algorithm is proposed for cooperative MIMO systems in the presence of transmission synchronization error.

The new technique principle performs a multiple sampling process and a signal combination from different sampled sequences to reconstruct the orthogonality of the transmission space-time sequences. The performance of the new space time combination technique over the traditional combination technique is then proved.

### • Chapter 6: Cooperative MIMO and Relay Cooperation Strategy

Relay techniques have been proposed as a simple and energy efficient technique to extend the transmission range in cooperative wireless networks. In this chapter, a comparison between relay and cooperative MIMO techniques in terms of performance and energy consumption shows that the best solution for WSN depends on the network topology, the position and number of cooperative (or relay) wireless nodes. In this context, an association strategy is proposed in order to exploit simultaneously the advantages of these two techniques. The energy consumption and the transmission delays of this cooperative strategy in comparison with the cooperative MIMO and cooperative relay techniques are investigated.

Finally, the thesis conclusion and some future works are given at the end of the thesis.

## Publications

[a] T. Nguyen, O. Berder and O. Sentieys, "Cooperative MIMO schemes optimal selection for wireless sensor networks", *IEEE 65th Vehicular Technology Conference (VTC Spring)*, Dublin, Ireland, May 2007, pp. 85-89.

[b] T. Nguyen, O. Berder and O. Sentieys, "Energy-efficiency Optimization for cooperative MIMO schemes in wireless sensor networks", *IRAMUS Thematic Informational Workshop*, Val Thorens, France, January 2007.

[c] T. Nguyen, O. Berder and O. Sentieys, "Optimisation énergétique des transmissions MIMO coopératives pour les réseaux de capteurs sans fil", *GRETSI'07*, Troyes, France, 2007, pp. 301-304.

- [d] T. Nguyen, O. Berder and O. Sentieys, "Impact of Transmission Synchronization Error and Cooperative Reception Techniques on the Performance of Cooperative MIMO Systems", *IEEE International Conference on Communications (ICC)*, Beijing, China, May 2008, pp. 4601-4605.
  
- [e] T. Nguyen, O. Berder and O. Sentieys, "Efficient Space Time Combination Technique for Unsynchronized Cooperative MISO Transmission", *IEEE Vehicular Technology Conference (VTC Spring)*, Singapore, May 2008, pp. 629-633.
  
- [f] T. Nguyen, O. Berder and O. Sentieys, "Efficient cooperative MIMO combination in the presence of transmission synchronization error", *submitted to IEEE International Conference on Sensor Networks, SECON 09*, Rome.



# Chapter 1

## Diversity and MIMO Techniques

### 1.1 Introduction

Wireless communications are a highly challenging design due to the complex, time varying propagation medium. Due to a non-existing line-of-sight transmission, scattering and reflection of radiated energy from objects (buildings, hills, trees...) as well as mobility effects, a signal transmitted through a wireless environment arrives at the receiver with different paths, referred to as multi-paths, which have different delays, angles of arrival, amplitudes and phases. As a consequence, the received signal varies as a function of frequency, time and space. These signal variations are referred to as the fading effect and cause a degradation of the signal quality.

The techniques where signals are transmitted through different media to combat fading effects in wireless communications are known as diversity techniques. Among different types of diversity techniques, spatial diversity using multiple transmit and receive antennas provides a very good performance without increasing bandwidth, delay or transmission power. Information theory results in [29, 98] showed that there is a huge advantage of using such spatial diversity. At the beginning, the receive diversity technique that uses multiple antennas at the receiver was the primary focus for space diversity systems due to the fact that diversity gain can be achieved by using simple but efficient combination techniques. Then, transmit diversity has been extensively studied as a method for combating fading effects and increasing transmission data rate [4, 79, 29, 97, 36, 94, 96, 95].

A multi layered space-time architecture that uses spatial multiplexing to increase the data rate but not necessarily provides transmit diversity was introduced by Foschini in [27]. The criterion to achieve the maximum transmit diversity was derived in [36] and a complete study for maximum diversity goals and coding gains in addition to the design of space-time trellis codes was proposed in [97]. The simple diversity transmission scheme in [4] and the introduction of space-time orthogonal block coding in [94] opened an interesting research domain in Multi-Input Multi-Output (MIMO) techniques.

The combination of transmit and receive diversity techniques, known as MIMO technique, not only achieves the reliability in wireless communications due to the diversity gain (which is equal to the product of transmit and receive antennas number) but also efficiently increases the channel capacity and the transmission data rate.

In this chapter, the principles and the different types of diversity techniques are firstly presented. The diversity gain and performance of combination techniques are then investigated, before the multi antenna system, the capacity and diversity gain of MIMO channel are reported. And finally, the three principal MIMO techniques: Space Time Block Code (STBC), Space Time Trellis Code (STTC) and Spatial Multiplexing (SM) are presented.

## 1.2 Diversity Techniques

The principle of diversity techniques is that copies of a transmitted signal are sent through different mediums like different time slots, different frequencies, different polarizations or different antennas for combating the fading effect. If these copies have independent fades, the possibility that all transmitted signals are simultaneously in deep fades is minimized. Therefore, using appropriate combining methods, the receiver can reliably decode the transmitted signal and the probability of error will be lower.

By sending two or more signal copies through independent fading channels, the transmit diversity gain can be exploited. The diversity gain  $G_d$  is defined as

$$G_d = \lim_{\gamma \rightarrow \infty} \frac{\log(P_e)}{\log(\gamma)} \quad (1.1)$$

where  $P_e$  is the error probability of the received signal and  $\gamma$  is the received Signal to Noise Ratio (SNR).

### 1.2.1 Time Diversity

When different time slots are used for the diversity transmission, it is called temporal diversity (Fig. 1.1). Copies of the transmitted signal are sent in separated time slots. The time interval between two time slots must be higher than the coherence time  $T_c$  of the channel to assure independent fades.

In the temporal diversity, the receiver suffers from a delay before it receives all transmitted signals and starts the combination and decoding processes. Temporal diversity is not bandwidth efficient because of this underlying redundancy.

### 1.2.2 Frequency Diversity

Frequency diversity uses different carrier frequencies to perform the diversity transmission [6]. In this technique, copies of transmitted signal are sent through different carrier

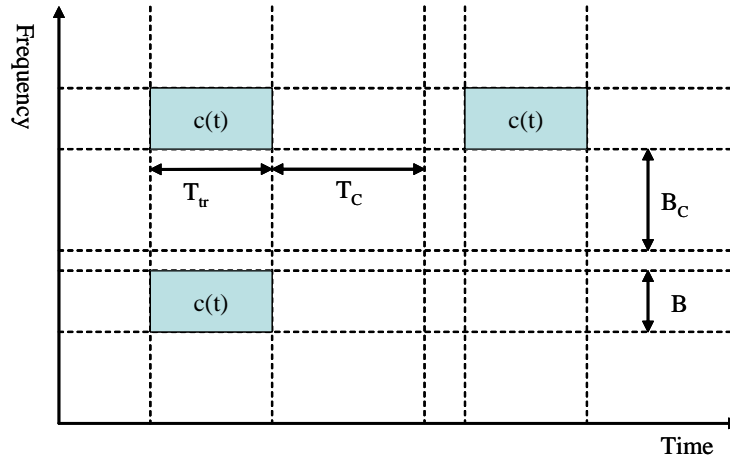


Figure 1.1: Principle of temporal diversity and frequency diversity

frequencies (Fig. 1.1) and these carrier frequencies should be separated by more than the coherence bandwidth  $B_c$  of the channel to ensure the independent fades. Similarly to temporal diversity, frequency diversity is not bandwidth efficient and the receiver needs to tune to different carrier frequencies for signal reception.

### 1.2.3 Spatial Diversity

Diversity techniques that may not suffer from bandwidth deficiency are spatial diversity [103] [5]. Spatial diversity uses multiple antennas at the receiver or the transmitter to achieve the diversity. If antennas are separated enough, more than half of the carrier wavelength, signals from different antennas are affected by independent channel fades.

- **Receive Diversity** uses multiple antennas at the receive side. The received signals from the different antennas have independent fades and are combined at the receiver to exploit the diversity gain. Receive diversity is characterized by the number of independent fading channels, and its diversity gain is almost equal to the number of receive antennas.
- **Transmit Diversity** uses multiple antennas at the transmit side. Information is processed at the transmitter and then spread across the multiple antennas for the simultaneous transmission. Transmit diversity was firstly introduced in [103] and becomes an active research area of space time coding techniques.

### 1.2.4 Antenna Diversity

Antenna diversity is another technique using antennas for providing the diversity. There are two main techniques of antenna diversity:

- Angular diversity uses directional antennas to achieve diversity. Different copies of the transmitted signal are received from different angles of the receive antenna. Unlike spatial diversity, angular diversity does not need a minimum separation distance between antennas. Therefore, angular diversity is also useful for small devices.
- Polarization diversity uses the difference of the vertical and horizontal polarized signals to achieve the diversity [52]. The arriving signal can be split into two orthogonal polarizations. If the signal goes through random reflections, the two polarization values are independent. Polarization diversity does not require the minimum separation distance for the antennas. However, polarization diversity can only provide a diversity order of two.

### 1.3 Combination Techniques

In order to exploit the gain of different diversity techniques to increase the overall SNR, copies of the transmitted signal must be combined at the receiver. The system performance depends on how many signal copies are combined at the receiver and which combination technique is used.

If the signal copies are fading independent, the source of diversity signals does not affect the method of combination with the exception of transmit antenna diversity. For example, receiving two versions of the transmitted signal by polarization diversity is the same as receiving two versions of signals from two receive antennas for the combining purpose. There exists four main types of signal combining technique: selection combining, switched combining, equal-gain combining (EGC) and maximum ratio combining (MRC) [80].

Fig.1.2 and Fig.1.3 show the block diagrams of the maximum ratio combiner and of the selection combiner. A hybrid scheme that combines these two techniques is also presented in Fig.1.4. The detail of these techniques is described in the following paragraphs.

#### 1.3.1 Maximum Ratio Combining

Let us consider a system that receives  $M$  copies of the transmitted signal  $s$  through  $M$  independent fading paths. Let us note  $r_k, k = 1, 2, \dots, M$ , as the  $k^{th}$  path received signal

$$r_k = \alpha_k s + \eta_k, \quad (1.2)$$

where  $\alpha_k$  is the independent channel fading,  $s$  is the transmit signal and  $\eta_k$  is an additive white Gaussian noise of the  $k^{th}$  copy of the signal.

A maximum likelihood decoder combines the  $M$  received signals to find the most likely transmitted signal. The receiver needs to find the optimal transmitted signal  $\hat{s}$  that

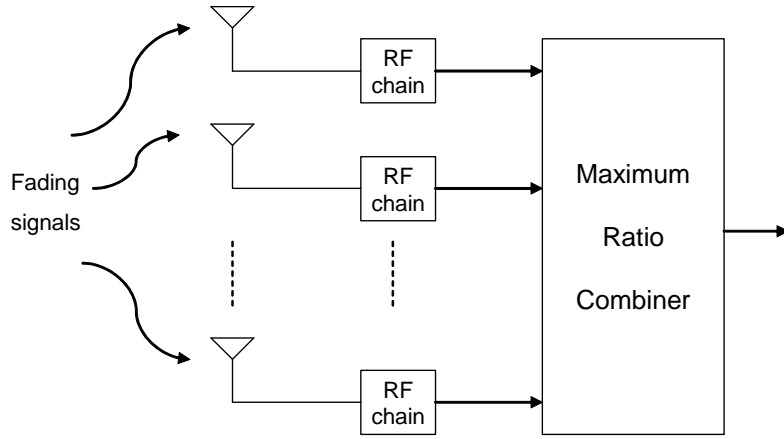


Figure 1.2: Principle of the Maximum Ratio Combining Technique

minimizes  $\sum_{k=1}^M |r_k - \alpha_k s|$ .

Considering that the receiver knows perfectly the channel path gains  $\alpha_k$ , the estimated value of transmitted signal can be combined as

$$\tilde{s} = \sum_{k=1}^M r_k \alpha_k^* = \sum_{k=1}^M (\alpha_k s + \eta_k) \alpha_k^* = \sum_{k=1}^M \|\alpha_k\|^2 s + \sum_{k=1}^M \eta_k \alpha_k^*. \quad (1.3)$$

MRC combines all  $M$  received signals with weighting factors  $\alpha_k^*$ . A Maximum-Likelihood (ML) decoder then finds the most likely transmitted signal  $\hat{s}$  which is the closest to the combined value  $\tilde{s}$  in the signal constellation. The SNR at the output of the maximum ratio combiner is

$$\gamma = \frac{\left(\sum_{k=1}^M \|\alpha_k\|^2\right)^2}{\sum_{k=1}^M \|\alpha_k\|^2} \frac{E_s}{N_0} = \sum_{k=1}^M \|\alpha_k\|^2 \frac{E_s}{N_0} = \sum_{k=1}^M \gamma_k. \quad (1.4)$$

Therefore, the effective received SNR is equivalent to the sum of the received SNRs of  $M$  different paths. Let us assume that all different paths have the same average SNR defined as  $A = E[\gamma_k]$ , the average SNR at the output of the maximum ratio combiner is

$$\bar{\gamma} = M \times A. \quad (1.5)$$

This  $M$ -fold increase in the average receive SNR results in a diversity gain of  $M$ . This is the maximum possible diversity gain when  $M$  copies of the signal are received over a Rayleigh fading channel.

Increasing the effective receive SNR reduces the error probability at the receiver. For a system with no diversity, the average error probability is proportional to the inverse of the SNR,  $SNR^{-1}$ , at high SNR [78]. Since each of the  $M$  paths follows an independent

Rayleigh fading distribution, the average error probability  $P_e$  of a system with  $M$  independent Rayleigh paths is proportional to  $SNR^{-M}$  [78]. As the above definition of diversity gain Eq. 1.1, the diversity gain of MRC with  $M$  independent paths is equal to  $M$ .

Equal Gain Combining (EGC) is a special case of maximum ratio combining where the receiver combines the different received signals with equal weight factors. In EGC, the average SNR at the output of the combiner is

$$\bar{\gamma} = \left[1 + \frac{\pi}{4}(M - 1)\right] A. \quad (1.6)$$

The SNR and diversity gains of EGC is smaller than those of the MRC technique.

### 1.3.2 Selection Combining

In the MRC technique with  $M$  independent signals arriving at the receiver antennas,  $M$  radio frequency processing chains (RF chains) are required to provide the  $M$  baseband signals for the MRC combination. Since each RF chain requires parts of the implementation using analog circuits, MRC will have a higher cost in the physical size and price. So, in some applications with a limitation in size and RF costs, a combining technique that uses only one RF chain is preferred.

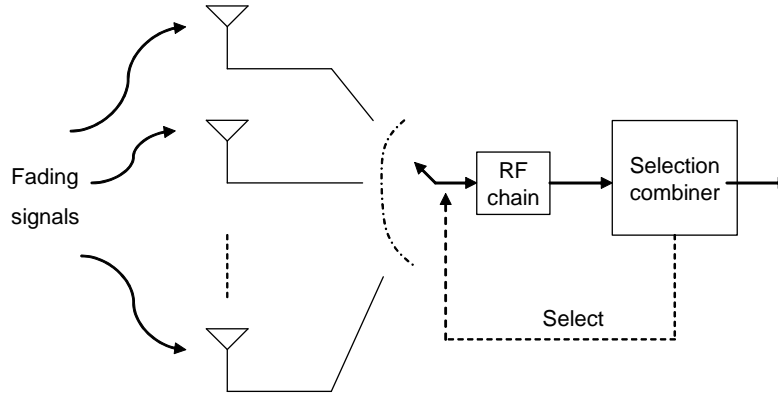


Figure 1.3: Principle of the Selection Combining Technique

Selection Combining (or antenna selection) chooses the signal having the highest SNR among all receive antennas and uses it for decoding. The average SNR at the output of the selection combiner,  $\bar{\gamma}$ , is

$$\bar{\gamma} = A \sum_{k=1}^M \frac{1}{k}. \quad (1.7)$$

As a result, without increasing the transmission power, selection combining provides

$\sum_{k=1}^M \frac{1}{k}$  times improvement in the average SNR, which is less than the maximum improvement ratio  $M$  of MRC. Selection combining does not provide an optimal SNR or diversity gain, but its complexity is lower than MRC. In other words, selection combining is a trade-off between RF complexity and performance.

### 1.3.3 Hybrid Combining Technique

In a system having  $M$  receive antennas ( $M$  is more than two receive antennas), it is possible to use a number of RF chains between one and  $M$  for a hybrid combining technique that mixes the MRC and selection combining [102]. Let us assume that the receiver contains  $J$  RF chains where  $1 < J < M$  and  $M > 2$ , the receiver chooses the  $J$  received signals among the  $M$  antennas with the highest SNR, and then combines them using MRC technique.

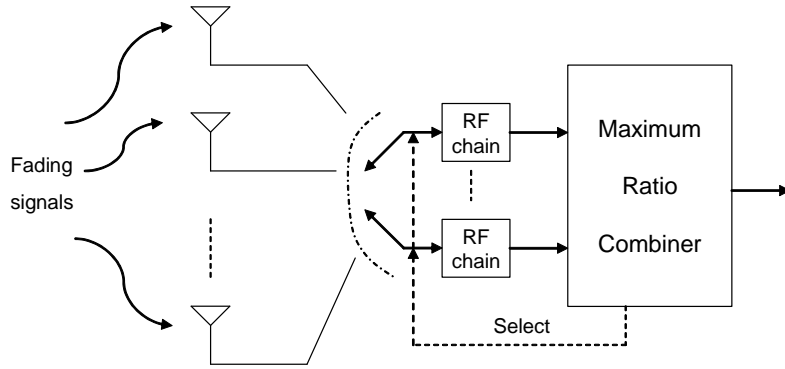


Figure 1.4: Principle of the Hybrid Combining Technique

The block diagram of this hybrid combining method is shown in Fig.1.4. The instantaneous SNR at the output of the hybrid selection/maximal ratio combining is

$$\gamma = \sum_{j=1}^J \gamma_j, \quad (1.8)$$

where  $\gamma_j$  is the SNR of the  $j^{th}$  selected signal. The average SNR at the output of the hybrid selection/maximal ratio combiner,  $\bar{\gamma}$ , is

$$\bar{\gamma} = AJ \left[ 1 + \sum_{m=J+1}^M \frac{1}{M} \right]. \quad (1.9)$$

Fig. 1.5 compares the SNR gains of different combining technique using 1 to 10 receive antennas. As expected, MRC provides a higher gain than EGC and selection combining while requiring the highest receiver complexity. When the number of receive antennas increases, the gap between the MRC (or EGC) and selection combining increases due to the trade-off of the lower complexity of selection combining technique. The gap between

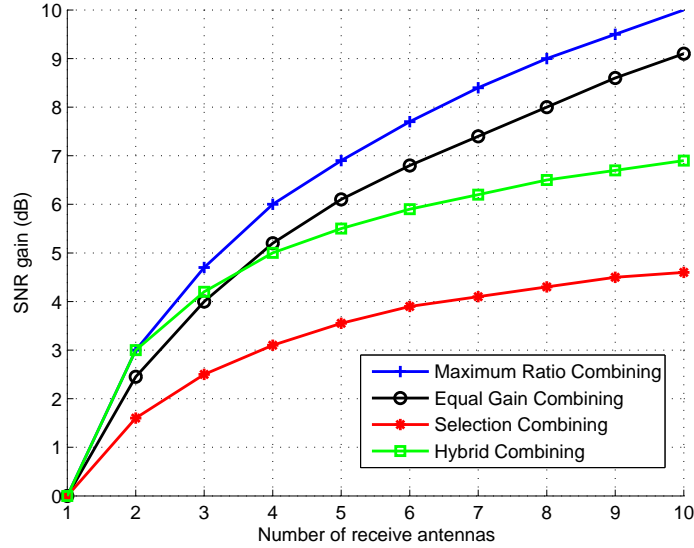


Figure 1.5: SNR gain of different combining methods

the hybrid selection/maximal ratio combiner with only  $J = 2$  RF chains and the MRC is small for a small number of receive antennas, but it increases with the number of receive antennas.

## 1.4 MIMO Techniques

MIMO stands for multiple-input multiple-output and means that multiple antennas are used at both transmission and reception sides of a communication system. The idea of MIMO is that multiple antennas of the transmitter and receiver are combined in such a way that the diversity is exploited to increase the performance of transmission or the data throughput. Information theory results in [29, 98] showed that the channel capacity and the system performance can be significantly increased by using multiple antennas at the transmission and at the reception. The core idea of MIMO techniques is that the signal processing in time is complemented with signal spatial distribution of multiple antennas at both link ends to increase the data rates or to provide the diversity gain.

Several MIMO transmission schemes which have been proposed for different goals can be divided in two categories: spatial multiplexing and space-time coding. A multi-layered architecture that uses spatial multiplexing to increase the data rate, but not diversity, was firstly introduced in [27]. On the other hand, space time coding exploits the maximum diversity gain to achieve a high reliability, high spectral efficiency and high performance gain. The criterion to achieve the maximum transmit diversity was derived in [36] and



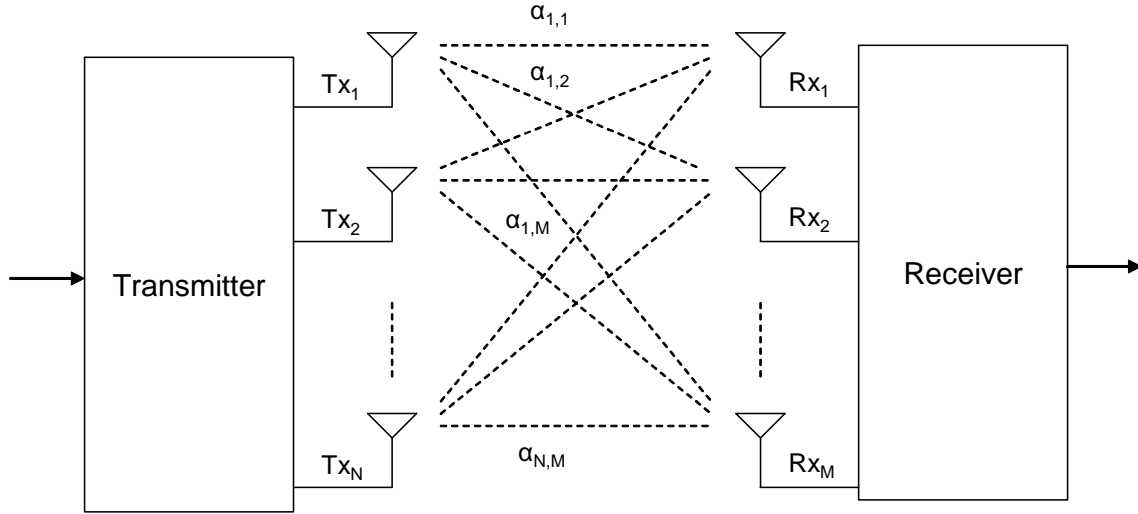


Figure 1.6: MIMO model with  $N$  transmit antennas and  $M$  receive antennas.

a complete study for maximum diversity goals and coding gains in addition with space-time trellis codes introduction was proposed in [97]. The simple diversity transmission scheme in [4] and the introduction of space-time orthogonal block coding in [94] opened an interesting domain of MIMO techniques that allow a maximum diversity gain with a low decoding complexity.

#### 1.4.1 MIMO Channel Model

Let us consider a point-to-point MIMO transmission channel with  $N$  transmit and  $M$  receive antennas, as illustrated by the block diagram given in Fig.1.6. At a certain time  $t$ , the complex signals  $c_{t,1}, c_{t,2}, \dots, c_{t,N}$  are transmitted via  $N$  transmit antennas, and the received signal at antenna  $m$  can be expressed as:

$$r_{t,m} = \sum_{n=1}^N \alpha_{n,m} c_{t,n} + \eta_{t,m} \quad (1.10)$$

where  $\eta_{t,m}$  is a noise term,  $\alpha_{n,m}$  is a complex channel gain between transmit antenna  $n$  and receive antenna  $m$ . Combining all received signals in a vector  $\mathbf{r} = [r_{t,1} \ r_{t,2} \ \dots \ r_{t,M}]$ , Eq. 1.10 can be easily expressed in the following matrix form

$$\mathbf{r} = \mathbf{c}\mathbf{H} + \boldsymbol{\eta} \quad (1.11)$$

where  $\mathbf{c} = [c_{t,1} \ c_{t,2} \ \dots \ c_{t,N}]$  is the transmit vector,  $\mathbf{H}$  and  $\boldsymbol{\eta}$  are the  $M \times N$  MIMO channel transfer matrix and receive AWGN noise vector which are defined as

$$\mathbf{H} = \begin{bmatrix} \alpha_{1,1} & \alpha_{1,2} & \dots & \alpha_{1,M} \\ \alpha_{2,1} & \alpha_{2,2} & \dots & \alpha_{2,M} \\ \vdots & \vdots & \ddots & \vdots \\ \alpha_{N,1} & \alpha_{N,2} & \dots & \alpha_{N,M} \end{bmatrix} \quad (1.12)$$

$$\boldsymbol{\eta} = \begin{bmatrix} \eta_{t,1} & \eta_{t,2} & \dots & \eta_{t,M} \end{bmatrix} \quad (1.13)$$

The noise is an additive white Gaussian noise (AWGN) and its elements  $\eta_{t,m}$  are independent from each other and have a complex Gaussian distribution for a complex baseband transmission.

The channel is considered as a frequency non-selective quasi-static flat fading model where the channel path gains are independent from each other and the channel matrix is constant over the frequency band of interest. If a Rayleigh fading channel is considered, the path gains are modeled by independent complex Gaussian random variables. The real and imaginary parts of the path gains at each time slot are i.i.d Gaussian random variables which have a zero mean and a variance equal to 0.5. The envelope of the channel path gains  $|\alpha_{n,m}|$  has a Rayleigh distribution, and that is the reason why the channel is called a Rayleigh fading channel. Also,  $|\alpha_{n,m}|^2$  is a chi-square random variable with two degrees of freedom and the average channel energy is  $E[|\alpha_{n,m}|^2] = 1$ .

Let us denote that the average power of the transmitted symbols  $c_{t,n}$  is  $E_s$ , and that the variance of the zero-mean complex Gaussian noise is  $N_0/2$  per dimension. Then, the average receive SNR is  $\gamma = NE_s/N_0$ . So that, for a fair comparison between two systems despite of the number of transmit antennas (for the same transmission power and average received SNR), the transmission power of each transmit antenna must be divided by  $N$  in comparison with the transmission power of a transmission with a single antenna.

### 1.4.2 MIMO Channel Capacity

Information-theoretic studies of wireless channels have proved that the MIMO capacity is significantly increased compare to the capacity of a Single-Input-Single-Output (SISO) system. One of the most important fields in the MIMO systems research area is how to exploit this potential of channel capacity in an efficient way.

The maximum error-free data rate that a channel can support is called the channel capacity. The channel capacity for SISO AWGN channels was first derived by Claude Shannon [88] as

$$C = \log_2(1 + \gamma). \quad (1.14)$$

In contrast to AWGN channels, multiple antenna channels combat fading and cover a spatial dimension. The capacity of a deterministic MIMO channel with an input-output relation  $\mathbf{r} = \mathbf{c}\mathbf{H} + \boldsymbol{\eta}$  is given by

$$C = \log_2\left(1 + \frac{\gamma}{N}\mathbf{H}^H\mathbf{H}\right). \quad (1.15)$$

where the normalized channel power transfer characteristic is  $\|\mathbf{H}\|^2$  and the average SNR at each receiver branch is  $\gamma$ .

For MIMO fading channel, the resulting capacity of the channel is a random variable because the capacity is a function of the channel matrix  $\mathbf{H}$ . The distribution of the capacity is determined by the distribution of the channel matrix  $\mathbf{H}$ .

### Capacity of random MIMO channel

Let us assume an equal distribution of the input power of transmit antennas. The channel capacity of a random MIMO channel is given by [29]

$$C = \log_2 \left[ \det\left(\mathbf{I} + \frac{\gamma}{N}\mathbf{H}^H\mathbf{H}\right) \right] \quad (1.16)$$

For the case of  $N \geq M$ , a lower bound on the capacity can be derived in terms of chi-square random variables [29] as

$$C > \sum_{k=N-M+1}^N \log_2 \left( 1 + \frac{\gamma}{N} \chi_k \right) \quad (1.17)$$

where  $\chi_k$  is a chi-square random variable with  $2k$  degrees of freedom. For the special case of  $N = M$ , the lower bound of capacity in (1.17) is

$$C_N = \sum_{k=1}^N \log_2 \left( 1 + \frac{\gamma}{N} \chi_k \right). \quad (1.18)$$

The mean channel capacity which is called the ergodic capacity is given by [98]

$$C = E \left[ \log_2 \left[ \det\left(\mathbf{I} + \frac{\gamma}{N}\mathbf{H}^H\mathbf{H}\right) \right] \right] \quad (1.19)$$

where  $E[x]$  denotes an expectation of random variable  $x$ . The ergodic capacity grows with the number  $N$  of antennas (under the assumption  $N = M$ ), which results in a significant capacity gain of MIMO fading channels compared to a SISO channel.

In Fig. 1.7, the ergodic channel capacity as a function of average SNRs is plotted for several uncorrelated MIMO systems with  $N = M$ . The channel capacity for the SISO system ( $N = 1$ ) at  $SNR = 10$  dB is approximately 2.95 bits/channel use. By applying multiple antennas, it is obvious that the channel capacity increases substantially. A  $2 \times 2$  MIMO system (two transmit and two receive antennas) can transmit more than 5.6 bits/channel use and the MIMO system with four transmit and receive antennas ( $4 \times 4$  MIMO) promises almost 11 bits/channel use at this SNR value.

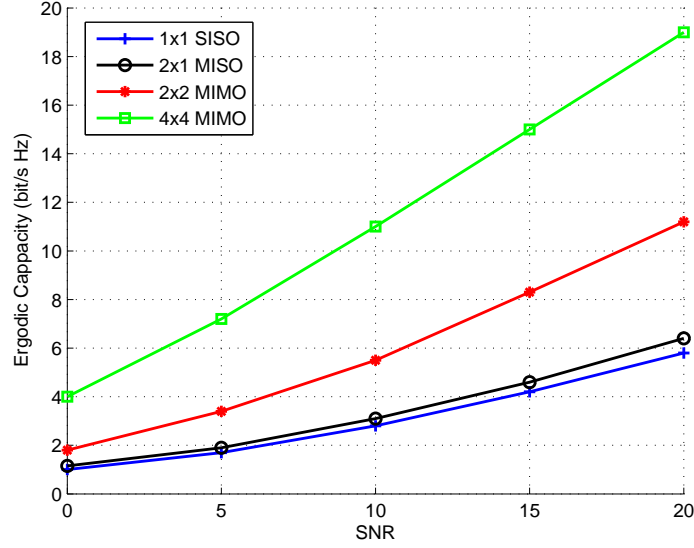


Figure 1.7: The ergodic channel capacity of MIMO channel

### Outage Capacity

A more useful capacity concept for performance measurement or coding purposes is the outage capacity defined in [29]. The outage capacity  $C_{out}$  is defined as a value that the channel capacity  $C$  (a random variable) is smaller than this value only with a probability  $P_{out}$  (outage probability).

$$P_{out} = P(C < C_{out}) \quad (1.20)$$

The importance of the outage probability is that if one wants to transmit  $C_{out}$  bits/channel use, the probability that the channel capacity is less than  $C_{out}$  is  $P_{out}$ . In other words, such a transmission is impossible with probability  $P_{out}$ . For a stationary channel, if we transmit a large number of frames with a rate of  $C_{out}$  bits/channel use, the number of failures is  $P_{out}$  times the total number of frames.

For a Rayleigh fading channel with  $N$  transmit antennas and  $M$  receive antennas, the Shannon capacity is a function of  $N \times M$  independent complex Gaussian random variables. For the case of one transmit antenna ( $N = 1$ ) and  $M$  receive antennas, using the equality  $\det[\mathbf{I} + \mathbf{A}\mathbf{B}] = \det[\mathbf{I} + \mathbf{B}\mathbf{A}]$ , the channel capacity is

$$C = \log_2 [\det(\mathbf{I}_M + \gamma \mathbf{H}^H \mathbf{H})] = \log_2(1 + \gamma \mathbf{H} \mathbf{H}^H) = \log_2 \left( 1 + \gamma \sum_{m=1}^M |\alpha_{1,m}|^2 \right). \quad (1.21)$$

Assuming independent Rayleigh fading, the channel capacity is then

$$C = \log_2(1 + \gamma \cdot \chi_r), \quad (1.22)$$

where  $\chi_r$  is a chi-square random variable with  $2M$  degrees of freedom and the outage probability can be calculated as

$$P_{out} = P(\chi_r < \frac{2^{C_{out}} - 1}{\gamma}). \quad (1.23)$$

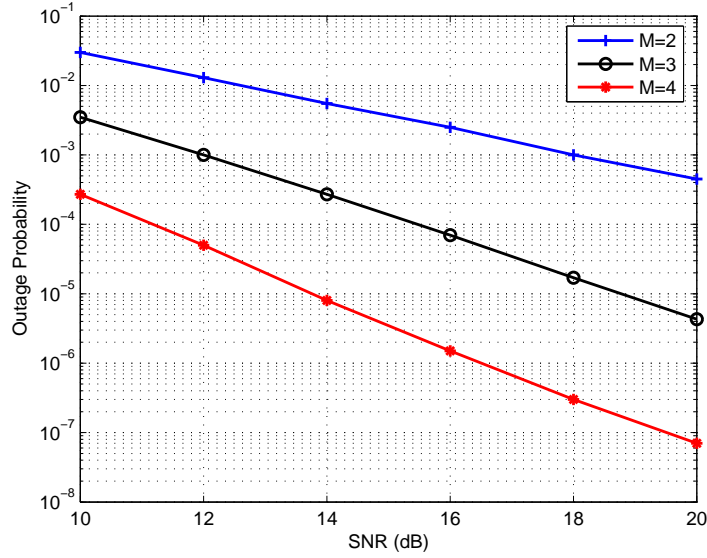


Figure 1.8: Outage probability with  $C_{out} = 2$  bits/(s Hz),  $M$  receive antennas, one transmit antenna

Fig. 1.8 shows the outage probability as a function of different SNRs for an outage capacity of  $C_{out} = 2$  bits/channel use of a MIMO channel with one transmit antenna and  $M = 2, 3, 4$  receive antennas.

Similarly, for a system with  $N$  transmit antennas and one receive antenna, the Shannon capacity can be calculated as

$$C = \log_2(1 + \frac{\gamma}{N} \cdot \chi_r) \quad (1.24)$$

where  $\chi_t$  is a chi-square random variable with  $2N$  degrees of freedom. The corresponding outage probability is then

$$P_{out} = P(\chi_r < N \frac{2^{C_{out}} - 1}{\gamma}). \quad (1.25)$$

As it is clear from Eq. 1.23 and 1.25, for a given outage capacity, a system with  $N$  transmit antennas and one receive antenna requires  $N$  times more SNR to provide the same outage probability as a system with one transmit antenna and  $N$  receive antennas.

Fig. 1.9 shows the outage probability as a function of varies SNRs for an outage capacity  $C_{out} = 2$  bits/channel use for MIMO channel with  $N = 2, 3, 4$  transmit antennas and one receive antenna.

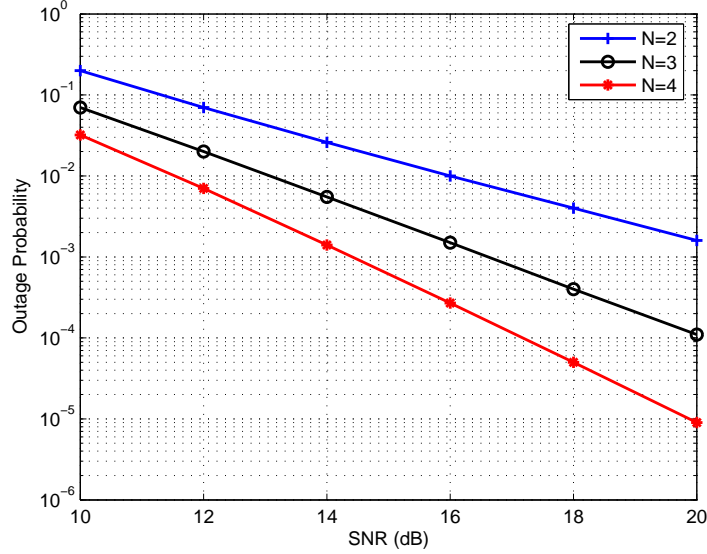


Figure 1.9: Outage probability with  $C_{out} = 2$  bits/(s Hz), one receive antenna,  $N$  transmit antennas

## 1.5 Space Time Coding

Basically, there are two different categories of space-time coding: space-time trellis codes (STTC) and space-time block codes (STBC). STTC has been introduced in [97] as a trellis coding technique for multiple transmission antennas that promises a full diversity with a substantial coding gain at the price of a high decoding complexity. To avoid this disadvantage, Alamouti has proposed a simple diversity transmission scheme [4] with a full diversity and a full data rate (one symbol per channel use) transmission for two transmit antennas. This scheme was generalized to an arbitrary number of transmit antennas by applying the theory of orthogonal design in [94, 32] and was named as space-time block codes.

The key feature of STBC is the orthogonality design between the transmitted signal vectors and a space time combination at the receiver to exploit the diversity gain. However, for more than two transmit antennas, no STBC for a complex symbols modulation with full diversity and full data rate exists [94]. Therefore, many different code design methods have been proposed for providing either full diversity or full data rate at the cost of a higher complexity like QOSTBC [44].

STBC can be concatenated with an additional outer code as an inner code to increase efficiently the coding gain. Such schemes have been proposed, like for example the Super Orthogonal Space-Time Trellis Codes (SOSTTC) [46].

### 1.5.1 Space-Time Block Codes

#### Alamouti Code

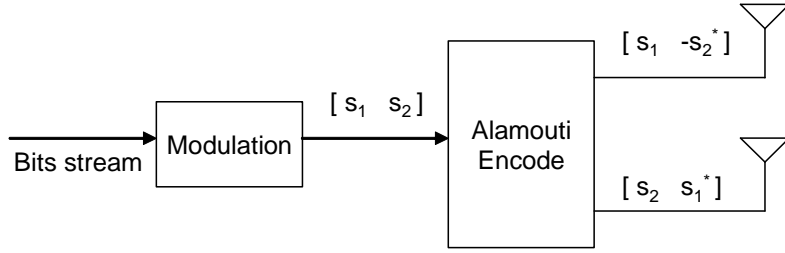


Figure 1.10: Alamouti encoding scheme

Alamouti code can be considered as the first STBC and provides full diversity at full data rate for two transmit antennas. A block diagram of the Alamouti space-time encoder is shown in Fig. 1.10. The Alamouti encoder takes the block of two modulated symbols  $s_1$  and  $s_2$  in each encoding operation and sends it to the transmit antennas according to the coding matrix

$$\mathbf{C}_2 = \begin{bmatrix} s_1 & s_2 \\ -s_2^* & s_1^* \end{bmatrix} \quad (1.26)$$

In the first transmission period, the symbols  $s_1$  and  $s_2$  are transmitted simultaneously from antenna one and antenna two. In the second period, the symbol  $-s_2^*$  and  $s_1^*$  are transmitted from antenna one and antenna two. The two rows and columns of  $\mathbf{C}_2$  are orthogonal:

$$\mathbf{C}_2 \mathbf{C}_2^H = \begin{bmatrix} s_1 & s_2 \\ -s_2^* & s_1^* \end{bmatrix} \begin{bmatrix} s_1^* & -s_2 \\ s_2^* & s_1 \end{bmatrix} = \begin{bmatrix} |s_1|^2 + |s_2|^2 & 0 \\ 0 & |s_1|^2 + |s_2|^2 \end{bmatrix} = (|s_1|^2 + |s_2|^2) \mathbf{I}_2 \quad (1.27)$$

where  $\mathbf{I}_2$  is a  $2 \times 2$  identity matrix. This orthogonal property implies that the receiver can detect  $s_1$  and  $s_2$  independently by a simple linear signal processing operation from the superposed received signals.

If one receive antenna is assumed to be available and the channel fading is considered constant during two consecutive transmit periods of duration  $T$ , the two received signals at  $t$  and  $t + T$  can then be expressed as

$$\begin{aligned} r_1 &= \alpha_1 s_1 + \alpha_2 s_2 + \eta_1 \\ r_2 &= -\alpha_1 s_2^* + \alpha_2 s_1^* + \eta_2 \end{aligned} \quad (1.28)$$

### Linear Combining and Maximum Likelihood Decoding of the Alamouti Code

From the two received signals in Eq. 1.28, a maximum likelihood (ML) detector decides a pair of symbols  $(\hat{s}_1, \hat{s}_2)$  from the signal modulation constellation that minimizes the decision metric

$$d^2(r_1, \alpha_1 s_1 + \alpha_2 s_2) + d^2(r_2, -\alpha_1 s_2^* + \alpha_2 s_1^*) = |r_1 - \alpha_1 s_1 - \alpha_2 s_2|^2 + |r_2 + \alpha_1 s_2^* - \alpha_2 s_1^*|^2 \quad (1.29)$$

Expanding this function and ignoring the common term  $|r_1|^2 + |r_2|^2$ , the cost function 1.29 can be decomposed into two parts:

$$|s_1|^2 \sum_{n=1}^2 |\alpha_n|^2 - (r_1 \alpha_1^* s_1^* + r_1^* \alpha_1 s_1 + r_2 \alpha_2^* s_1 + r_2^* \alpha_2 s_1^*) \quad (1.30)$$

is only a function of  $s_1$ , and

$$|s_2|^2 \sum_{n=1}^2 |\alpha_n|^2 - (r_1 \alpha_2^* s_2^* + r_1^* \alpha_2 s_2 - r_2 \alpha_1^* s_2 - r_2^* \alpha_1 s_2^*) \quad (1.31)$$

is only a function of  $s_2$ . Therefore, instead of minimizing the cost function of Eq. 1.29 over all possible values of  $(s_1, s_2)$ , the receiver can independently minimize the cost functions 1.30 and 1.31 over all possible values of  $s_1$  and  $s_2$  respectively.

If the constellation symbols have equal energy distribution, the ML receiver minimizes

$$|s_1 - r_1 \alpha_1^* - r_2^* \alpha_2|^2 \quad (1.32)$$

to decode  $s_1$ , and minimizes

$$|s_2 - r_1 \alpha_2^* + r_2^* \alpha_1|^2 \quad (1.33)$$

to decode  $s_2$ .

The ML decoding consists of two simple linear combinations of the received signals with the channel coefficients. The channel coefficients  $\alpha_1$  and  $\alpha_2$  are considered to be perfectly estimated at the receiver.

$$\begin{aligned} \tilde{s}_1 &= r_1 \alpha_1^* + r_2^* \alpha_2 = (|\alpha_1|^2 + |\alpha_2|^2) s_1 + \alpha_1^* \eta_1 + \alpha_2 \eta_2^* \\ \tilde{s}_2 &= r_1 \alpha_2^* - r_2^* \alpha_1 = (|\alpha_1|^2 + |\alpha_2|^2) s_2 - \alpha_1 \eta_2^* + \alpha_2^* \eta_1 \end{aligned} \quad (1.34)$$

Then, the decoder finds the closest symbol  $\hat{s}_1$  and  $\hat{s}_2$  to  $\tilde{s}_1$  and  $\tilde{s}_2$  in the symbol constellation.

$$\begin{aligned} \hat{s}_1 &= \underset{s_1 \in S}{\operatorname{argmin}} d^2(\tilde{s}_1, s_1) \\ \hat{s}_2 &= \underset{s_2 \in S}{\operatorname{argmin}} d^2(\tilde{s}_2, s_2) \end{aligned} \quad (1.35)$$



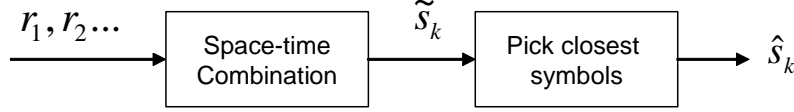
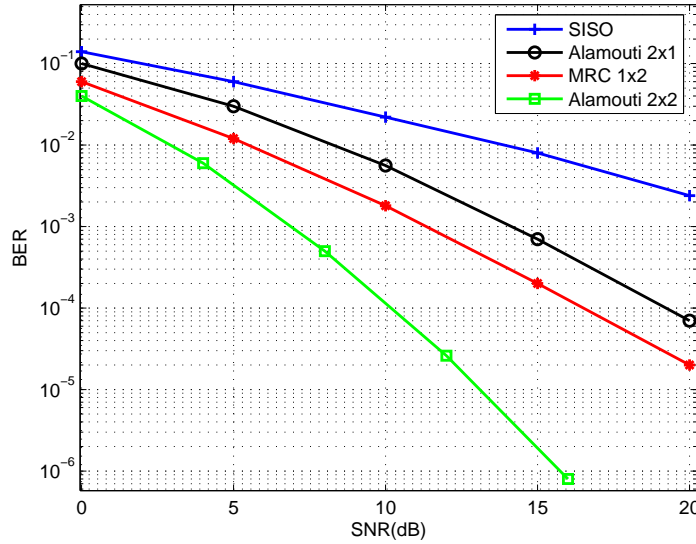


Figure 1.11: STBC decoding scheme

We note that the decoding complexity of the code increases linearly, instead of exponentially, with the number of transmit antennas.

Alamouti scheme is a simple transmit diversity technique which improves the SNR at the receiver by using a simple signal coding algorithm at the transmitter and a linear complexity ML detection at the receiver. The diversity gain obtained is equal to the MRC technique with one antenna at the transmitter and two antennas at the receiver.

The performance of the Alamouti ( $2 \times 2$ ) scheme, Alamouti ( $2 \times 1$ ) scheme, MRC ( $1 \times 2$ ) scheme and no diversity ( $1 \times 1$ ) scheme using QPSK modulation (with Gray coding) over a slow independent Rayleigh fading channels is shown in Fig.1.12. The channel state information (CSI) is considered to be known at the receiver.

Figure 1.12: BER performance of the QPSK Alamouti Codes,  $N = 2$ ,  $M = 1, 2$ .

The simulation results show that the Alamouti ( $2 \times 1$ ) scheme achieves the same diversity as the ( $1 \times 2$ ) scheme using MRC. However, the performance of Alamouti scheme is  $3dB$  worse than MRC due to the fact that the transmit power from each antenna in the Alamouti scheme is half of that of the single antenna of the MRC. The Alamouti ( $2 \times 2$ )

scheme with two receive antennas shows a better performance than other schemes because the order of diversity is  $N \times M = 4$ .

### Orthogonal Space-Time Block Codes (OSTBC)

Orthogonal STBCs are an important subclass of linear STBCs that guarantee that the ML detection of different symbols is decoupled and that at the same time, the transmission scheme achieves a diversity order equal to  $N \times M$ . The main disadvantage of OSTBCs is the fact that for more than two transmit antennas and complex-valued signal modulation, full diversity OSTBCs only exist for code rates smaller than one.

**Definition of Orthogonal Design:** An OSTBC is a linear space-time block code  $\mathbf{C}$  that has the following unitary property:

$$\mathbf{C}^H \mathbf{C} = \sum_{n=1}^N |s_n|^2 \mathbf{I}_N \quad (1.36)$$

The  $i^{th}$  column of  $\mathbf{C}$  corresponds to the symbols transmitted from the  $i^{th}$  transmit antenna, while the  $j^{th}$  row of  $\mathbf{C}$  represents the symbols transmitted simultaneously through  $N$  transmit antennas at time  $j$ . According to Eq. 1.36, the columns of the transmission matrix  $\mathbf{C}$  are orthogonal to each other. It means that, in each block, the signal sequences from any two transmit antennas are orthogonal. The orthogonality enables us to achieve full transmit diversity and allows a simple ML decoding at the receiver.

**Example of Real Orthogonal OSTBC:** For real signal modulation, there exist OSTBCs that can achieve a full rate for any given number  $N$  of transmit antennas. For example, the code matrices  $\mathbf{C}_4$  and  $\mathbf{C}_8$  for four and eight transmit antennas are

$$\begin{aligned} \mathbf{C}_4 &= \begin{bmatrix} s_1 & s_2 & s_3 & s_4 \\ -s_2 & s_1 & -s_4 & s_3 \\ -s_3 & s_4 & s_1 & -s_2 \\ -s_4 & -s_3 & s_2 & s_1 \end{bmatrix} \\ \mathbf{C}_8 &= \begin{bmatrix} s_1 & s_2 & s_3 & s_4 & s_5 & s_6 & s_7 & s_8 \\ -s_2 & s_1 & -s_4 & s_3 & -s_6 & s_5 & -s_8 & -s_7 \\ -s_3 & s_4 & s_1 & -s_2 & -s_7 & s_8 & -s_5 & -s_6 \\ -s_4 & -s_3 & s_2 & s_1 & s_8 & -s_7 & s_6 & -s_5 \\ -s_5 & s_6 & -s_7 & -s_8 & s_1 & -s_2 & s_3 & s_4 \\ -s_6 & -s_5 & -s_8 & s_7 & s_2 & s_1 & -s_4 & -s_3 \\ -s_7 & -s_8 & s_5 & -s_6 & -s_3 & s_4 & s_1 & s_2 \\ -s_8 & s_7 & s_6 & s_5 & -s_4 & -s_3 & -s_2 & s_1 \end{bmatrix} \end{aligned} \quad (1.37)$$

For a number of transmit antennas less than four or eight, the coding matrix can be obtained by removing the last column of the matrix  $\mathbf{C}_4$  and  $\mathbf{C}_8$ . For example, the coding matrix for three transmit antennas is

$$\mathbf{C}_3 = \begin{bmatrix} s_1 & s_2 & s_3 \\ -s_2 & s_1 & -s_4 \\ -s_3 & s_4 & s_1 \\ -s_4 & -s_3 & s_2 \end{bmatrix} \quad (1.38)$$

**Example of Rate 1/2 Complex Orthogonal STBC:** For any arbitrary complex signal constellation, there are OSTBCs that can achieve a rate of 1/2 for any given number of  $N$  transmit antennas. For example, the following code matrices  $\mathbf{G}_3$  and  $\mathbf{G}_4$  with transmission rate 1/2 are OSTBCs for three and four transmit antennas [94]

$$\mathbf{G}_3 = \begin{bmatrix} s_1 & s_2 & s_3 \\ -s_2 & s_1 & -s_4 \\ -s_3 & s_4 & s_1 \\ -s_4 & -s_3 & s_2 \\ s_1^* & s_2^* & s_3^* \\ -s_2^* & s_1^* & -s_4^* \\ -s_3^* & s_4^* & s_1^* \\ -s_4^* & -s_3^* & s_2^* \end{bmatrix}, \mathbf{G}_4 = \begin{bmatrix} s_1 & s_2 & s_3 & s_4 \\ -s_2 & s_1 & -s_4 & s_3 \\ -s_3 & s_4 & s_1 & -s_2 \\ -s_4 & -s_3 & s_2 & s_1 \\ s_1^* & s_2^* & s_3^* & s_4^* \\ -s_2^* & s_1^* & -s_4^* & s_3^* \\ -s_3^* & s_4^* & s_1^* & -s_2^* \\ -s_4^* & -s_3^* & s_2^* & s_1^* \end{bmatrix} \quad (1.39)$$

With the code matrix  $\mathbf{G}_3$  or  $\mathbf{G}_4$ , four complex symbols are taken at a time and transmitted via three or four transmit antennas in eight time slots. Thus, the symbol rate is 1/2.

**Example of Rate 3/4 Complex Orthogonal STBC:** For full diversity OSTBC designs with complex signal constellation, the maximum data rate 3/4 can be achieved by using respectively the following code matrices  $\mathbf{H}_3$  and  $\mathbf{H}_4$ , proposed by Tarokh in [94]

$$\mathbf{H}_3 = \begin{bmatrix} s_1 & s_2 & \frac{s_3}{\sqrt{2}} \\ -s_2^* & s_1^* & \frac{s_3^*}{\sqrt{2}} \\ \frac{s_3}{\sqrt{2}} & \frac{s_3^*}{\sqrt{2}} & \frac{-s_1 - s_1^* + s_2 - s_2^*}{2} \\ \frac{s_3}{\sqrt{2}} & -\frac{s_3^*}{\sqrt{2}} & \frac{s_2 + s_2^* + s_1 - s_1^*}{2} \end{bmatrix}$$

$$\mathbf{H}_4 = \begin{bmatrix} s_1 & s_2 & \frac{s_3}{\sqrt{2}} & \frac{s_3}{\sqrt{2}} \\ -s_2^* & s_1^* & \frac{s_3^*}{\sqrt{2}} & -\frac{s_3^*}{\sqrt{2}} \\ \frac{s_3}{\sqrt{2}} & \frac{s_3^*}{\sqrt{2}} & \frac{-s_1 - s_1^* + s_2 - s_2^*}{2} & \frac{-s_2 - s_2^* + s_1 - s_1^*}{2} \\ \frac{s_3}{\sqrt{2}} & -\frac{s_3^*}{\sqrt{2}} & \frac{s_2 + s_2^* + s_1 - s_1^*}{2} & -\frac{s_1 + s_1^* + s_2 - s_2^*}{2} \end{bmatrix} \quad (1.40)$$

### Linear Signal Combining and Maximum Likelihood Decoding of the OSTBC

Similarly to the Alamouti STBC, the problem of minimizing the decision metric of OSTBC can be expanded to independent decision and the linear complexity combination for each transmit symbol. For the case of OSTBC  $\mathbf{G}_4$ , assuming that all signals in constellation are equi-probable and that the channel coefficients can be perfectly estimated at the receiver, the decoding algorithm is the following.

At first, the receiver combines the received signals  $r_1, r_2, r_3$  and  $r_4$  and the channel coefficients as follows

$$\begin{aligned}
\tilde{s}_1 &= \sum_{m=1}^M (r_{1,m}\alpha_{1,m}^* + r_{2,m}\alpha_{2,m}^* + r_{3,m}\alpha_{3,m}^* + r_{4,m}\alpha_{4,m}^* \\
&\quad + r_{5,m}^*\alpha_{1,m} + r_{6,m}^*\alpha_{2,m} + r_{7,m}^*\alpha_{3,m} + r_{8,m}^*\alpha_{4,m}) \\
\tilde{s}_2 &= \sum_{m=1}^M (r_{1,m}\alpha_{2,m}^* - r_{2,m}\alpha_{1,m}^* - r_{3,m}\alpha_{4,m}^* + r_{4,m}\alpha_{3,m}^* \\
&\quad + r_{5,m}^*\alpha_{2,m} - r_{6,m}^*\alpha_{1,m} - r_{7,m}^*\alpha_{4,m} + r_{8,m}^*\alpha_{3,m}) \\
\tilde{s}_3 &= \sum_{m=1}^M (r_{1,m}\alpha_{3,m}^* + r_{2,m}\alpha_{4,m}^* - r_{3,m}\alpha_{1,m}^* - r_{4,m}\alpha_{2,m}^* \\
&\quad + r_{5,m}^*\alpha_{3,m} + r_{6,m}^*\alpha_{4,m} - r_{7,m}^*\alpha_{1,m} - r_{8,m}^*\alpha_{2,m}) \\
\tilde{s}_4 &= \sum_{m=1}^M (r_{1,m}\alpha_{4,m}^* - r_{2,m}\alpha_{3,m}^* + r_{3,m}\alpha_{2,m}^* - r_{4,m}\alpha_{1,m}^* \\
&\quad + r_{5,m}^*\alpha_{4,m} - r_{6,m}^*\alpha_{3,m} + r_{7,m}^*\alpha_{2,m} - r_{8,m}^*\alpha_{1,m})
\end{aligned} \tag{1.41}$$

Then, these estimated signal values are sent to ML detectors to find the closest symbol  $\hat{s}_1, \hat{s}_2, \hat{s}_3$  and  $\hat{s}_4$  to  $\tilde{s}_1, \tilde{s}_2, \tilde{s}_3$  and  $\tilde{s}_4$  in the constellation. We note that this combination and ML decoding can be separated into four independent decoding for  $\hat{s}_1, \hat{s}_2, \hat{s}_3$  and  $\hat{s}_4$ , leading to a linear complexity algorithm.

Fig.1.13 shows the BER simulation result for the transmission of 3 bits/channel use using one (un-coded SISO), two, three and four transmit antennas. The 8-PSK modulation was used for the case of one and two transmit antennas with Alamouti code and the 16-QAM modulation was used for the case of three and four transmit antennas with the rate 3/4 OSTBCs  $\mathbf{H}_3$  and  $\mathbf{H}_4$  from Eq. 1.40. It can be noticed that, at the BER of  $10^{-3}$ , the rate 3/4 16-QAM code  $\mathbf{H}_4$  provides about 8dB gain over an uncoded 8-PSK data transmission. At  $BER = 10^{-4}$ , the code  $\mathbf{H}_4$  for four transmit antennas provides about 5dB gain over the Alamouti code.

Fig.1.14 shows the BER simulation result for the transmission of 2 bits/channel use using one (un-coded SISO), two, three and four transmit antennas. The 4-PSK modulation was used for the case of one and two transmit antennas with Alamouti code and the 16-QAM modulation was used for the case of three and four transmit antennas with the rate 1/2 OSTBCs  $\mathbf{G}_3$  and  $\mathbf{G}_4$  from Eq. 1.39. It can be observed that, at the BER of  $10^{-3}$ ,

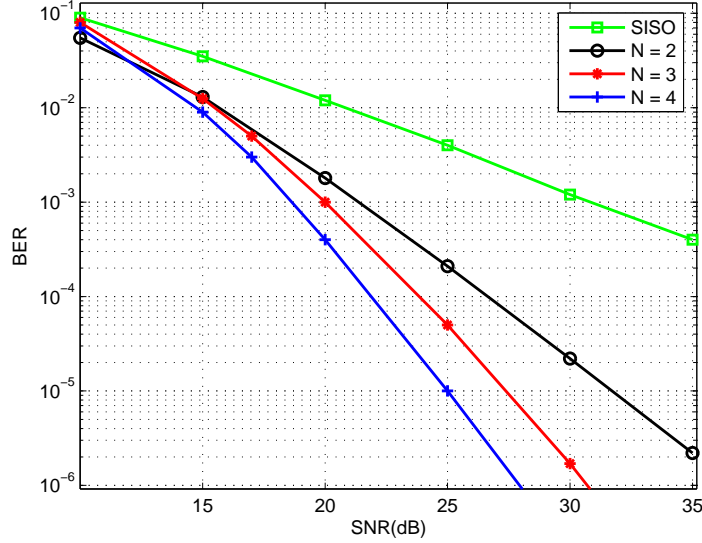


Figure 1.13: Bit error performance for OSTBC of 3 bits/channel use on  $N \times 1$  channels with i.i.d Rayleigh fading.

the rate 1/2 16-QAM code  $\mathbf{G}_4$  provides about 8 dB gain over an uncoded 4-PSK data transmission. For BER smaller than  $10^{-3}$ , the code  $\mathbf{G}_4$  is not as good as the Alamouti code. At a BER of  $10^{-4}$ , the code  $\mathbf{G}_4$  for four transmit antennas provides about 2 dB gain over the Alamouti code.

From these simulation results, we can see that increasing the number of transmit antennas provides a significant performance gain. One of the most important advantages of OSTBCs is that the complexity increases linearly with the number of transmit antennas due to the fact that only linear processing is required for combination and ML decoding at the receiver.

### 1.5.2 Quasi-Orthogonal Space-Time Block Codes (QSTBC)

A complex orthogonal design of STBC which provides full diversity and full transmission rate is not possible for more than two transmit antennas. The main advantages of an OSTBC design are the full diversity gain and the linear complexity ML decoding with an independent separated symbol detection. To design full-rate codes, we relax the separated decoding property and approach the codes for which decoding pairs of symbols independently is possible. A new family of STBC so called Quasi Orthogonal Space-Time Block Codes (QSTBC), has been introduced in [44, 77] to achieve the full rate data transmission with some trade-offs in complexity and performance.

The only full-rate full-diversity complex space-time block code using orthogonal designs

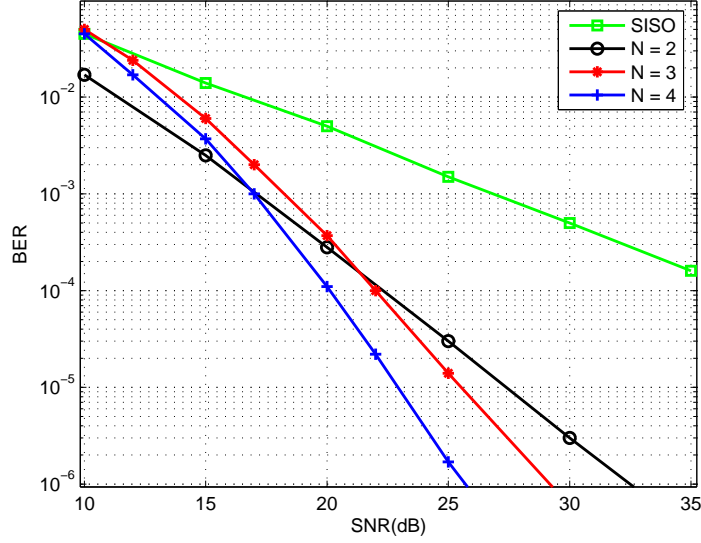


Figure 1.14: Bit error performance for OSTBC of 2 bits/channel use on  $N \times 1$  channels with i.i.d Rayleigh fading.

is the Alamouti code

$$\mathbf{G}(s_1, s_2) = \mathbf{C}_2 = \begin{bmatrix} s_1 & s_2 \\ -s_2^* & s_1^* \end{bmatrix} \quad (1.42)$$

Let us consider the following QOSTBC for four transmit antennas [44]:

$$\mathbf{G}(s_1, s_2, s_3, s_4) = \begin{bmatrix} \mathbf{G}(s_1, s_2) & \mathbf{G}(s_3, s_4) \\ -\mathbf{G}^*(s_3, s_4) & \mathbf{G}^*(s_1, s_2) \end{bmatrix} = \begin{bmatrix} s_1 & s_2 & s_3 & s_4 \\ -s_2^* & s_1^* & -s_4^* & s_3^* \\ -s_3^* & -s_4^* & s_1^* & s_2^* \\ s_4 & -s_3 & -s_2 & s_1 \end{bmatrix} \quad (1.43)$$

where a matrix  $\mathbf{G}^*$  is the complex conjugate matrix of  $\mathbf{G}$

$$\mathbf{G}^*(s_1, s_2) = \mathbf{G}(s_1^*, s_2^*) = \begin{bmatrix} s_1^* & s_2^* \\ -s_2 & s_1 \end{bmatrix} \quad (1.44)$$

The encoding for QOSTBC is very similar to the encoding of orthogonal STBC, and these codes achieve full data rate at the expense of a slightly reduced diversity. In this quasi-orthogonal code designs, the columns of the transmission matrix are divided into groups. While the columns within each group are not orthogonal to each other, different groups are orthogonal to each other. This is the reason why the name prefix of this STBC class is "quasi orthogonal". Denoting the  $i^{th}$  column of matrix  $\mathbf{G}$  by vector  $\mathbf{v}_i$ , we have

$$\langle \mathbf{v}_1, \mathbf{v}_2 \rangle = \langle \mathbf{v}_1, \mathbf{v}_3 \rangle = \langle \mathbf{v}_2, \mathbf{v}_4 \rangle = \langle \mathbf{v}_3, \mathbf{v}_4 \rangle = 0 \quad (1.45)$$

where  $\langle \mathbf{v}_i, \mathbf{v}_j \rangle$  is the inner product of vectors  $\mathbf{v}_i$  and  $\mathbf{v}_j$ . Using quasi-orthogonal design, pairs of transmitted symbols can be decoded independently at the receiver [44]. This means that the ML detection complexity for the QOSTBC is higher than for the OSTBC.

For regular symmetric constellations like M-ary PSK or M-ary QAM modulation, the minimum rank of the difference matrix  $D(\mathbf{C}_i, \mathbf{C}_j)$  is two for QOSTBC in Eq. 1.43. Therefore, the diversity of the code is two, which is smaller than the diversity four of OSTBC while the rate of this code is one.

### Rotated QOSTBC

The maximum diversity of  $4M$  for a full rate complex QOSTBC is impossible if all symbols are chosen from the same constellation. In order to provide full diversity, a different constellation for different transmitted symbols is proposed in [92], [89]. For example, the symbols  $s_3$  and  $s_4$  can be rotated before transmission. Let us denote  $s'_3$  and  $s'_4$  the rotated versions of  $s_3$  and  $s_4$ . It is possible to achieve a full-diversity QOSTBC by replacing  $(s_3, s_4)$  with  $(s'_3, s'_4)$ ; the examples of such full-diversity QOSTBC are provided in [89, 92, 45]. The resulting code is very powerful since it provides full diversity and full rate transmission.

Fig. 1.15 provides simulation results for the transmission of 2 bits/channel use with four transmit antennas and one receive antenna using orthogonal and quasi-orthogonal STBC. QPSK modulation is used for the full rate QOSTBC and the SISO system and 16-QAM for the rate 1/2 orthogonal STBC. A rotation of  $\pi/4$  is used for the case of rotated QOSTBC.

Fig. 1.15 shows that the full transmission rate QOSTB has an advantage over the rate 1/2 OSTBC for low SNRs, while OSTBC with full-diversity benefits more from increasing the SNR. Interestingly, the  $\pi/4$  rotated QOSTBC provides both full diversity and full rate and therefore performs better than OSTBC and QOSTBC at all SNR range, at the cost of a more complex signal modulation and a higher complexity ML detection at the receiver.

### 1.5.3 Space Time Trellis Codes

For OSTBC, it is impossible to design a full data rate full diversity complex coding matrix for a transmit antenna number greater than two. The goal of Space Time Trellis Codes (STTC) design is to satisfy the space-time coding design criteria: achieve full diversity at full rate transmission for any number of transmit antenna. STTCs combine modulation and trellis coding to transmit information over multiple transmit antennas and is considered as the Trellis Code Modulation (TCM) for MIMO channel.

The first example of a rate one full diversity space-time trellis code for BPSK, 4-PSK, 8-PSK, and 16-QAM constellations are designed in [97]. Like a TCM, a STTC can be represented by a trellis with pair of symbols for each trellis path.

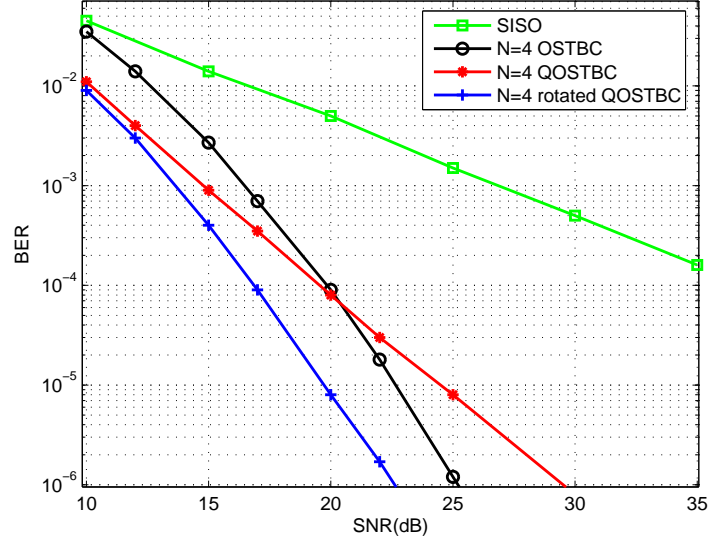


Figure 1.15: Bit error probability plotted against SNR for different space-time block codes at 2 bits/(s Hz); four transmit antennas, one receive antenna.

### Encoding STTC

Let us consider the coding trellis of the full rate 2 bits/channel use STTC with two transmit antennas represented in Fig. 1.16. The STTC can be represented by a trellis and pairs of symbols that are transmitted from the two antennas for every paths in the trellis. We use the corresponding indices of the symbols (of the 4-PSK modulation) to present the transmitted symbols for each path in the Fig. 1.16.

For a STTC that sends  $b$  bits/s/Hz,  $2^b$  branches leave every state. A set of  $2^b$  pairs of indices next to every state represents the  $2^b$  pairs of symbols for the  $2^b$  outgoing branches from top to bottom. For example, Fig. 1.16 illustrates a rate one space-time trellis code to transmit  $r = 2$  bits/s/Hz. The code uses a 4-PSK modulation,  $b = 2$ , that includes indices 0, 1, 2, 3 to represent 1,  $j$ ,  $-1$ ,  $-j$ , respectively.

Similar to a TCM encoder, the encoding always starts at state 0. Let us assume that the encoder is at state  $S_t$  at time  $t$ . Then,  $b = 2$  bits arrive at the encoder to pick one of the  $2^b = 4$  branches leaving at state  $S_t$ . The corresponding indices of the selected branch  $i_1 i_2$  are used to choose two symbols  $c_{t,1} c_{t,2}$  from the symbols constellation. These symbols are respectively sent from the two transmit antennas simultaneously. The encoder moves to state  $S_{t+1}$  which is at the right-hand side of the selected branch. At the end, similar to the encoding for a TCM, extra branches are picked to make sure that the encoder stops at state 0.

To design a good STTC, no parallel path exists in the STTC trellis and the rank



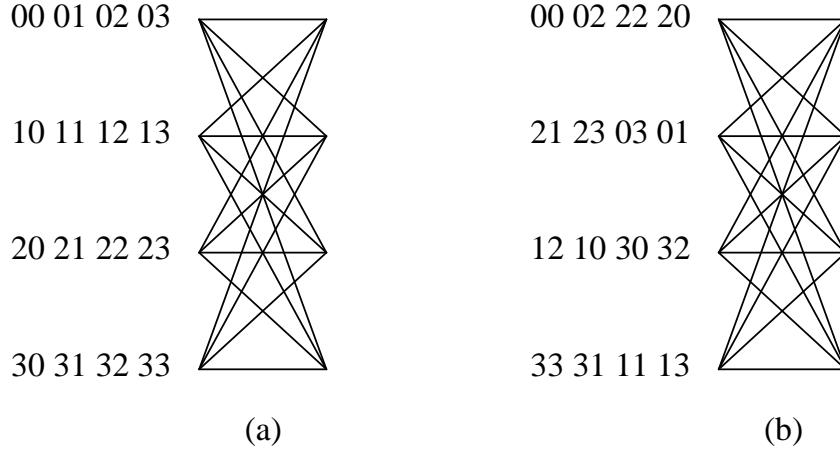


Figure 1.16: Two four state STTC, two transmit antennas, 2 bits/s/Hz using 4-PSK modulation.

criterion must guarantees a full diversity [97]. The following two design rules have been suggested to achieve full diversity for two transmit antennas:

- Transitions diverging from the same state should differ in the second symbol,
- Transitions merging to the same state should differ in the first symbol.

For a STTC with a spectral efficiency  $b$  bits/s/Hz and a diversity of  $r$ , at least  $2^{b(r-1)}$  states are required to achieve a diversity order  $r$ .

Whilst the rank criterion is important, the determinant (for low number of antennas) or trace (for large number of antennas) must also be taken into account as they determine the coding gain. On a figure representing the FER versus the SNR, both are equally important in the region of interest since the rank gives the steepness and the coding gain the horizontal SNR shift.

### Decoding STTC

The maximum-likelihood decoding finds the most likely valid path in the trellis that starts from state zero and merges to state zero after  $T + Q$  time slots. Let us assume that we receive  $r_{1,m}, r_{2,m} \dots r_{T+Q,m}$  at time slots  $t = 1, 2 \dots T + Q$  at the receive antenna  $m$ . Similar to the case of TCM, the Viterbi algorithm can be used for the ML decoding of STTCs. If a branch of the trellis transmits symbols  $s_1$  and  $s_2$  from antennas one and two, respectively, the corresponding branch metric is given by

$$\sum_{m=1}^M |r_{t,m} - \alpha_{1,m}s_1 - \alpha_{2,m}s_2|^2 \quad (1.46)$$

The path metric of a valid path is the sum of all branch metrics in the path. The most likely path is the path that has the minimum path metric and the ML decoder finds the sequence of symbols that constructs this minimum metric path:

$$\min_{c_{1,1}, c_{1,2}, \dots, c_{T+Q,1}, c_{T+Q,2}} \sum_{t=1}^{T+Q} \sum_{m=1}^M |r_{t,m} - \alpha_{1,m}s_1 - \alpha_{2,m}s_2|^2. \quad (1.47)$$

### Performance of STTC

In the case of STTC, the minimum value of CGD (Coding Gain Distance) among all possible pairs of codewords is used as an indication of the performance of the code [3]. Another four-state STTC for a 4-PSK  $b = 2$  bits/(s Hz) transmission is given in Fig. 1.16b. The CGD of this code is 8 which is more than the CGD of the STTC in Fig. 1.16a

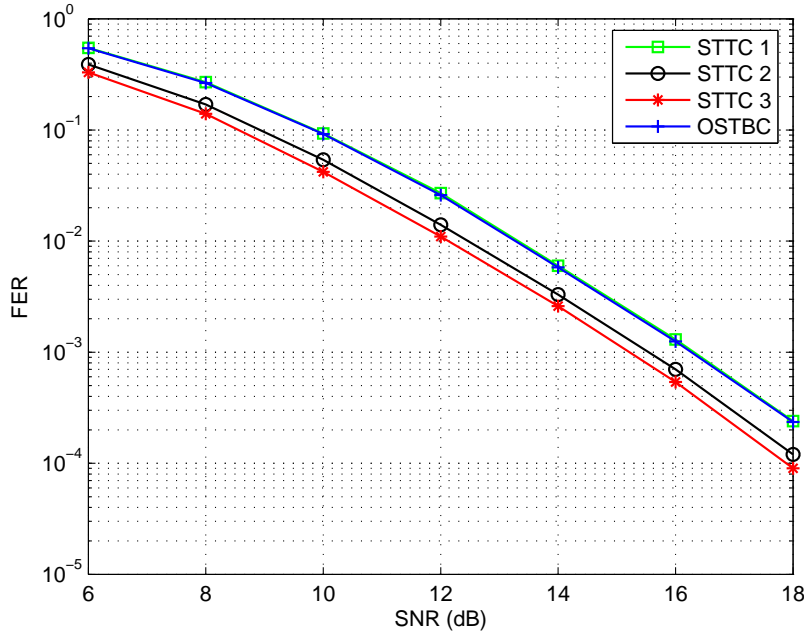


Figure 1.17: A four-state STTC; 2 bits/(s Hz) using two receive antennas

Fig. 1.17 shows the simulation results for a 4-PSK 2 bits/s/Hz transmission using two receive antennas for the full diversity STTC in Fig. 1.16a (legend *STTC1*) and Fig. 1.16b (legend *STTC3*). The STTC in Fig. 1.16b outperforms the STTC in Fig. 1.16a by about 1 dB. As argued in [3], CGD is a good measure for a large number of receive antennas. For one receive antenna, these STTCs provide almost identical results despite the difference between their minimum CGDs [97].

It can be seen in the Fig. 1.17 that the performance of the well designed STTC (of Fig. 1.16b) is better than the OSTBC performance due to the coding gain of STTC.

## 1.6 Spatial Multiplexing

The main objective of space-time codes is to achieve the maximum possible diversity; space-time codes provide a diversity gain equal to the product of the transmit and receive antennas numbers  $N \times M$ . However, the data rate of space-time codes is equal or less than that of SISO channel for any number of transmit antennas. The increase of MIMO channel capacity, compared to SISO channels, can only be achieved by using more bits/symbols modulation.

Another approach to achieve the highest possible throughput is Spatial Multiplexing (SM) [27, 104, 28]. Instead of using the multiple antennas to achieve the maximum possible diversity gain, SM uses multiple antennas to increase the transmission rate. The principle of spatial multiplexing is to demultiplex the data stream into  $N$  separate sub-streams, using a serial-to-parallel converter, and then each sub-stream is transmitted from an independent antenna. As a result, the throughput is  $N$  symbols/channel use for a MIMO channel with  $N$  transmit antennas.

This  $N$ -fold increase in throughput generally comes at the cost of a lower diversity gain compared to space-time coding and a higher complexity in the decoding technique. Therefore, spatial multiplexing is a better choice for high data rate systems operating at relatively high SNR, while space-time coding is more appropriate for non high data rate transmission at low SNR.

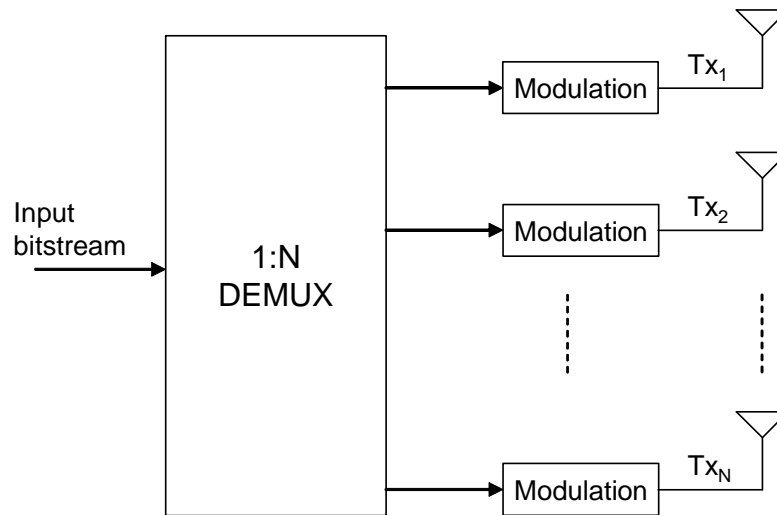


Figure 1.18: Spatial Multiplexing Transmission Technique

### Spatial Multiplexing Encoding

A simple example of spatial multiplexing is shown in Fig. 1.18. A serial to parallel demultiplexer generates  $N$  separate sub-streams from the input stream. Each sub-stream is processed separately and is transmitted from a different antenna. Denoting the transmitted  $1 \times N$  vector by  $\mathbf{c}$ , the  $1 \times M$  output vector  $\mathbf{r}$  is

$$\mathbf{r} = \mathbf{c}\mathbf{H} + \boldsymbol{\eta} \quad (1.48)$$

where  $\mathbf{H}$  is the  $N \times M$  channel matrix and  $\boldsymbol{\eta}$  is the  $1 \times M$  noise matrix. The maximum likelihood decoding finds the codeword  $\mathbf{c}$  that minimizes the Frobenius norm

$$\|\mathbf{r} - \mathbf{c}\mathbf{H}\|_F \quad (1.49)$$

Using a full search to find the optimal codeword is computationally non trivial. If the modulation uses a constellation with  $2^b$  points to transmit  $b$  bits/symbol, the number of possibilities of  $\mathbf{c}$  is  $2^{bN}$ . For four transmit antennas using 16-QAM modulation ( $b = 4$ ), there are 65536 possibilities of  $\mathbf{c}$ , which is impractical to compute in most cases. When a simpler ML decoding does not exist, sub-optimal decoding methods have been proposed to reduce the complexity of the receiver.

### Sphere Decoding Technique

The principle of sphere decoding technique is to limit the number of searching codewords by considering only the codewords that are within a sphere centered by the received signal vector [99]. So that, the overall complexity of the sphere decoding is lower than that of the full search in all codewords space.

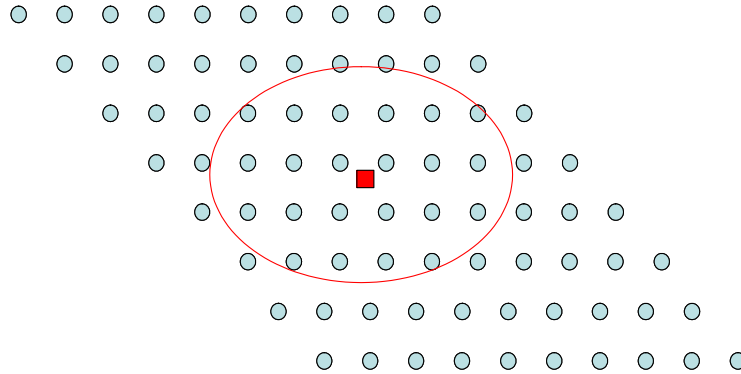


Figure 1.19: Sphere Decoding Technique.

This concept is depicted in Fig.1.19, in which the received signal vector and the possible codewords are represented by a small square and circle points. The distribution of the transmitted signal and the received signal depends on the instantaneous power of the noise and interferences. Therefore, the search region in codewords space depends on the received SNR and it is more likely to have the most possible codeword (in a search region) close to the received signal. The idea of limiting the search region and a survey of closest point search methods is presented in [1].

### Equalization Decoding Techniques

One general approach with a complexity lower than that of ML decoding is to use equalization techniques to separate different symbols. In fact, this class of techniques first tries to find the best signal that represents each of the symbols and then decodes the symbol using the detected signal.

In detecting the best representation of each symbol, the effects of other symbols are considered as interference. Therefore, the equalization ideas to remove inter-symbol interference (ISI) can be used. The two popular equalization techniques are the zero-forcing (ZF) equalizer and the minimum mean-squared error (MMSE) equalizer.

#### Zero-forcing

A zero-forcing equalizer uses an inverse filter to compensate for the channel response matrix. If possible, this results in the removal of the interference from all other symbols. Let us assume the case that  $\mathbf{H}$  is a full rank square matrix ( $N = M$ ). In this case the inverse of the channel matrix  $\mathbf{H}$  exists, multiplying both sides of Eq. 1.48 by the inverse matrix  $\mathbf{H}^{-1}$ , we have

$$\mathbf{r}\mathbf{H}^{-1} = (\mathbf{c}\mathbf{H} + \boldsymbol{\eta})\mathbf{H}^{-1} = \mathbf{c} + \boldsymbol{\eta}\mathbf{H}^{-1} \quad (1.50)$$

As it can be seen from Eq. 1.50, the symbols are separated from each other. The noise is still Gaussian and the  $n^{th}$  symbol can be decoded by finding the closest constellation point to the  $n^{th}$  element of  $\mathbf{r}\mathbf{H}^{-1}$ .

However, the power of the effective noise  $\boldsymbol{\eta}\mathbf{H}^{-1}$  may be more than the power of the original noise  $\boldsymbol{\eta}$ . Zero forcing is a linear equalization method that does not consider the effects of noise. In fact, the noise may be enhanced in the process of eliminating the interference.

In the general case, if the number of transmit and receive antennas are not the same, we may multiply by the Moore-Penrose generalized inverse, pseudo-inverse  $\mathbf{H}^+$ , of channel matrix  $\mathbf{H}$  to achieve a similar zero-forcing result [42]. Note that if  $\mathbf{H}$  is a square and

non-singular matrix, we have  $\mathbf{H}^+ = \mathbf{H}^{-1}$ . Also, if  $M > N$  and  $\mathbf{H}$  is full rank, we have  $\mathbf{H}^+ = \mathbf{H}^H(\mathbf{H}\mathbf{H}^H)^{-1}$ . Therefore, multiplying (1.48) by  $\mathbf{H}^+$  results in

$$\mathbf{r}\mathbf{H}^+ = \mathbf{c}\mathbf{H}\mathbf{H}^H(\mathbf{H}\mathbf{H}^H)^{-1} + \boldsymbol{\eta}\mathbf{H}^+ = \mathbf{c} + \boldsymbol{\eta}\mathbf{H}^+ \quad (1.51)$$

Again, a separate decoding of the symbols is possible by finding the closest constellation point to the  $n^{th}$  element of  $\mathbf{r}\mathbf{H}^+$ .

### Minimum mean-squared error

The ZF equalization does not consider the effects of the equalization in enhancing the noise. To address this problem, a linear MMSE equalizer is proposed to minimize the total effective noise. MMSE equalizer multiplies Eq. 1.48 by a matrix such that the resulting effective noise is minimized. Using the MMSE criterion, the linear least-mean-squares estimation of  $\mathbf{c}$  is

$$\mathbf{r}\mathbf{H}^H \cdot \left( \frac{\mathbf{I}_N}{\gamma} + \mathbf{H}\mathbf{H}^H \right)^{-1} \quad (1.52)$$

where  $\gamma$  is the received SNR. Unlike the ZF method, the received vector is multiplied by a matrix that is a function of SNR. When the noise is negligible (SNR is high), that is  $\gamma \rightarrow \infty$ , the MMSE equalizer matrix  $\mathbf{H}^H[(\mathbf{I}_N/\gamma) + \mathbf{H}\mathbf{H}^H]^{-1}$  converges to  $\mathbf{H}^{-1}$  which is the detection matrix for the ZF method.

The above linear equalization methods are based on multiplying the received vector by a detection matrix and then decoding the symbols separately. Another equalization approach is decision feedback equalization (DFE) [78].

### V-BLAST Technique

Instead of decoding all symbols jointly, one approach to a lower complexity design is the consecutive symbols decoding algorithm V-BLAST (Vertical Bell Laboratories Layered Space-Time Architecture) [104]. Symbols are detected from one by one and the optimal order is the detection from the strongest symbol to the weakest one. This technique only works if the number of receive antennas is higher than the number of transmit antennas  $M \geq N$ .

First, the algorithm decodes the strongest symbol. Then, it cancels the effects of this strongest symbol from all received signals and detects the next strongest symbol. The algorithm continues canceling the effects of detected symbols and decoding the next strongest symbol until all symbols are detected.

The algorithm includes three steps: Ordering, Interference Cancellation and Interference Nulling. The purpose of the ordering step is to decide which transmitted symbol to be detected at each stage of the decoding. The symbol with the highest SNR is the best pick

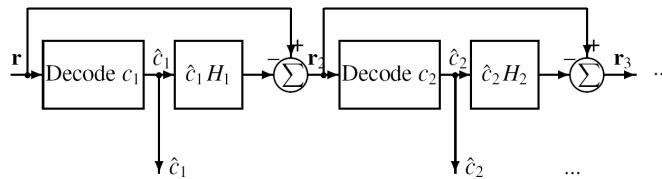


Figure 1.20: VBLAST decoder block diagram.

in this step. The goal of the interference cancellation is to remove the interference from the already detected symbols in decoding the next symbol. Finally, interference nulling finds the best estimate of a symbol from the updated equations. This step is called interference nulling (using Zero-forcing or MMSE nulling) since it can be considered as removing the interference effects of undetected symbols from the one that is being decoded.

Another BLAST technique is the D-BLAST (Diagonal Bell Laboratories Layered Space-Time Architecture) [27]. The encoder of D-BLAST is very similar to V-BLAST. The main difference is in the way that the signals are transmitted from different antennas. In V-BLAST, all signals in each layer are transmitted from the same antenna. However, in D-BLAST, the signals are shifted before transmission. The receiver of a D-BLAST architecture is similar to that of a V-BLAST system although the shifting creates a higher complexity.

### Spatial Multiplexing Performance

Fig.1.21 shows the simulation results of spatial multiplexing technique using sphere decoding, ZF equalizer, MMSE equalizer and V-BLAST decoding techniques. QPSK modulation is used for two transmit and two receive antennas to provide a 4 (bits/channel use) transmissions over independent flat Rayleigh fading channel. ZF nulling and MMSE nulling techniques have been used for two different cases of V-BLAST receiver.

As expected, linear decoding methods like ZF and MMSE perform worse than the interference cancellation and nulling techniques V-BLAST while requiring a much lower decoding complexity. The sphere decoding technique has the highest performance, but requires the most complex decoding algorithm. The MMSE outperforms ZF in both linear equalizer and iterative decoding, V-BLAST, methods at the cost of a higher complexity.

## 1.7 Conclusion

In this chapter, the performance of combination techniques for exploiting the spatial diversity are presented. Then, the capacity of MIMO channels and the three main MIMO

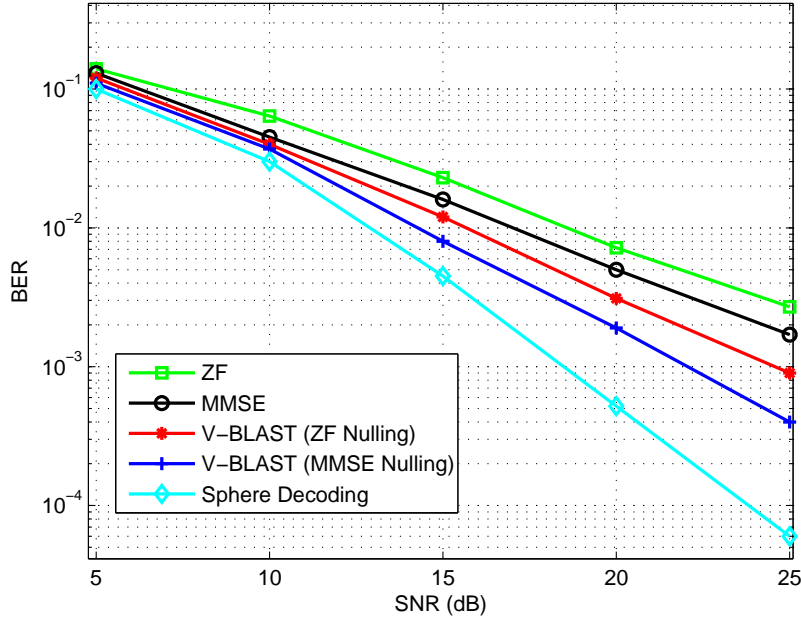


Figure 1.21: Bit error probability plotted against SNR for spatial multiplexing using QPSK, 4 bits/s/Hz; two transmit and receive antennas.

techniques: Space Time Block Code (STBC), Space Time Trellis Code (STTC) and Spatial Multiplexing (SM), are also investigated. The combination of transmit and receive diversity techniques, known as MIMO technique, not only achieves the reliability in wireless communications due to the diversity gain but also increases efficiently the channel capacity and the data transmission rate.

As the purpose of this thesis work is the energy consumption optimization in the WSN context, STBC are practically attractive, thanks to the diversity gain and the low complexity of ML decoding.

Based on the diversity gain of receive diversity and MIMO techniques, cooperative transmission techniques like cooperative relays and cooperative MIMO have been proposed for wireless distributed networks, where multiple antennas can not be integrated in a single wireless node. Cooperative techniques help to exploit the spatial and temporal diversity gain in order to reduce the fading effect and to increase the system performance. The application and the performance of cooperative techniques in wireless distributed networks are investigated in the next chapter of this thesis.



## Chapter 2

# Cooperative techniques in Wireless Sensor Networks

### 2.1 Introduction

In Wireless Sensor Networks (WSN), energy consumption is the most important constraint since each node is powered by a small battery that may not be rechargeable or renewable for long term. In various WSN applications, the network is considered to be alive while all nodes (or some important nodes) still have some energy. Therefore, maximizing the minimum node lifetime by reducing energy consumption are an important design consideration for such networks.

Since all layers of the protocol stack contribute to the energy consumption in WSN transmission applications, energy minimization requires an energy constrained design across all system layers from application to physical layers. The energy consumption in physical layer plays an important role in which a transmission energy consumption is the dominant part for medium and long range transmission. In this thesis, the energy consumption of circuit and data transmission is focused and some cooperative strategies are investigated in order to increase the energy efficiency in WSN.

Cooperative techniques help to reduce the transmission energy consumption by different manners. Three types of cooperation strategies are investigated in this thesis: multi-hop, relaying and cooperative MIMO transmissions.

- In wireless transmission, the received power typically falls off as the  $K^{th}$  power of distance, with the path loss factor  $2 < K < 6$ . Therefore, multi-hop transmission technique can conserve the transmission energy by dividing the transmission channel into multiple transmissions.
- The temporal and spatial diversity of multiple antennas are very attractive due to their simplicity and their performance for wireless transmission over fading channel.

In a wireless distributed network, when multiple antennas can not be integrated in a small wireless node, cooperative relay technique can exploit the spatial and temporal diversity gain in order to reduce the path loss effect in wireless channels. The result is that the system performance is improved or less transmission energy consumption is needed. Cooperative relaying technique is also known as user cooperation diversity, virtual antenna diversity or coded cooperation.

- The performance of space-time diversity Multi-Input Multi-Output (MIMO) have been known for radio transmission over fading channel. Space-time coding MIMO systems need less transmission energy than SISO system for the same error rate requirement. This transmission energy efficiency is particularly useful for Wireless Sensor Networks (WSN) where the energy consumption is the most important constraint.

Since the direct application of the multi-antenna technique to distributed WSN is impractical, wireless sensor nodes can cooperate in transmission and reception in order to deploy a space-time coding transmission. This cooperation technique is referred to as the cooperative MIMO transmission which allows space-time diversity gain to reducing the transmission energy consumption in WSN.

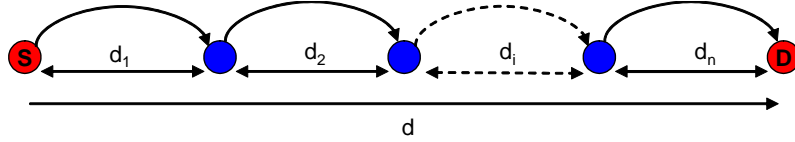
In this chapter, the traditional multi-hop transmission and the efficient relay techniques are firstly represented in Section 2.2 and Section 2.3. Then, the cooperative MIMO transmission scheme is presented in Section 2.4. In section 2.5, the CAPTIV, an intelligent transport system project in Bretagne, France is presented. Some cooperative strategies for energy constrained data transmission in CAPTIV are also proposed at the end of this chapter.

## 2.2 Multi-Hop Technique

In a multi-hop transmission network, one node decodes the received signal from the previous hop and forwards it to the next hop. An example of a wireless multiple hop model is shown in Fig. 2.1. Instead of transmitting over a long distance from source node S to destination node D, the path is divided into several single transmissions, this is the multi-hop technique.

Let us consider the multi-hop network with  $n$  hops as shown in Fig.2.1;  $d_i$  is the distance between two hops and the wireless link between a source and a destination consists of  $n$  hops formed by  $n - 1$  collinear radio nodes willing to cooperate. The distance between the source node S and the the destination node D is

$$d = \sum_{i=1}^n d_i \quad (2.1)$$


 Figure 2.1: Multi-hop transmission model with  $n$  hops.

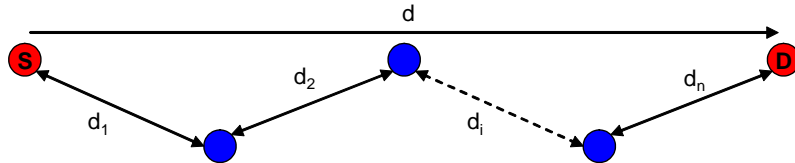
where  $d_i$  is the distance between two nodes  $i$  and  $i + 1$ . The path loss between two wireless nodes with distance  $d_i$  is given by

$$P(d_i) = P(d_0) \left( \frac{d_i}{d_0} \right)^K \quad (2.2)$$

where  $K$  is the path loss exponent of the wireless channel,  $P(d_i)$  is the transmission power at distance  $d_i$  and  $P(d_0)$  is the reference power at distance  $d_0$ . The needed transmission power  $P(d_i)$  increases quickly with the power factor of the path loss  $K$ . If the transmission channel is divided into multi-hop transmission, the total transmission power consumption is the sum of each single-hop transmission, and increases linearly with the transmission distance. Multi-hopp technique allows us to save some transmit power, the transmission power consumption gain  $G_p$  is

$$G_p = \frac{P(d)}{\sum_{i=1}^n P(d_i)} = \frac{(\sum_{i=1}^n d_i)^K}{\sum_{i=1}^n d_i^K}. \quad (2.3)$$

Equation 2.3 shows that increasing the number of hops increases the transmit power savings for wireless transmission. However, in some sensor networks where the nodes are densely distributed, and the average distance between nodes is usually below  $10m$ , the circuit energy consumption along the signal path becomes comparable to or even dominates the transmission energy in the total energy consumption. Thus, in order to find efficient transmission schemes, the overall energy consumption including both transmission and circuit energy consumption needs to be considered.


 Figure 2.2: Multi-hop transmission model with  $n$  hops.

If the multi-hop transmission scheme is in the zigzag form like in Fig.2.2 where  $d <$

$\sum d_i$ , the transmission power consumption gain is

$$G = \frac{P(d)}{\sum_{i=1}^n P(d_i)} = \frac{(d)^K}{\sum_{i=1}^n d_i^K} \quad (2.4)$$

which is smaller than the power gain in Eq. 2.3. An important drawback of the multi-hop technique is the transmission delay through multi-hop cooperation nodes.

Multi-hop transmission can save significantly the energy consumption only when the transmission energy is considered. However, when the circuit energy is included, single-hop transmissions may be more efficient than multi-hop transmission scheme for a short range communication where circuit consumption is comparable to transmission consumption. This will be discussed in chapter 3.

## 2.3 Relay Cooperation Techniques

Relaying between radio nodes has been observed to reduce the aggregate path loss and to improve performance in wireless channels. Relays can also be used to assist communication between two hops in a multi-hop wireless route. The relay channel formulation and protocols have been recently studied in various works in which the gains achievable with cooperation are observed to be promising [14], [85], [86] and [57]. In fact, these papers can be considered as a reborn, since Amplify and Forward (A-F) and Decode and Forward (D-F) relaying protocols have been known in parts by the satellite community for nearly five decades [54, 39, 12, 100, 9] and by the radio community for almost a century already [41, 19].

In relay cooperative networks, the received signal comes from different independent fading channels, so that the probability of deep fading is minimized. This diversity gain helps to decrease the error rate, or to decrease the transmission power for the same required error rate. The traditional model for relay diversity technique with one relay node shown in Fig. 2.3, consists in a source node S, a destination node D and a relay node R.

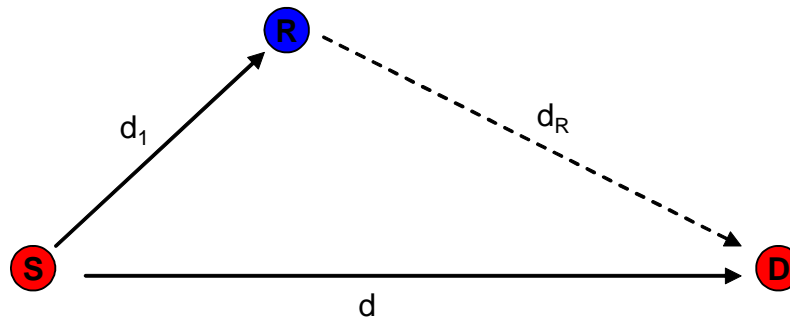


Figure 2.3: Three terminal relay diversity scheme.

The relay transmission from S to D can be performed by a two-time slot transmission scheme explained below:

### Time slot 1

In the first time slot, signals are transmitted by the source S to the destination node D and the relay node R at the same time. Let  $c$  be the transmit signal of the source, the received signal at the destination node is

$$r_1 = \alpha_{sd}c + \eta_1 \quad (2.5)$$

and the received signal at the relay node is

$$r_R = K_R \alpha_{sr}c + \eta_R \quad (2.6)$$

where  $\alpha_{sd}, \alpha_{sr}$  are the channel gains from the source node to the destination node and the relay node respectively,  $\eta_1$  and  $\eta_R$  are noise vectors having complex Gaussian distribution with zero mean and unit variance (0.5 per dimension) at the destination and relay nodes.  $K_R$  is the power gain factor of the signal at the relay node because the distance between source and relay nodes is smaller than the distance between source and destination nodes,

$$K_R = \left(\frac{d}{d_1}\right)^K. \quad (2.7)$$

### Time slot 2

In the second time slot, the relay node transmits the vector  $c'$  based on the received vector  $r_R$ . The received signal at the destination node is

$$r_2 = \alpha_{rd}c' + \eta_2 \quad (2.8)$$

At node D, the receiver combines the signals  $r_1, r_2$  by using a diversity combination technique (MRC, EGC...) before symbol detection.

In other relay schemes, the source node can also re-send the frame in the second time slot. The source to destination channel and the relay to destination channel must be orthogonal to each other to avoid interferences (e.g. a different frequency channel for a source to destination re-transmission), unless a multi-user detection can be performed.

Relay techniques can be classified according to their forwarding strategy, there are three main methods for the relay node to transmit the received frame to the destination node: Amplify and Forward, Decode and Forward, and Re-encode and Forward.

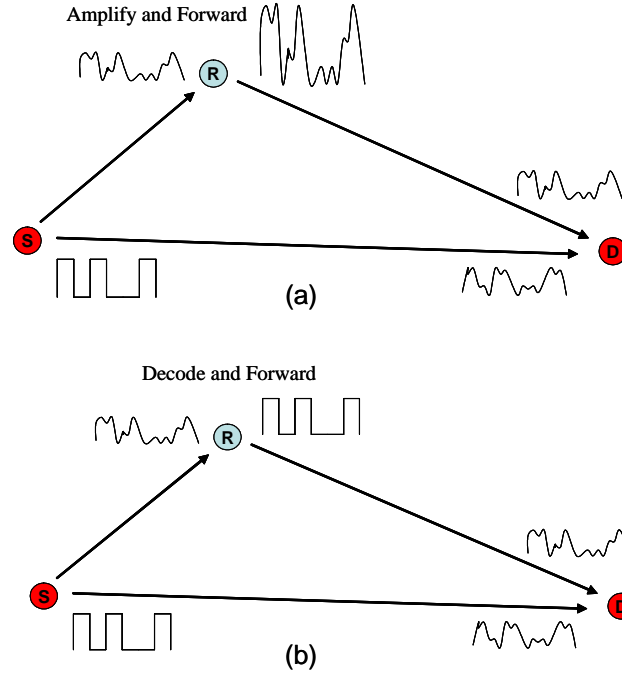


Figure 2.4: Amplify-and-Forward (a) and Decode-and-Forward (b) techniques in relay networks

### 2.3.1 Amplify and Forward

The most simple relay technique is the Amplify-and-Forward (A-F) method which was analyzed in [57]. It has been shown that this method achieves a diversity order of two, which is the best possible outcome at high SNR.

In amplify and forward technique, after receiving a noisy version of the signal transmitted from source node S, the relay node R just amplifies and then retransmits this noisy version to the destination node D (Fig. 2.4.a).

With the normalized transmit signal at the relay node  $c' = r_R/K_R = \alpha_{sr}c + (\eta_R/K_R)$ , the received signal at the destination node D is

$$r_2 = \alpha_{rd}c' + \eta_2 = \alpha_{rd}\alpha_{sr}c + \alpha_{rd}\frac{\eta_R}{K_R} + \eta_2. \quad (2.9)$$

The destination node combines the two received signals sent from the source and relay nodes by using the maximal ratio combining (MRC) technique, and makes a final decision on the transmitted bits. Although noise is amplified by this Amplify-and-Forward relay cooperation, the destination node receives two independently faded versions of the transmit signal. Therefore, it can exploit the diversity gain to make a better decision on the final combined information. The estimated information can be combined by using MRC method as follows:

$$\tilde{c} = r_1\alpha_{sd}^* + r_2(\alpha_{rd}\alpha_{sr})^* = (||\alpha_{sd}||^2 + ||\alpha_{rd}\alpha_{sr}||^2)c + \eta_1\alpha_{sd}^* + \eta_2\alpha_{rd}^*\alpha_{sr}^* + ||\alpha_{rd}||^2\alpha_{sr}^* \frac{\eta_R}{K_R} \quad (2.10)$$

It can be intuitively seen that, if the signals are maximal ratio combined, then the performance benefit will be totally dependent on the source-relay channel quality. On this basis, a weighted combining scheme has been proposed in [58], [86].

### 2.3.2 Decode and Forward

Beside the Amplify-and-Forward technique, another basic relay technique is Decode-and-Forward (D-F). An example of the Decode-and-Forward relaying scheme can be found in [59]. This method is perhaps closest to the idea of an information relay.

In the Decode-and-Forward technique, instead of just amplifying the analog received signal, the relay node R attempts to detect the received signal to bits and then retransmits the detected bits to the destination node like in Fig 2.4.b. If the signal at the relay node is decoded perfectly, i.e.  $c' = c$ , , the received signal at the destination node is

$$r_2 = \alpha_{rd}c' + \eta_2 = \alpha_{rd}c + \eta_2. \quad (2.11)$$

Then, the estimated signal can be combined by using MRC as:

$$\tilde{c} = r_1\alpha_{sd}^* + r_2\alpha_{rd}^* = (||\alpha_{sd}||^2 + ||\alpha_{rd}||^2)c + \eta_1\alpha_{sd}^* + \eta_2\alpha_{rd}^*. \quad (2.12)$$

By using this Decode-and-Forward technique, relay node can eliminate the noise amplification drawback of the Amplify-and-Forward technique. If the signal at the relay node is decoded perfectly, the total performance at the destination node is better. However, if the detection at the relay node is not reliable, it will affect the performance of the MRC combination at the destination node D. The final performance is limited by the error occurred in the source-relay channel and will be less than the Amplify-and-Forward technique.

The choice between these two relay techniques depends on the quality of source-relay channel. In general case, if the relay node is near to the source node, the Decode-and-Forward technique is selected, and if the relay node is far from the source node, the Amplify-and-Forward technique is better.

In Fig. 2.5, the performance comparison between the traditional SISO transmission and the relay techniques is shown. Non-coded QPSK transmission is used over a Rayleigh fading channel. It is obvious that the two relay techniques have a better performance or need less SNR at the receiver (i.e. less transmission energy) for the same error rate requirement than the SISO technique.

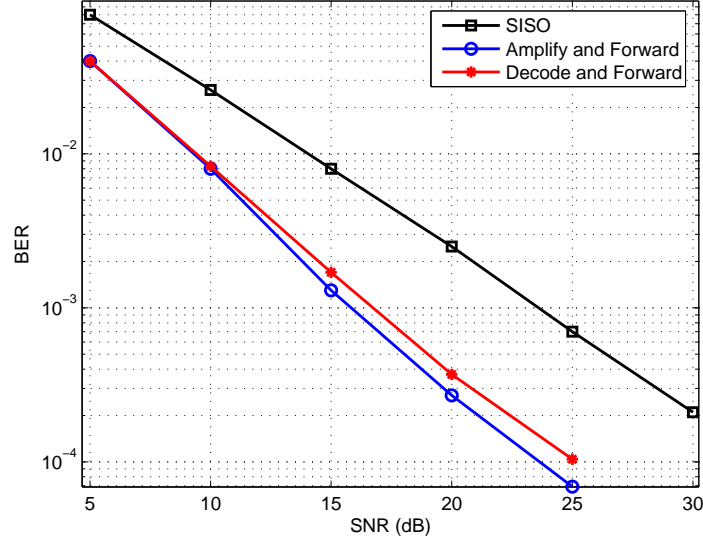


Figure 2.5: Performance of Amplify-and-Forward and Decode-and-Forward relay techniques

### 2.3.3 Re-encode and Forward

For the Amplify-and-Forward and Decode-and-Forward, the MRC combination is used at the destination node to exploit the diversity gain. Another more complex relay technique is the Re-encode-and-Forward (or Code Cooperation Relay) which allows diversity and coding gains at the same time.

Re-encode and Forward (R-F) [43] is a method that integrates a relay cooperation into channel coding. The principle is that the relay node decodes the received codewords, re-encodes and sends codewords (different from source node codewords) through an independent fading path. This coded cooperation has a better performance than the two previous relay techniques, at the expense of a higher encoding and decoding complexity.

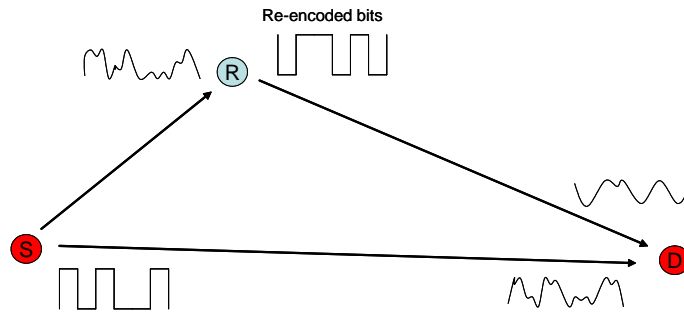


Figure 2.6: Coded cooperation or Re-encode-and-Forward technique in relay networks



In Fig. 2.6, the idea is that the relay node R decodes a received signal, re-encodes the information, and then retransmits the codeword (different from the received codeword) or just the redundancy part of the codeword to the destination node, therefore providing the coding gain to the receiver from the diversity of the original and the re-encoded signals.

For example, the original codeword of source node S is considered having  $N_1 + N_2$  bits ( $N_1$  is information bits and  $N_2$  is coded redundant bits for example). Relay node receives  $N_1 + N_2$  bits from source node S in the first time slot, decodes the message and transmits just  $N_2$  bits repartition in the second time slot to the destination node D. In some cases, the  $N_2$  bits can be processed through a bit interleaver before transmission in order to exploit the interleaver gain at the error control decoding stage at the destination node. One should note that Decode and Forward and Re-encode and Forward are now considered as equivalent since most DF protocols assume the signal is re-encoded at the relay.

## 2.4 Parallel Relay Networks

In typical one-relay-node network, the transmission range can be extended due to the diversity gain and the more transmission power from relay node. This principle can be extended to a parallel relay network where multiple relay nodes are used to receive the signal and then to retransmit respectively to the destination node D. Such an architecture is called a "parallel relay" architecture in [82], [68].

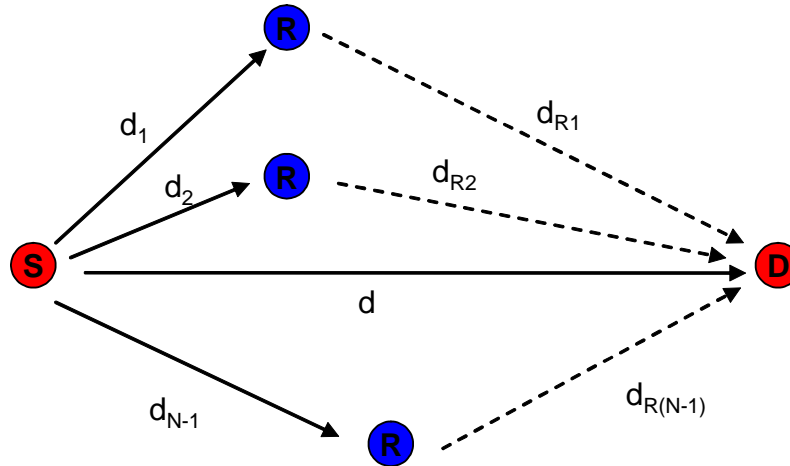


Figure 2.7: Transmission scheme in a parallel relay network with  $N - 1$  relay nodes.

Let us consider a parallel relay network composed of  $N$  transmit nodes like in Fig. 2.7. This network has one source node, and  $N - 1$  other nodes act as relays. Like in the three terminal relay diversity model, at first time slot, the source transmits a signal vector  $c$  to

the destination node and all relay nodes. The received signal at relay node  $k$  is

$$r_R^k = \alpha_{sr}^k c + \eta_R^k, k = 1 \dots N - 1. \quad (2.13)$$

where  $\alpha_{sr}^k$  is the complex fading coefficient between the source node and the  $k^{th}$  relay node,  $\eta_R^k$  is AWGN noise vector with zero mean and unit variance.

In the second to  $N$  time slots, each relay node transmits respectively its signal to the destination node D. After  $N - 1$  time slots, the destination node receives the  $N - 1$  independent fades of the transmit signal from  $(N - 1)$  relay nodes.

The multiple relay system can use the Amplify-and-Forward technique or the Decode-and-Forward technique to retransmit the received signals to the destination node. For the case where the Decode-and-Forward technique is used, the  $N - 1$  received signals from relay nodes at the destination node are

$$r_{k+1} = \alpha_{rd}^k c + \eta_{k+1}, k = 1 \dots N - 1, \quad (2.14)$$

where  $\alpha_{rd}^k$  is the complex fading coefficient between the source and the  $k^{th}$  relay node,  $\eta_{k+1}$  is the AWGN noise with zero mean and unit variance. The destination node is considered to know perfectly the channel coefficients, the MRC can be performed at the destination and the final combined signal is

$$\tilde{c} = r_1 \alpha_{sd}^* + \sum_{k=1}^{N-1} r_{k+1} (\alpha_{rd}^k)^* = (|\alpha_{sd}|^2 + \sum_{k=1}^{N-1} |\alpha_{rd}(k)|^2) c + \eta_1 \alpha_{sd}^* + \sum_{k=1}^{N-1} \eta_{k+1} (\alpha_{rd}^k)^* \quad (2.15)$$

The diversity gain increases with the number of the independent fading transmission signal, i.e. the number of relay nodes. In perfect conditions, the diversity gain of this parallel relays system with  $N$  transmission nodes is equal to the MRC technique with  $N$  reception nodes.

## 2.5 Cooperative MIMO Techniques

Relay technique is the simplest method to exploit the diversity gain to reduce the transmission error rate or reduce the transmission energy consumption. In chapter 1, the diversity gain of the MIMO technique is presented and it was explained that space-time diversity Multi-Input Multi-Output (MIMO) systems need less transmission energy than SISO system for the same Bit Error Ratio (BER) requirement. The energy efficiency of MIMO transmission is particularly useful for Wireless Sensor Network (WSN) where the energy consumption is the most important constraint.

However, the direct application of multi-antenna technique to WSN is impractical due to the limited physical size of sensor nodes which can typically support only a single

antenna. Fortunately, some individual nodes can cooperate in transmission and reception by using MIMO cooperative technique which allows space time diversity gain, reduces the energy consumption and increases the system capacity.

The trade-off of cooperative MIMO system is additional delays in communication due to the need for information transfer between cooperating nodes in both transmission and reception sides.

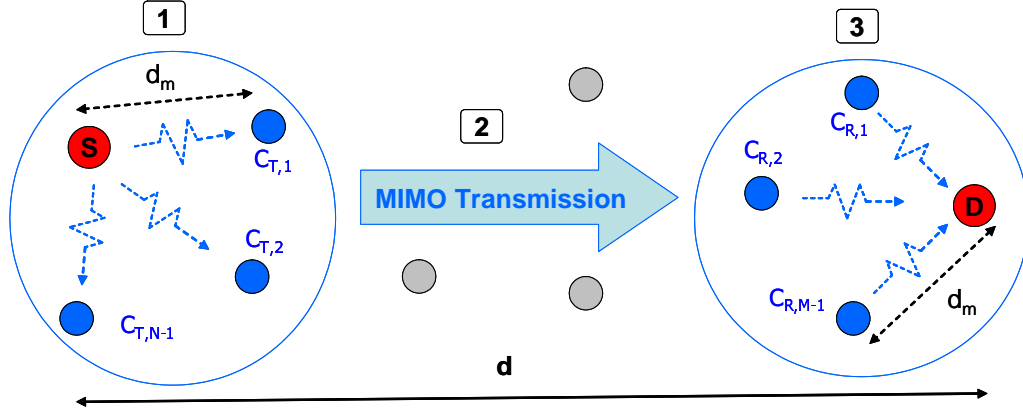


Figure 2.8: Cooperative MIMO transmission scheme from S to D with  $N - 1$  cooperative transmission nodes ( $C_{T,1}, C_{T,2}..C_{T,N-1}$ ) and  $M - 1$  cooperative reception nodes ( $C_{R,1}, C_{R,2}..C_{R,M-1}$ ).

The principle of cooperative MIMO transmission using space-time block codes (STBC) was presented in [17]. As illustrated by Fig. 2.8, the cooperative MIMO transmission from source node S to destination node D over a transmission distance  $d$  is composed of three phases:

1. Local data exchange,
2. Cooperative MIMO transmission,
3. Cooperative reception.

These three transmission phases are detailed in the following paragraphs.

### 2.5.1 Local Data Exchange

At the transmission side, the source node S must cooperate with its neighbors and exchange its data in order to perform a MIMO transmission in phase 2. Node S can broadcast the transmission bits to the other  $N - 1$  cooperative transmission nodes. The distance between cooperating nodes  $d_m$  is much smaller than the transmission distance  $d$ .

### 2.5.2 Cooperative MIMO Transmission

After  $N-1$  neighbor nodes receive the data from source node S,  $N$  cooperative transmission nodes will modulate and encode their received bits to the QPSK STBC symbols and then transmit simultaneously to the destination node (or multi-destination nodes) like a traditional MIMO systems (each cooperative node plays role of one antenna of the MIMO system).

For low-speed and energy constrained transmissions in WSN, MIMO Space-Time Block Code transmission techniques are referred. The simplicity of STBC encoding and decoding is practical for WSN due to the calculation limitation of the wireless sensor nodes.

### 2.5.3 Cooperative Reception

At the reception side, the cooperative neighbor nodes of destination node D firstly receive the MIMO modulated symbols, and then sequentially retransmit them to the destination node D for joint MIMO signals combination and data decoding.

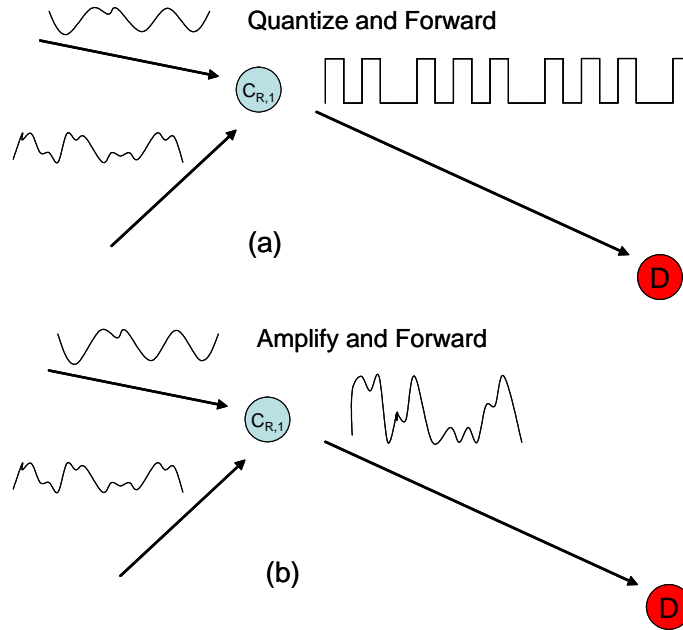


Figure 2.9: Cooperative reception techniques in cooperative MIMO networks.

In a cooperative MIMO system, the decoder at destination node D requires the analog value of received signals at all cooperative nodes for the space time combination. Therefore, each cooperative node must transmit their received value through a wireless channel to the destination node D.

The cooperative reception technique presented in [17] considers that a cooperative reception node quantizes one received symbol to  $N_{sb} = 10$  bits and then forwards the bits

sequences to the destination node D. At the destination node, the space-time signals from other cooperative reception nodes are reconstruct from the received bits sequences and then are space-time combined.

This technique increases the number of transmission bits. For a short range SISO transmission of this cooperative reception phase, the circuit energy consumption dominates the total system consumption (as illutrated in Fig. 3.3). The strategy of quantizing one symbol to  $N_{sb}$  bits will increase the transmission data, i.e. increase the transmission time and the circuit consumption (which depends on the transmission time). The total consumption increases and affects the energy efficiency of cooperative reception technique.

This effect is investigated in chapter 4 and two new cooperative reception technique (Forward and Combine, Combine and Forward) based on the idea of relay techniques are also proposed for a better energy consumption in the cooperative reception phase.

#### 2.5.4 Multi-hop Cooperative MIMO Technique

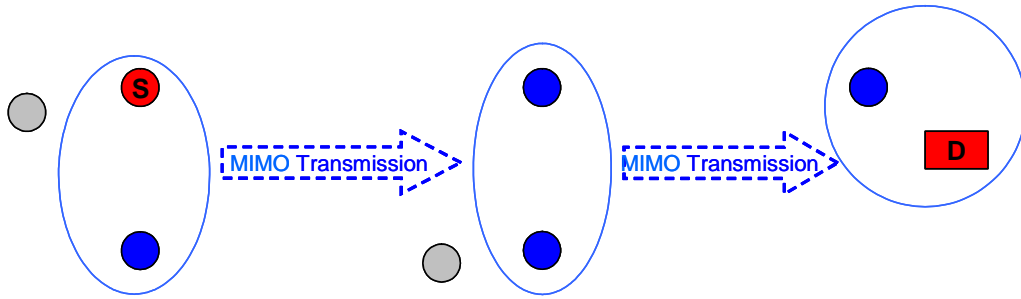


Figure 2.10: Multi-hop cooperative MIMO transmission.

Like the traditional SISO multi-hop technique, the cooperative MIMO technique can be used with multi-hop cooperation strategy in order to reduce the transmission consumption over long distance, or in the case that a greater number of transmit and receive nodes can not be deployed.

In Fig.2.10, a multi-hop cooperative MIMO transmission scheme with two cooperation nodes in each hop is presented. In such network, each hop transmission is one cooperative MIMO transmission and, in the general case, the number of cooperative nodes in one group is not limited to a number of two (e.g. three and four cooperative nodes). As cooperative MIMO transmission with two transmit and two receive nodes is the best compromise between complexity and performance, the cooperative MIMO configuration 2-2 will be preferred in multi-hop cooperative MIMO transmission.

## 2.6 Cooperative MIMO Transmission in the CAPTIV Project

### 2.6.1 CAPTIV Project Overview

As a result of increased motorization, urbanization, population growth and changes in population density, traffic congestion has been increasing world-wide, reducing efficiency of transportation infrastructure and increasing travel time, air pollution, fuel consumption and accident occurrences. In this context, information and communication systems play a key role in driving assistance, floating car data, and traffic management in order to make the road safer. To reduce traffic accidents, researchers have proposed several vehicle-to-vehicle (V2V) collision warning systems to avoid vehicle collisions. However, few systems based on infrastructure-to-vehicle (I2V) communications exist.

A scientific coordination group devoted to Intelligent Transportation Systems, called GIS ITS Bretagne, has been set up in the Brittany region, to investigate this research area. One of its projects, CAPTIV, aims at using existing infrastructure, i.e. road signs but also every infrastructure along the road, to transmit information inside a wireless network including equipped vehicles. This network is an ad-hoc network and can be considered as a Wireless Sensor Network, whose size depends on the area to be covered.

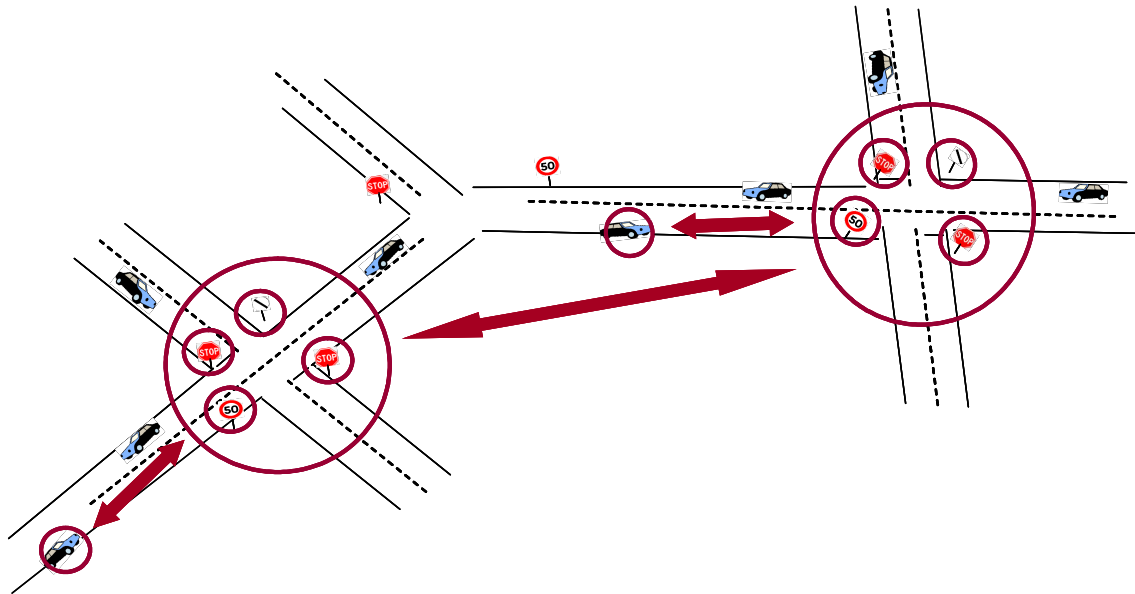


Figure 2.11: Infrastructure-to-Infrastructure and Infrastructure-to-Vehicle wireless communications in the CAPTIV, Intelligent Transport System Project.

The first applications offered by CAPTIV are road signs anticipated displays (including dynamic situations as temporary works on the road) and arriving vehicle indications. In such a network, every kinds of information can be transmitted, leading then to more advanced applications which integrate live data and feedback from a number of other

sources, such as parking guidance and information systems, weather information, and so on. The main advantages of CAPTIV over existing schemes are dynamicity, low power consumption and low cost.

Dynamicity means that the system can be very easily and quickly re-programmed, and that it can quickly take into account particular and temporary situations. The low power consumption is obtained thanks to a global optimization. The design of adapted antennas allows to optimize the link budget. Channel characterizations and modeling lead to signal processing techniques, such as cooperative MIMO (Multi-Input Multi- Output) techniques, particularly useful in such a context.

### 2.6.2 Description of the CAPTIV System

In the CAPTIV system, information is transmitted thanks to vehicles and existing infrastructure within a network whose typical size is metropolitan. The communications can occur from a vehicle to vehicle (V2V), vehicle to road infrastructure (V2I), road infrastructure to vehicle (I2V) or road infrastructure to road infrastructure (I2I) until the information reaches a communication node or cluster where road sign density is high (e.g. crossroads). From a signal processing point of view, this can lead to several types of communications:

- MISO (Multiple Input - Single Output) and SIMO (Single Input - Multiple Output) transmissions between a vehicle close to the crossroads and the communication cluster formed by the road signs of the crossroads.
- MIMO (Multiple Input - Multiple Output) communications between crossroads. MIMO techniques can then be used to optimize the power consumption of the whole system.

The main technical characteristics of the CAPTIV system are the following:

- Coverage : at least 100 meters.

The driver needs to be informed far before the crossroads, and 100 meters is really a lower bound. But there are some road signs before crossroads that can be included in the communication cluster, thus extending the coverage.

- Mobility : 90 km/h.

CAPTIV system is dedicated to any kind of road (rural or urban) except motorways.

- Reactivity : 100 ms.

Taking into account the human reactivity, the system has to be very reactive to let the driver the time to analyze information and act consequently.

- Bit rate : about 40 kbit/s.

The amount of information is not too high, and only one or two frames of 256 bits are needed to inform drivers of any direction of arrival, but the reactivity has to be very short.

- Maximum number of devices at a junction : 100.

The system has to support any kind of traffic situation, from very fluid to congested.

- Consumption : between 25 and 40 mA.

The transceivers on the road signs have to be autonomous and are fed with solar energy, so the consumption is a very critical point. On the other hand, on-board transceivers are less constrained because they can take advantages of the vehicle battery.

- Frequency : 2.4 GHz.

Several frequencies and standards have been investigated apart from the characteristics mentioned here above. Most of standards did not respect this schedule of conditions because of consumption or coverage aspects. Only the 802.15.4 standard, i.e. Zigbee physical and MAC layers, was able to respect it in part. We decided therefore to adopt the 2.4 GHz frequency band, but developed our own transmission protocol to optimize the power consumption.

### 2.6.3 Proposed Cooperative Transmission Schemes in CAPTIV

In plenty of communication scenarios in CAPTIV, the transmission between the infrastructure and the vehicle are usually from a medium to long distance that direct transmission can not support (or need plenty of transmission energy). Firstly, multi-hop routing technique can be used for such transmission but it is not efficient enough in terms of energy consumption in many cases. Relay and cooperative MIMO techniques are the better strategies in terms of energy efficiency.

Consider that the circle and the rectangle stand respectively for the road sign and the vehicle in the transport system, some cooperative transmission strategies, illustrated in the following figures, have been proposed for energy efficiency transmissions in CAPTIV.

#### SISO multi-hop transmission in CAPTIV

The most simple cooperation scheme is the multi-hop SISO transmission like in Fig. 2.12. A message from a road sign (source node S) in one cross road can be transmitted through multi road signs (cooperation nodes) to a vehicle (destination node D).



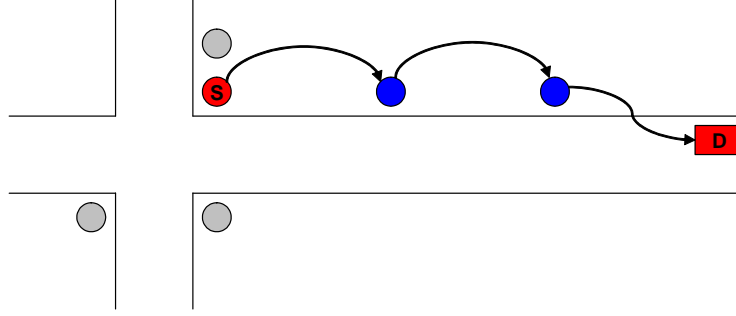


Figure 2.12: Multi-hop SISO transmission between infrastructure and vehicle.

### Relay transmission in CAPTIV

Relay technique is known as the simplest diversity technique. In Fig.2.13, a message from the road sign can be transmitted to the vehicle (destination node D) and another road sign (relay node R). Then, the message is relayed from this relay road sign to the vehicle for signal combination. This technique is more energy efficient than multi-hop SISO for medium range transmission.

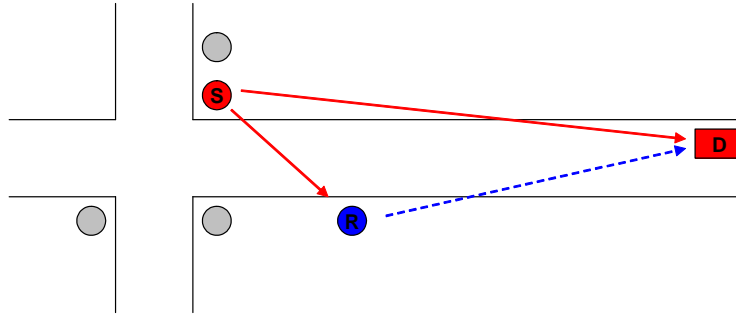


Figure 2.13: Relay transmission between infrastructure and vehicle

### Cooperative MIMO transmission in CAPTIV

Cooperative MIMO is an energy efficient cooperative techniques for medium and long range transmission (the energy efficiency of the cooperative MIMO is investigated in chapter 3). Depending on the system topology (the available nodes) and the transmission distance, the optimal selection of transmit and receive node number can be chosen in order to minimize the total energy consumption. The selection scheme will be presented in chapter 3.

In Fig. 2.14, a road sign (source node S) can cooperate with its neighbor road signs to employ a cooperative MISO technique to transmit a message to the vehicle (destination node D).

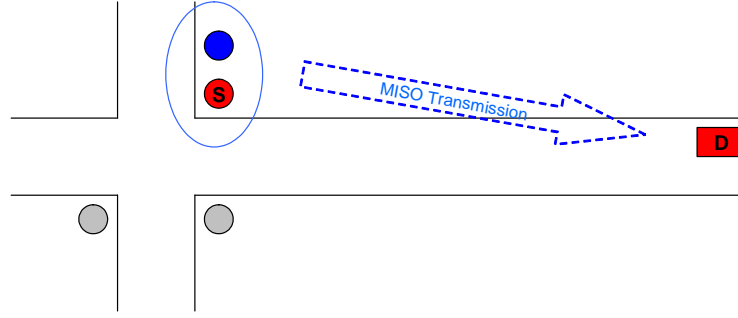


Figure 2.14: Cooperative MISO transmission between infrastructure and vehicle

In Fig.2.15, the road sign (source node S) and the vehicle (destination node D) can cooperate with its neighbor road signs to employ a cooperative MIMO transmission over a long distance. The optimal number of the employed cooperative transmit and receive nodes depends on the transmission distance and the available nodes.

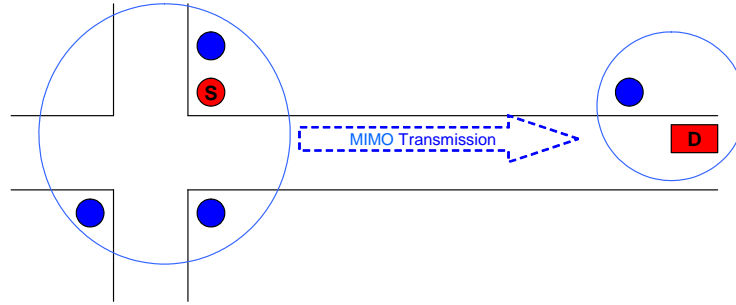


Figure 2.15: Cooperative MIMO transmission between infrastructure and vehicle

Another example of cooperative MIMO transmission in CAPTIV is shown in Fig. 2.16, the road sign (source node S) can cooperative with other road signs in one cross-road to transmit the message by using a cooperative MIMO technique to the cooperative reception road signs in the other cross-road.

### Multi-hop cooperative MIMO transmission

For a long distance communication, the cooperative MIMO technique with the number of transmit and receive nodes greater than 2 has the energy consumption advantages (proved in chapter 3), but this scenario can not be always employed because of the lack of available nodes. In this condition, a multi-hop technique using cooperative MIMO for each transmission hop is a suitable solution.

For example, the communication between two crossroads with distance greater than 1km in Fig. 2.17, two road signs in the middle of the transmission line can be employed

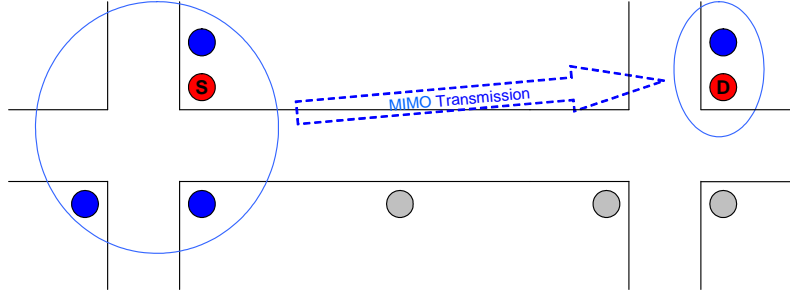


Figure 2.16: Cooperative MIMO transmission between infrastructure and infrastructure

(and cooperate together) to perform a multi-hop cooperative MIMO transmission.

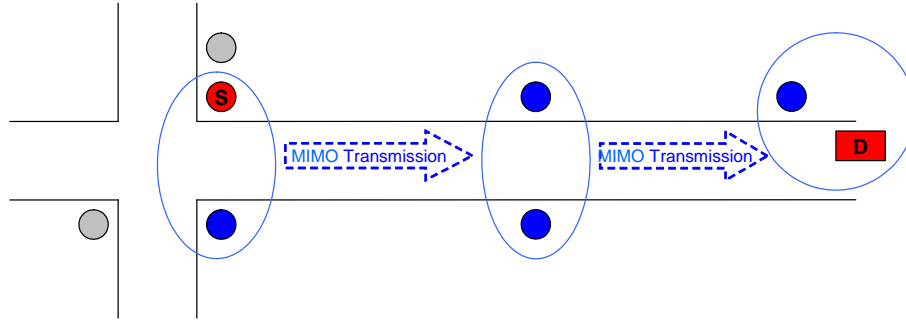


Figure 2.17: Multi-hop cooperative MIMO transmission between infrastructure and vehicle

## 2.7 Conclusion

Cooperative techniques can exploit the transmission diversity gain in order to increase the performance or to reduce the transmission energy consumption of the system. In this chapter, the multi-hop, cooperative relay and cooperative MIMO techniques were presented.

Some detail on CAPTIV, an ITS application project, where the energy consumption is an important constraint, was also presented in this chapter. Cooperative techniques can help to reduce the transmission energy consumption in a medium to long distance transmission WSN like the CAPTIV. Some cooperative strategies, based on the multi-hop, cooperative relay and cooperative MIMO techniques, have been proposed in order to deploy an energy efficient transmissions between the vehicles and road infrastructures in CAPTIV.

Among the presented cooperative transmissions in this chapter, cooperative MIMO techniques have a great potential to perform an energy efficient transmission scheme in

distributed wireless networks. The performance and the energy efficiency of cooperative MIMO techniques will be studied in Chapter 3. The energy consumption comparisons between the cooperative MIMO technique and the multi-hop and relay techniques will be also investigated in chapter 3 and chapter 6.

## Chapter 3

# Energy Efficiency of Cooperative MIMO Techniques

### 3.1 Introduction

For wireless transmission over fading channel, a MIMO space time coding system needs less transmission energy than a SISO system for the same Bit Error Rate (BER) target. The MIMO energy-efficiency transmission scheme is particularly useful for WSN where each wireless node has to operate without battery replacement for a long time and energy consumption is the most important constraint.

When multi-antenna can not be integrated into a single sensor node, some individual sensor nodes can cooperate at the transmission and at the reception in order to deploy a cooperative MIMO transmission scheme [24], [61], [59], [49], [63]. Cooperative MIMO schemes can deploy the energy-efficiency of MIMO technique which plays an important role in long range transmission where transmit energy is dominant in the total energy consumption. In various WSN applications, such as area surveillance for agriculture or intelligent transportation systems, middle and long range transmissions are indeed often required because of the weak density of the wireless sensor networks.

Nonetheless, a cooperative MIMO scheme requires extra energy for the local cooperative data exchange, extra circuit consumption of the cooperative nodes and extra energy of the more complex digital processing [48]. Therefore, it is not practical for short range transmission in which circuit energy consumption is dominant in the total energy consumption. Another draw-back of the cooperative MIMO technique is the delay of the cooperative local data exchange.

The energy-efficiency of the cooperative MIMO scheme versus the SISO scheme was shown in [16] [50] with the case of two transmit nodes using Alamouti STBC [4]. Depending

on the energy model of [15], we propose an extension of this cooperative principle to MIMO systems with three and four antennas using Tarokh orthogonal STBC (1.40).

An energy-efficient antenna subset selection that depends on the transmission distance is performed in this chapter and a new multi-hop cooperative MIMO technique is proposed. This technique represents a good trade-off between classical multi-hop SISO and more complex MIMO cooperative schemes.

The advantage of Orthogonal STBC technique (Alamouti and Tarokh) over SISO technique and their application to the cooperative MIMO scheme are presented in Section 3.2. In Section 3.3, the energy consumption model for an RF system is investigated and the energy consumption of SISO, non-cooperative MIMO and SISO multi-hop systems are compared. The extra consumption cost of cooperative MIMO system in comparison with non cooperative MIMO system is investigated in Section 3.4. The energy efficiency of the cooperative MIMO technique over the SISO and multi-hop SISO techniques for long distance transmission is proved through simulation results.

### 3.2 Application of STBC to Wireless Sensor Networks

For MIMO transmission techniques, Spatial Multiplexing is designed for increasing high rate transmission systems operating at relatively high Signal-to-Noise Ratio (SNR), while space-time coding is more appropriate for non high-rate transmission at low SNR. The diversity gain and the performance at low SNR of MIMO space-time coding is useful for WSN to reduce the transmission power consumption.

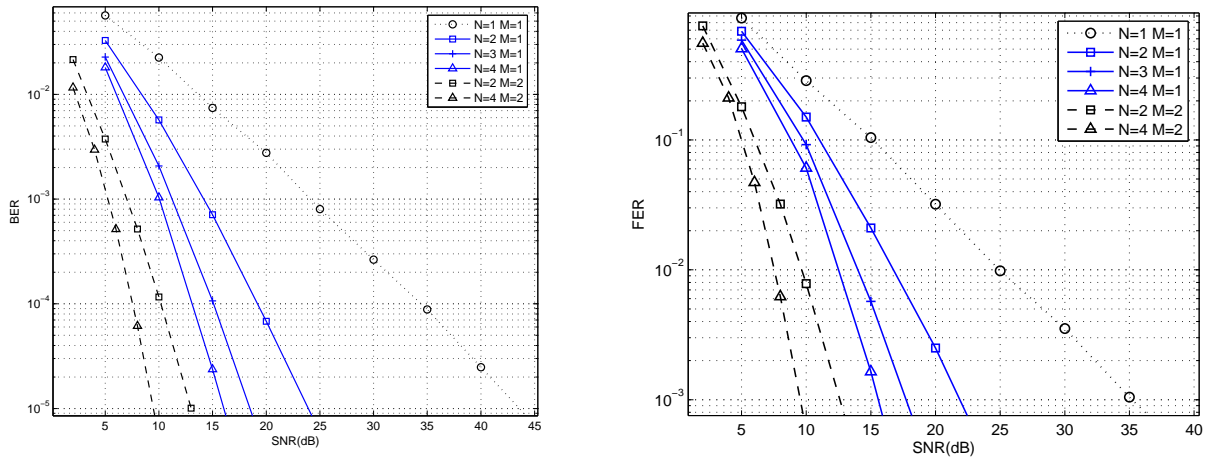


Figure 3.1: BER and FER performance of STBC for various number of transmit and receive antennas ( $N$  and  $M$ ) over a Rayleigh fading channel.

Between two space-time coding techniques, Space-Time Block Codes and Space-Time

Trellis Codes, STBC is the most practical for WSN [21][37][25]. The simplicity of block coding and the low complexity of a maximum likelihood decoding of STBC corresponds to the processing limitation of a wireless sensor node.

The performance of STBC with  $N = 2, 3$  and 4 transmission antennas using Alamouti [4] and Tarokh STBCs for complex symbol [94] over a Rayleigh fading channel is shown on Fig. 3.1. Modulation is uncoded QPSK and we assume that we have perfect synchronization, perfect channel estimation and Maximum Likelihood detection at the receiver.

$SNR$	$N = 1$	$N = 2$	$N = 3$	$N = 4$
$M = 1$	43.5 dB	24 dB	18.5 dB	16.2 dB
$M = 2$	20.7 dB	13 dB	10.5 dB	9.4 dB
$M = 3$	13.3 dB	8.7 dB	7.4 dB	6.6 dB
$M = 4$	9.7 dB	6.4 dB	5.4 dB	4.9 dB

Table 3.1:  $SNR$  requirement of STBC for  $BER = 10^{-5}$ , non-coding QPSK modulation, Rayleigh block fading channel

$SNR$	$N = 1$	$N = 2$	$N = 3$	$N = 4$
$M = 1$	35.2 dB	22 dB	17.7 dB	15.8 dB
$M = 2$	19.5 dB	12.7 dB	10.4 dB	9.2 dB
$M = 3$	12.5 dB	8.8 dB	7.5 dB	6.7 dB
$M = 4$	9.7 dB	6.5 dB	5.4 dB	5 dB

Table 3.2:  $SNR$  requirement of STBC for  $FER = 10^{-3}$ , non-coding QPSK modulation, Rayleigh block fading channel, 120 bits per frame

Due to the diversity gain of transmission and reception, error rate performance (FER and BER) of MIMO STBC can easily outperform SISO systems under the same SNR. It means that, with the same BER requirement, a MIMO system requires less energy for transmission than a SISO system. The required  $SNR$  for the error rate  $BER = 10^{-5}$  and  $FER = 10^{-3}$  is presented in Tab. 3.1 and 3.2.

It is obvious that a cooperative MIMO technique using STBC transmission is very useful for long range transmission in WSN where transmission energy dominates the total energy consumption of the system. For a system with two cooperative transmit nodes, Alamouti code [4] can be used, whereas the orthogonal STBC developed by Tarokh [94] is used for systems with three or four transmit nodes (some other OSTBC like max-SNR STBC or quasi-orthogonal STBC can be used too).

The limitation of orthogonal STBC is that a full-diversity and full-rate coding matrix

for complex symbols modulation with the number of transmit antennas greater than two does not exist. The maximum rate for a complex OSTBC is  $3/4$  for three and four antennas and the coding rate for a complex OSTBC with a number of transmit antennas greater than four is just  $1/2$ .

### 3.3 Energy Consumption Model

Energy consumption of one RF system consists in the transmission consumption and the circuit energy consumption. MIMO technique can help to reduce the transmission energy consumption based on the performance advantages over SISO technique, but a higher circuit energy consumption is needed due to the multiple antennas and RF processing chain implementation.

Typical RF system blocks of transmitters and receivers are shown in Fig. 3.2. For the simplicity of energy consumption estimation, the digital base-band signal processing blocks (coding, pulse-shaping, digital modulation, combination, detection ...), which do not cost as much energy consumption as other RF processing blocks, are omitted.

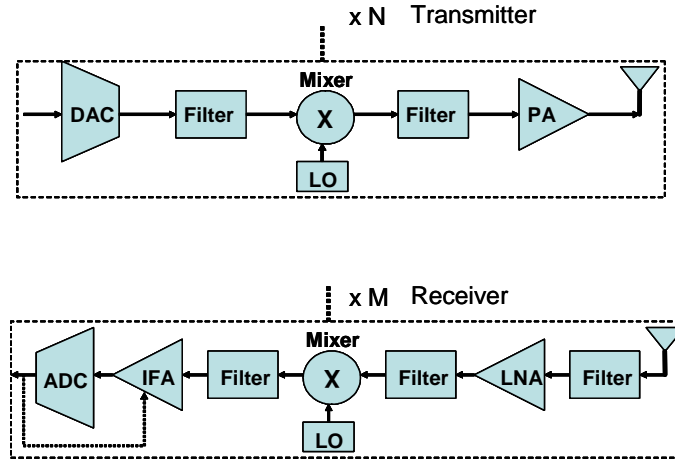


Figure 3.2: Transmitter and receiver blocks with  $N$  transmit and  $M$  receive antennas.

#### 3.3.1 Energy Consumption of Non Cooperative Systems

In this thesis, a traditional MIMO system where all antennas are implemented in one wireless node is called a non-cooperative system. A cooperative MIMO system is a system where the multiple antennas are distributed in different wireless nodes and cooperate to perform a MIMO transmission.

Let us consider a non-cooperative MIMO system with  $N$  transmit and  $M$  receive antennas, the total power consumption of a typical RF non-cooperative system consists of



two components : the transmission power  $P_{pa}$  of the power amplifier and the circuit power  $P_c$  of all RF circuit blocks.

$P_{pa}$  depends on the output transmission power  $P_{out}$ . If the channel is  $K$ -law path loss, the needed transmission power can be calculated as

$$P_{out}(d) = \bar{E}_b R_b \times \frac{(4\pi d)^K}{G_t G_r \lambda^2} M_l N_f \quad (3.1)$$

where  $\bar{E}_b$  is the mean required energy per bit for ensuring a given error rate requirement,  $R_b$  is the bit rate,  $d$  is the transmission distance.  $G_t$  and  $G_r$  are the transmission and reception antenna gain,  $\lambda$  is the carrier wave length,  $M_l$  is the link margin,  $N_f$  is the receiver noise figure defined as  $N_f = M_n/N_0$  with  $N_0 = -174$  dBm/Hz single-side thermal noise Power Spectral Density (PSD) and  $M_n$  is the PSD of the total effective noise at receiver input [15].

Depending on the number of transmit and receive antennas ( $N$  and  $M$ ), and the Power Spectral Density (PSD) of thermal noise  $N_0$ , we can calculate  $\bar{E}_b$  based on  $SNR$  value given by Tab. 3.2 for error rate requirement  $FER = 10^{-3}$  (or by Tab. 3.1 for error rate requirement  $BER = 10^{-5}$ ).

The power consumption  $P_{pa}$  can be approximated as

$$P_{pa} = (1 + \alpha)P_{out} \quad (3.2)$$

where  $\alpha = \frac{\xi}{\eta} - 1$  with  $\xi$  the drain efficiency of the RF power amplifier and  $\eta$  the Peak-to-Average Ratio (PAR) which depends on the modulation scheme and the associated constellation size.

The total circuit power consumption of  $N$  transmit and  $M$  receive antennas is given by

$$\begin{aligned} P_c \approx & N(P_{DAC} + P_{mix} + P_{filt} + P_{syn}) \\ & + M(P_{LNA} + P_{mix} + P_{IFA} + P_{filr} + P_{ADC} + P_{syn}) \end{aligned} \quad (3.3)$$

where  $P_{DAC}$ ,  $P_{mix}$ ,  $P_{LNA}$ ,  $P_{IFA}$ ,  $P_{filt}$ ,  $P_{filr}$ ,  $P_{ADC}$ ,  $P_{syn}$  stand respectively for the power consumption values of the digital-to-analog converter, the mixer, the low noise amplifier, the intermediate frequency amplifier, the active filter at the transmitter and receiver, the analog-to-digital converter and the frequency synthesizer whose values are presented in [15].

For traditional non-cooperative systems, the total energy consumption per bit  $E_{bt}$  can be obtained as

$$E_{bt} = (P_{pa} + P_c)/R_b \quad (3.4)$$

Then, the total energy consumption can be calculated as

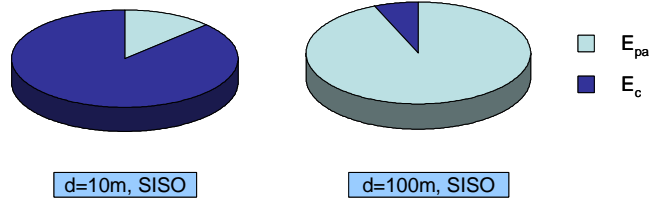
$f_c = 2.5$ GHz	$\eta = 0.35$
$G_t G_r = 5$ dBi	$\frac{N_0}{2} = -174$ dBm/Hz
$B = 10$ kHz	$\beta = 1$
$P_{mix} = 30.3$ mW	$P_{syn} = 50$ mW
$\bar{P}_b = 10^{-3}$	$T_s = \frac{1}{B}$
$P_{filt} = P_{filr} = 2.5$ mW	$P_{LNA} = 20$ mW
$N_f = 10$ dB	$M_L = 40$ dB

Table 3.3: System parameters for the energy consumption evaluation.

$$E_{total} = E_{bt} N_b \quad (3.5)$$

For energy consumption estimation, evaluation and comparison purposes, the reference energy model in [15] with the system parameters in Table 3.3 is used in this thesis.

In Fig. 3.3, the energy consumption partition of a traditional SISO system is shown. For a small distance, the circuit energy ( $E_c$ ) dominates the total energy consumption. Transmission energy consumption increases quickly with the path-loss power factor  $K = 2$ , and apart from  $d = 100m$ , transmission energy ( $E_{pa}$ ) dominates the total energy consumption. MIMO technique can consequently be used to reduce significantly the transmission energy consumption in that case.

Figure 3.3: Transmission energy ( $E_{pa}$ ) and circuit energy ( $E_c$ ) repartitions of a SISO system for transmission distances  $d = 10m$  and  $d = 100m$ .

In Fig. 3.4, the energy consumption of SISO and traditional MIMO systems with two transmit and two receive antennas is illustrated. It can be seen that MIMO systems can help to reduce significantly the transmission energy consumption at the cost of a higher circuit energy consumption.

### 3.3.2 Multi-Hop SISO System

As previously discussed in chapter 2, in order to reduce the needed transmission power  $P_{pa}(d)$ , which increases quickly with the path loss power factor  $K$ , a SISO multi-hop technique can be used. If the transmission channel is divided into multi-hop transmission by using the multi-hop technique, the total transmission consumption is the sum of

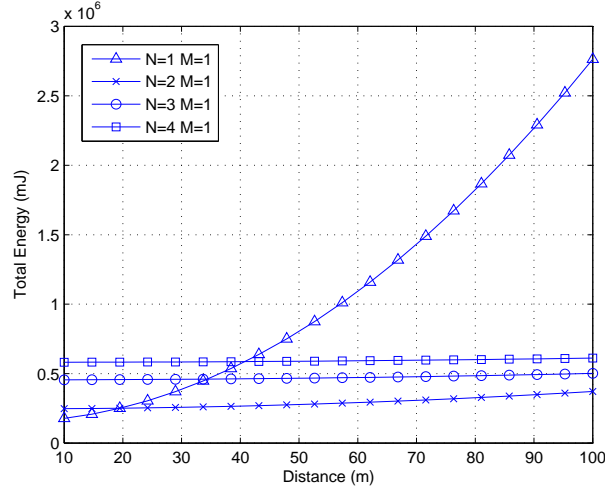


Figure 3.4: Energy consumption in function of the distance of SISO and non-cooperative MIMO systems with 2, 3 and 4 transmit antennas.

each single-hop transmission, which consequently increases linearly with the transmission distance.

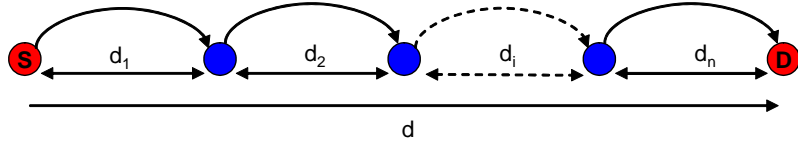


Figure 3.5: Multi-hop transmission scheme with  $n$ -hop SISO transmissions from  $S$  to  $D$ .

Let us consider the network topology for multi-hop in Fig. 3.5 with a hop distance  $d_{hop}$ . In the optimal case where all nodes are in a straight line and the distances between two nodes is  $d_{hop}$  (i.e.  $d_{hop} = d_i$  with  $i = 1..n_{hop}$ ), the total energy consumption is the sum of each hop energy consumption. The optimal distance  $d_{hop}$  between two nodes can be determined by the tangent line (apart from  $d = 0$ ) of the energy consumption curve of SISO system like in Fig. 3.6.

In Fig. 3.6, the energy consumption of SISO and multi-hop SISO systems is shown. With the optimal  $d_{hop} = 25m$  and for transmission distance  $d = 100m$  (4 hops), the multi-hop technique can save 53% of the total energy consumption of the SISO system. However, the multi-hop system needs four hops for multi signal transmission, which costs approximatively four times the transmission delay of the SISO system.

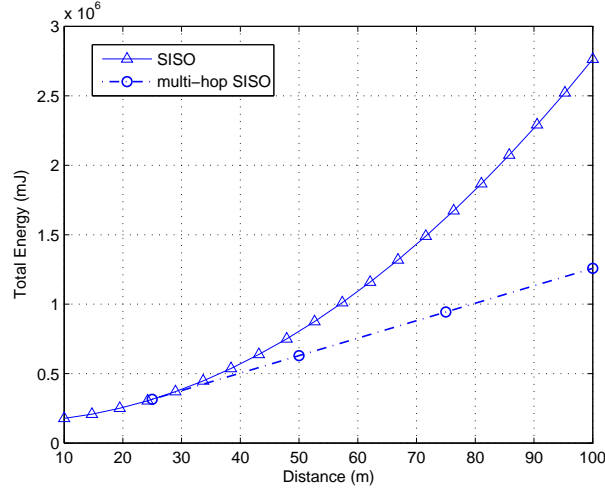


Figure 3.6: Energy consumption in function of transmission distances of SISO and multi hop SISO systems,  $FER = 10^{-3}$  requirement, Rayleigh block fading channel with power path-loss factor  $K = 2$ .

### 3.4 Cooperative MIMO System

Differing from non-cooperative MIMO systems, the energy consumption of a cooperative MIMO system must include the energy consumption of cooperative data exchanges and cooperative reception phases. The extra energy of the local cooperative data exchanges depends on the number of cooperative transmit nodes and the local inter-node distance  $d_m$  between two cooperating nodes at both transmission and reception sides. Distance  $d_m$  is expected to vary from 1 meter to 10 meters depending on the geographical configuration of the network.

Let us assume that there are  $N_b$  bits to transmit from a source node S to a destination node D (separated by distance  $d$ ) and there are  $N$  nodes and  $M$  nodes cooperating at transmission and reception sides, respectively.

At the transmission side, node S must firstly broadcast its  $N_b$  bits to  $N - 1$  cooperative nodes. For this short local distance transmission  $d_m$ , we know that SISO is the most energy-efficient technique (Fig. 3.4).

For a short distance transmission, the channel is considered as an Additive White Gaussian Noise (AWGN) channel with a path loss factor  $K = 3.5$  [71], and let us assume that there are just single-hop SISO transmissions between two cooperative nodes, and that an uncoded 16-QAM modulation is used ( $SNR = 9.4$  dB is needed for ensuring a  $FER = 10^{-3}$  requirement over an AWGN channel). The 16-QAM allows to decrease circuit consumption by reducing the transmission time.

Assuming the broadcast is possible from node S to  $N - 1$  cooperative nodes (over a

short distance  $d_m$ ), we can calculate the needed energy per bit for a local data exchange phase  $E_{pb_{coop}T_x}$  based on the non-cooperative energy consumption model in the previous section (one transmit antenna and  $N - 1$  receive antennas scheme).

The extra cooperative energy consumption at the transmission side  $E_{coopT_x}$  depends on the energy consumption per bit  $E_{pb_{coop}T_x}$  and can be calculated as

$$E_{coopT_x} = N_b E_{pb_{coop}T_x}. \quad (3.6)$$

After receiving  $N_b$  bits from source node S,  $N - 1$  cooperative transmission nodes and S will modulate and encode the information to the QPSK STBC symbols and then transmit simultaneously to the destination node (or multi-destination nodes) over a MIMO Rayleigh fading channel.

At the reception side, the  $M - 1$  cooperative receive nodes firstly receive the MIMO encoded symbols, quantize one STBC symbol to  $N_{sb}$  bits and then retransmit their quantized bits respectively to the destination node D using uncoded 16-QAM modulation. The energy consumption per bit for this cooperative reception phase  $E_{pb_{coop}R_x}$  can be calculated by using non-cooperative energy model for a SISO 16-QAM transmission with distance  $d = d_m$ .

The extra cooperative energy consumption at the reception side  $E_{coopR_x}$  depends on the number of cooperative nodes  $M - 1$ , the number of symbol-to-bit quantization  $N_{sb}$  and the needed energy per bit  $E_{pb_{coop}R_x}$ .

$E_{coopR_x}$  can then be calculated as

$$E_{coopR_x} = N_{sb}(M - 1)N_b E_{pb_{coop}R_x}. \quad (3.7)$$

The energy consumption of the MIMO transmission phase (transmission energy  $P_{pa}$  and circuit energy  $P_c$ ) can be calculated like a non-cooperative MIMO system

Finally, the total energy consumption of a cooperative MIMO system is

$$E_{total} = E_{coopT_x} + (E_{pa} + E_c) + E_{coopR_x} \quad (3.8)$$

The energy consumption repartition of cooperative MISO 2-1 system presented in Fig. 3.7 consists of three parts: the transmission energy  $E_{pa}$ , the circuit energy  $E_c$  and the cooperative energy  $E_{coop}$  (which consist of the transmission and the circuit energy consumptions of the cooperative phases). In comparison with the SISO system, the cooperative MIMO system can reduce significantly the transmission energy repartition, at the cost of higher circuit and cooperative energy consumptions.

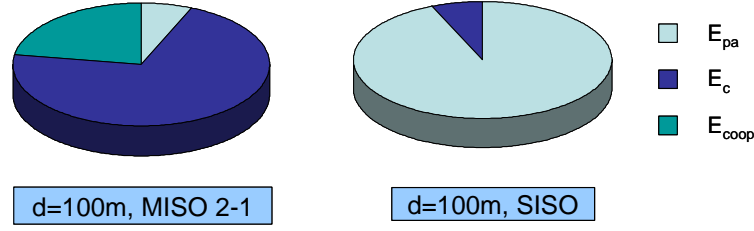


Figure 3.7: Transmission energy ( $E_{pa}$ ), circuit energy ( $E_c$ ) and cooperative energy ( $E_{coop}$ ) repartitions of the SISO and the cooperative MISO systems for the transmission distance  $d = 100m$ .

### 3.5 Energy Efficiency of Cooperative MIMO Systems

The simulation were performed using the system parameters presented in Table 3.3. The following figures in this chapter represent the total energy consumption to transmit  $10^7$  bits with the error rate requirement  $FER = 10^{-5}$  from a source node S to a destination node D separated by a distance  $d$  (over a Rayleigh quasi-static channel). The local distance between cooperative nodes is  $d_m = 5m$  and  $N_{sb} = 10$  bits/symbols quantization.

#### 3.5.1 Cooperative MISO vs. SISO Techniques

Fig. 3.8 shows the total energy consumption of the SISO system and cooperative MISO systems with two, three and four transmission nodes ( $N = 2, 3$  and  $4$ ). It can be seen that when the transmission distance  $d < 30m$ , the cooperative MISO is less energy-efficient than the traditional SISO because of the extra circuit and the cooperative energy consumptions. However, when  $d > 30m$ , the transmission energy saved by MISO technique can be greater than the extra energy cost and the cooperative MISO outperforms the SISO.

At distance  $d = 100m$ , 85% energy is saved by using a 2-1 cooperative MISO strategy instead of SISO. The more the distance increases, the more the transmission energy dominates in the total energy consumption. This is the reason why the cooperative 3-1 MISO outperforms 2-1 and the cooperative 4-1 MISO outperforms 3-1 respectively at the distances  $d = 180m$  and  $d = 310m$ .

#### 3.5.2 Cooperative MIMO vs. Cooperative MISO Techniques

Fig. 3.9 shows the total energy consumption of the cooperative MISO 4-1 system and the cooperative MIMO systems with two reception nodes ( $M = 2$ ). It can be seen that the cooperative MIMO 3-2 outperforms 2-2 and the cooperative MIMO 4-2 outperforms 3-2 respectively at distances  $d = 650m$  and  $d = 850m$ . For a small distance, the cooperative MISO 4-1 is better than cooperative MIMO systems, but for  $d > 650m$ , the cooperative

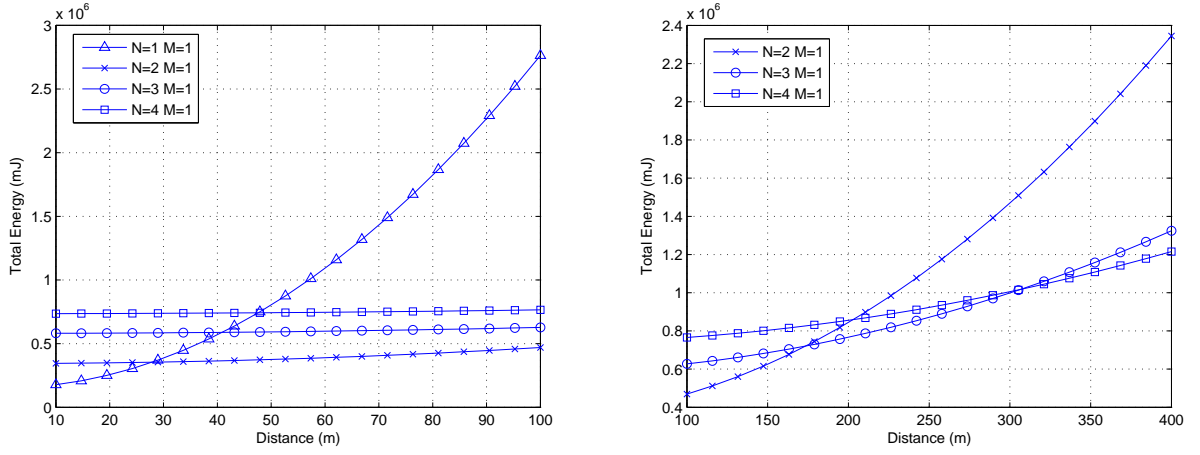


Figure 3.8: Energy consumption in function of transmission distances of cooperative MISO and SISO systems,  $N = 2, 3$  and 4 cooperative transmit nodes,  $FER = 10^{-3}$  requirement, Rayleigh block fading channel with power path-loss factor  $K = 2$ .

MIMO 2-2 outperforms the cooperative MISO 4-1.

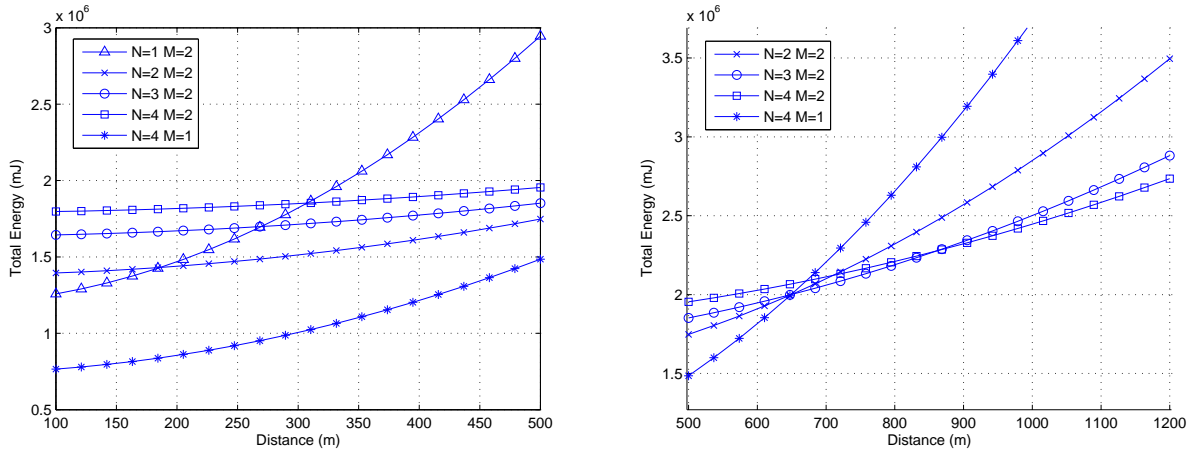


Figure 3.9: Energy consumption of cooperative MIMO and cooperative MISO systems,  $N = 2, 3, 4$  and  $M = 2$  cooperative transmit and receive nodes,  $FER = 10^{-3}$  requirement, Rayleigh block fading channel with power path-loss factor  $K = 2$ .

Similar results are obtained for 3 or 4 cooperative reception nodes. For each range of transmission distance  $d$ , based on the energy calculation result, we can find the best energy-efficient antenna selection strategy, as shown in Fig. 3.10.

By employing the optimal number of transmit-receive nodes  $N - M$  for each transmission range like in Fig. 3.10, the lower bound of total energy consumption of the cooperative MIMO system is represented on Fig. 3.11.

As illustrated by Fig. 3.10, increasing the number of transmission nodes is better than increasing the number of reception nodes because of the smaller cooperative energy consumption. The number of transmit cooperative bits  $N_{b-coopRx} = N_{sb}(M - 1)N_b$  at

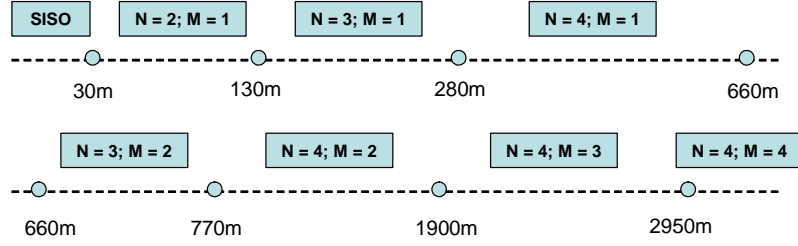


Figure 3.10: Optimal  $N - M$  transmit and receive antennas set selection as a function of transmission distance,  $FER = 10^{-3}$  requirement, Rayleigh block fading channel with power path-loss factor  $K = 2$ .

the reception side is greater than  $N_{b-coopTx} = N_b$  at the transmission side ( $N_{sb} = 10$  for energy calculation), which leads to a much higher cooperative energy consumption at the reception side. Therefore, two cooperative reception techniques, which have a better energy consumption efficiency than this quantization technique, are proposed in Chapter 4.

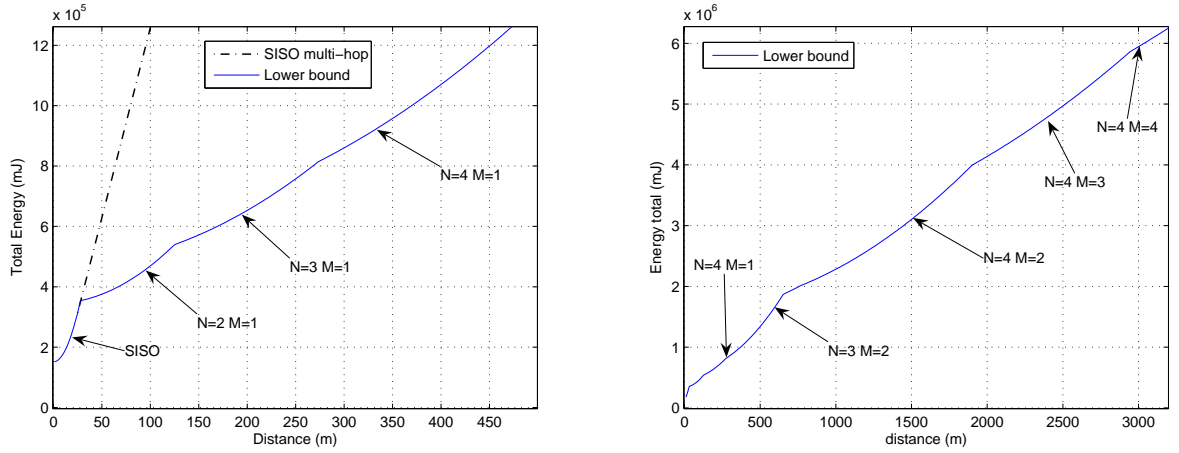


Figure 3.11: Energy consumption lower bound of cooperative MIMO systems,  $FER = 10^{-3}$  requirement, Rayleigh block fading channel with power path-loss factor  $K = 2$ .

### 3.5.3 Cooperative MISO vs. Multi-hop SISO Techniques

The energy consumption comparison between multi-hop SISO and the cooperative MISO is presented on Fig. 3.12 with the optimal hop distance  $d_{hop} = 25m$ . For the transmission distance  $d = 100m$ , four hops are needed for the multi-hop SISO system to transmit the data to the destination.

Fig. 3.12 shows that the multi-hop SISO system is 69% less energy-efficient than the cooperative 2-1 MISO system. Moreover, for  $d = 200m$  and  $d = 500m$ , multi-hop SISO



technique is 83% and 89% less energy efficient than cooperative 2-1 MISO and cooperative 3-1 MISO respectively.

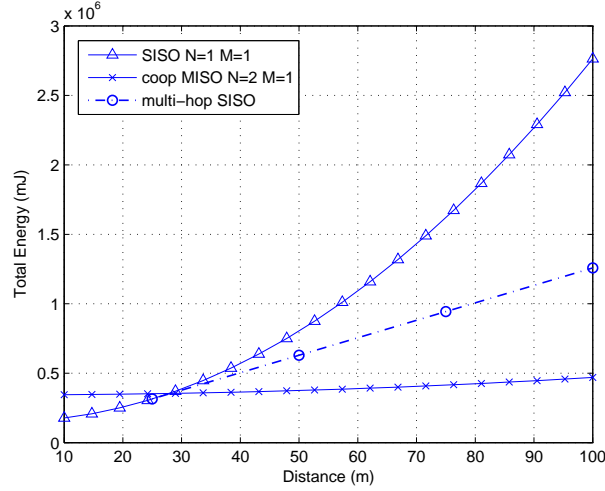


Figure 3.12: Energy consumption in function of transmission distances of cooperative MISO, SISO and multi-hop SISO systems,  $FER = 10^{-3}$  requirement, Rayleigh block fading channel with power path-loss factor  $K = 2$ .

Like the cooperative MISO technique, the multi-hop technique draw-back is also the delay of long distance transmission. It is evident that the cooperative MISO transmission delay (just in cooperative transmission side) is less than the 4-hops delay of the multi-hop SISO technique for  $d = 100m$ .

### 3.5.4 Cooperative MIMO vs. Multi-hop Cooperative MIMO Techniques

For a very long range transmission ( $d$  from 1000 to 4000m), the best energy-efficiency strategy is to use 4-2, 4-3 and 4-4 cooperative MIMO schemes. However, due to the geographical distribution of WSN, we cannot always have enough neighbor nodes to set up a 4-3 or 4-4 cooperative MIMO transmission scheme. In this condition, a multi-hop cooperative MIMO technique is proposed.

A cooperative MIMO 2-2 configuration which requires less resources in the network is practical for the multi-hop cooperative MIMO transmission. The optimal distance for one 2-2 cooperative MIMO hop is around 900m (as shown in Fig. 3.13).

In Fig. 3.13, it can be seen that for the distance  $d = 2700$  m (3 hops), 2-2 multi-hop technique can save 39% energy consumption in comparison with 2-2 cooperative MIMO technique and just 32% less energy efficient than the best 4-4 cooperative solution. It is also interesting to note that in terms of energy consumption, the 2-2 multi-hop cooperative MIMO technique can outperform 3-2 cooperation and 4-2 cooperation for 3 and 4 hops,

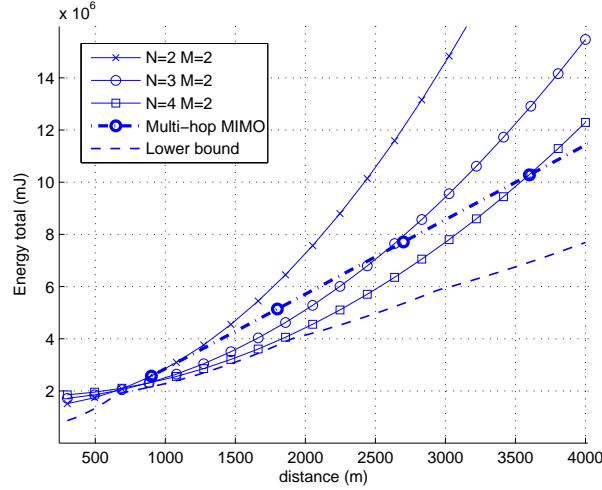


Figure 3.13: Energy consumption in function of transmission distances of cooperative MIMO and multi-hop MIMO 2 – 2 systems,  $FER = 10^{-3}$  requirement, Rayleigh block fading channel with power path-loss factor  $K = 2$ .

respectively.

### 3.5.5 Influence of the distance between cooperative nodes

The transmission energy consumption of the cooperative phases (phase one and phase three) increases when the local cooperative transmission distance increases. However, for a short distance transmission of cooperative phases, the circuit consumption dominates the total energy consumption  $E_{coop}$  (as shown in Fig. 3.3). Moreover, the energy consumption of cooperative phases is usually significantly smaller than the circuit energy consumption of phase 2 (as shown in Fig. 3.7) or the transmission energy consumption for a long distance transmission. Therefore, the variation of the cooperative transmission distance  $d_m$  affects very slightly the total energy consumption of the cooperative MIMO system.

Fig. 3.14 shows the energy consumption of the cooperative MISO systems with different cooperative transmission distance  $d_m = 5, 10$  and  $20\text{m}$ .

### 3.5.6 Impacts of the Error Rate Requirement and the Power Path Loss Factor

If all the RF parameters and the transmission distance are fixed, the transmission energy consumption depends on the required energy per bit  $E_b$  (as shown in Eq. 3.1), which is linked to the error rate requirement according to Tab. 3.1 and 3.2, and the power path-loss factor  $K$ . The error rate requirement depends on a specific LLC (Logical Link Layer) protocol. As an example for the Zigbee specification, the desired Packet-Error-Rate (can

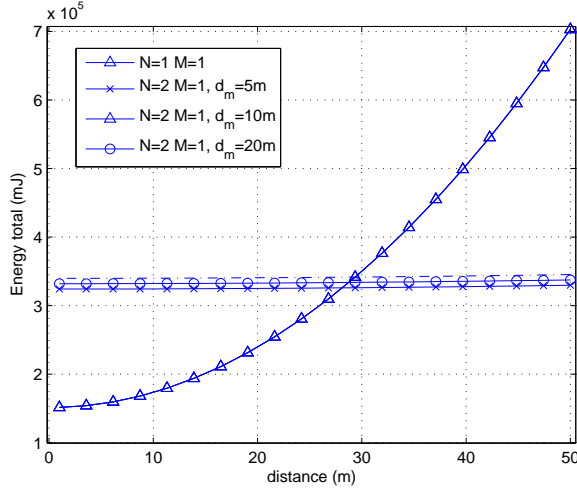


Figure 3.14: Energy consumption of the cooperative MISO 2 – 1 with different cooperative transmission distances  $d_m = 5, 10$  and  $20\text{m}$ ,  $FER = 10^{-3}$  requirement, Rayleigh block fading channel with power path-loss factor  $K = 2$ .

be considered as a FER) is  $10^{-3}$ . As the required FER decreases, the transmission energy consumption will decrease, reducing the energy efficiency advantage of the cooperative MIMO over the SISO technique.

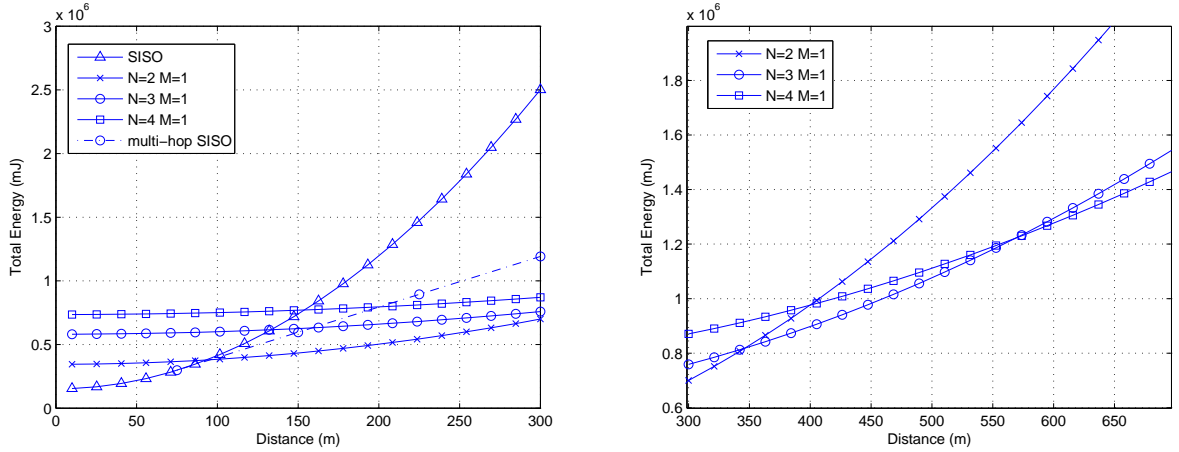


Figure 3.15: Energy consumption in function of transmission distances of cooperative MISO and SISO systems,  $N = 2, 3, 4$  cooperative transmit nodes,  $FER = 10^{-2}$  requirement, Rayleigh block fading channel with power path-loss factor  $K = 2$ .

Fig. 3.15 shows the energy consumption comparison between SISO, multi-hop SISO and cooperative MISO systems with the error rate requirement  $FER = 10^{-2}$ . In comparison with the result in Fig. 3.8 and 3.12 (error rate requirement  $FER = 10^{-3}$ ), it can be seen that the advantage of the cooperative MISO over SISO and multi-hop SISO

techniques is reduced.

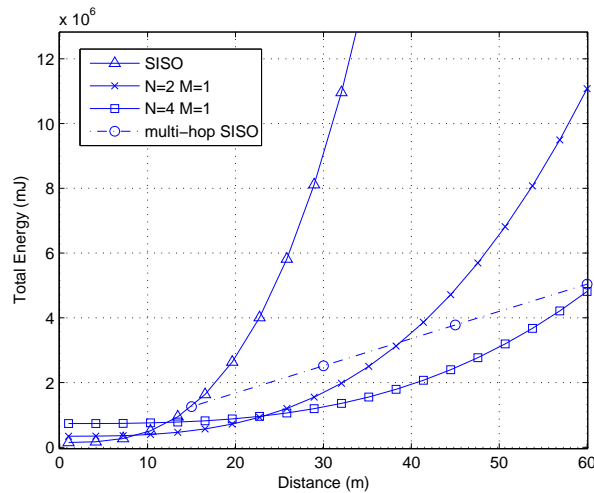


Figure 3.16: Energy consumption in function of transmission distances of cooperative MIMO and multi-hop MIMO 2 – 2 systems,  $FER = 10^{-2}$  requirement, Rayleigh block fading channel with power path-loss factor  $K = 3$ .

As far as the channel is concerned, if the path-loss factor  $K$  increases, the transmission energy consumption increases quickly (as a power function of the path-loss factor  $K$ ). Fig. 3.16 shows the energy consumption comparison between SISO, multi-hop SISO and cooperative MISO systems with the error rate requirement  $FER = 10^{-2}$  and the power path-loss factor  $K = 3$ . It can be seen that the cooperative MIMO has a bigger advantage over SISO technique. Fig. 3.16 also shows that the efficiency of the multi-hop technique increases with the path loss factor  $K$ .

### 3.5.7 Energy Consumption of the Coding Systems

Error control coding (ECC) helps to increase the performance in wireless fading transmission at the cost of a higher complexity in encoding and decoding processes. The performance evaluation of STBC and ECC concatenation can be found in [8], [10], [35] and [87]. ECC can increase effectively the performance of space-time coding technique.

The energy consumption of the ECC [56, 53, 40] is usually lower than the RF circuit consumption, and can be negligible in the following energy consumption estimation. However, the cost of the integrated hardware circuit for ECC encoding/decoding may be higher than the cost of the low-cost transceiver for WSN node. Therefore, finding the ECC allowing the best trade-off between the performance and complexity is also an important criterion.

Fig. 3.17 shows the performance simulation result of the STBC in concatenation with a

low-complexity rate 1/2 convolutional codes (CONV) [7 4 3] (with the encoding constraint length four). In comparison with the FER result in Fig 3.1, it can be seen that ECC helps to reduce the SNR for the same required FER, therefore reducing the transmission energy consumption.

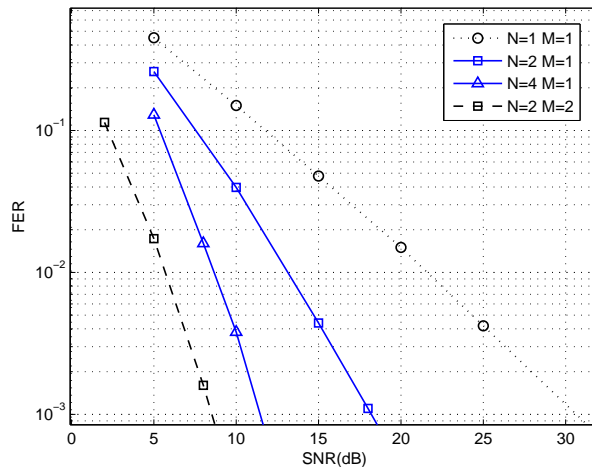


Figure 3.17: FER performance of STBC in concatenation with CONV [7 4 3] codes over a Rayleigh block fading channel.

Fig. 3.18 shows the energy consumption comparison between the SISO, multi-hop SISO and cooperative MISO systems with and without the ECC CONV [7 4 3] and the error rate requirement  $FER = 10^{-3}$ . In the presence of ECC, the advantages of the cooperative MIMO over SISO techniques is reduced. However, as the ECC reduces the transmission rate (rate 1/2 for this CONV), the transmission time increases which leads to a higher circuit energy consumption. As a consequence, error control coding systems are less energy efficient than non-coded systems for a short distance transmission.

### 3.6 Conclusion

In this chapter, the energy consumption of cooperative MIMO techniques was investigated. Cooperative MIMO techniques can exploit the energy-efficiency of MIMO transmission in distributed wireless sensor networks. It is shown that cooperative MISO and MIMO techniques are more energy-efficient than SISO and traditional multi-hop SISO techniques for medium and long range transmissions in WSN.

An optimal cooperative MIMO scheme selection was presented in order to find the optimal  $N$ - $M$  antenna configuration for a given transmission distance. The multi-hop cooperative MIMO technique for a 2-2 antenna configuration which demands less network

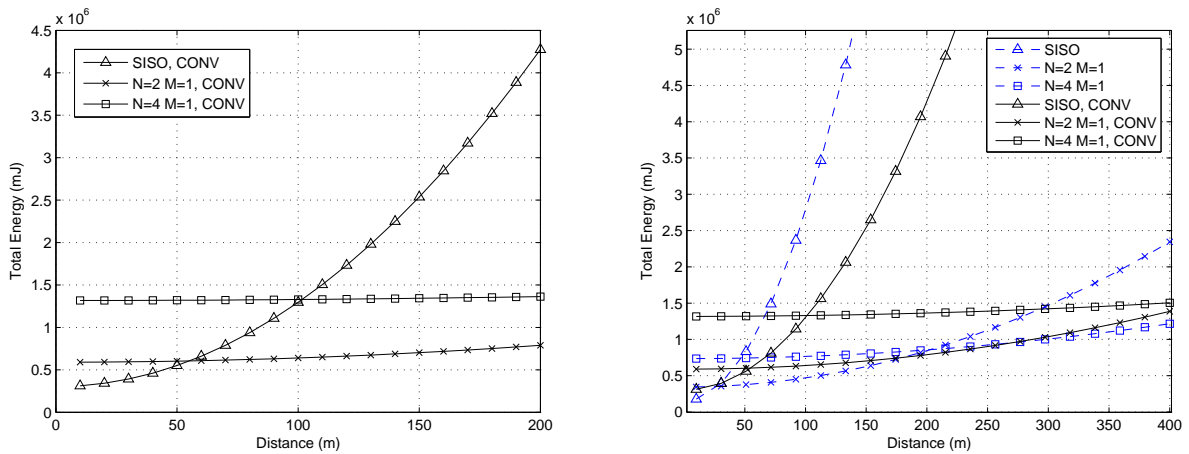


Figure 3.18: Energy consumption in function of transmission distances of cooperative MISO and SISO systems, CONV [7 4 3],  $FER = 10^{-3}$  requirement, Rayleigh block fading channel with power path-loss factor  $K = 2$ .

resources was also proposed.

The cooperative MIMO approach seems better than the traditional SISO, but it is more sensible to channel estimation errors and requires a precise MIMO transmission synchronization. The impact of transmission synchronization errors, channel estimation errors and cooperative reception techniques in the performance of cooperative MIMO technique is investigated in the next chapter. Another trade-off is the delay of cooperative transmission. However, comparing with a multi-hop SISO approach, the cooperative MIMO technique is not only better in terms of energy consumption but also in terms of transmission delay.

## Chapter 4

# Effect of Transmission Synchronization Errors and Cooperative Reception Techniques

### 4.1 Introduction

In chapter 3, the cooperative MIMO technique and the energy consumption of cooperative MIMO techniques were investigated. Cooperative MIMO can exploit the diversity gain of space-time coding technique to increase the energy consumption efficiency. It is obvious that cooperative MISO and MIMO systems are more energy-efficient than SISO and traditional multi-hop SISO systems for medium and long range transmission in wireless distributed sensor networks.

Since the nodes are physically separated in a cooperative MIMO system, their different respective clocks lead to de-synchronized transmission and reception. That generates Inter-Symbol Interference (ISI), decreases the desired signal amplitude at the receiver and makes it more difficult to estimate the Channel State Information (CSI). Precise synchronization techniques in [90][69][26][5][67] can be used for a greater timer synchronization precision but they cost much energy and time. At the reception side, each cooperative node has to forward its received signal through the wireless channel to the destination node for signal combination, which leads to additional noise in the final received signal. The effect of synchronization error at the transmission side and this additive noise at the cooperative reception side lead to some performance degradations of cooperative MIMO system. The error rate increases with the same SNR or the transmission energy needs to be increased for the same error rate requirement, which lead to an increase in the transmission energy and the total energy consumption.

Energy efficiency of cooperative MIMO technique was presented in [73] but the effect of transmission synchronization error was not considered. The performance of Alamouti and MRC diversity technique in the presence of transmission synchronization error were investigated in [47]. The cooperative MISO system has a good tolerance to small synchronization errors, but the study is limited to two transmit antennas, the CSI is considered to be known at the receiver and the effect of synchronization error is presented for a low SNR range. This thesis extends to the case of 3 and 4 transmit antennas using Tarokh STBC [94] or max-SNR STBC [31], and the system performances are investigated also in the presence of channel estimation errors.

The cooperative reception technique presented in [16] considers that cooperative nodes quantize one received symbol to  $N_{sb}$  bits and then forwards the bit sequences to the destination node, increasing the transmission data and the circuit energy. In order to achieve a better energy efficiency, two cooperative reception techniques derived from amplify-and-forward strategies [75] are also proposed in this chapter and their effect on the system performance and energy consumption is explored.

The rest of this chapter is organized as follows. The performance of cooperative MISO systems using Alamouti and Tarokh STBC is analyzed in the presence of transmission synchronization error and the absence of CSI at the receiver. The performance of different cooperative reception techniques is then investigated in Section 4.3. Finally, the performance of cooperative MIMO systems and their energy efficiency are illustrated by simulation results.

Simulations of cooperative MISO performance using Alamouti codes (two cooperative transmission nodes) and Tarokh OSTBC (three and four cooperative transmission nodes) in the presence of transmission synchronization error are performed in this chapter. The system uses an uncoded quadrature phase shift keying (QPSK) modulation, the channel is considered to be Rayleigh fading (independent for each frame of 120 symbols) and the raised cosine pulse shape  $p(t)$  has a roll-off factor of 0.25.

## 4.2 Effect of Transmission Synchronization Error

The nature of STBC [4][94] considers that the signals from different transmit antennas must be received synchronously at each cooperative node to perform the orthogonal combination. The precision of the synchronization process in a wireless node depends on the algorithm complexity and the processing time. Furthermore, the clock of each wireless node can be drifted during transmission times and the transmission delay can vary for each MIMO channel.



Consequently, it is impossible to have a perfectly synchronized transmission in distributed cooperative MIMO systems, leading to a un-synchronized received signal at the receiver. Therefore, ISI is generated, the desired symbol amplitude is decreased and the CSI is more difficult to be estimated at the receiver.

#### 4.2.1 Cooperative Transmission Synchronization Error

Since space-time combination can be performed independently at each cooperative reception node in cooperative MIMO systems, the impact of transmission synchronization error in a cooperative MIMO system is the same as in the corresponding cooperative Multi-Input Single-Output (MISO) system (e.g. the effect is the same on cooperative MIMO 4-2 and cooperative MISO 4-1 systems). Therefore, only the cooperative MISO system with  $N$  cooperative transmission nodes and one reception node is considered in the rest of the chapter.

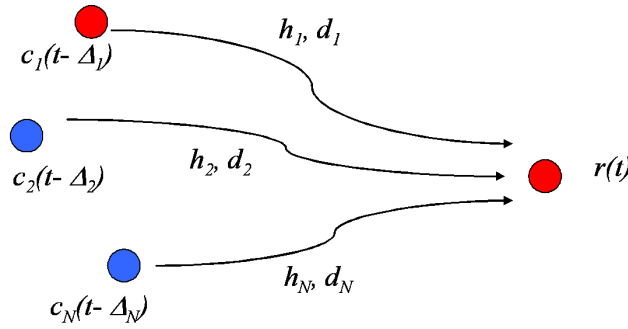


Figure 4.1: Un-synchronized cooperative MISO transmission.

After the local data exchange and the signal space-time coding [73], all the  $N$  cooperative nodes must transmit their STBC symbols simultaneously to the reception node. Due to the imperfect synchronous timer clocks between cooperative nodes, the node  $k$  among the  $N$  cooperative nodes will transmit its space-time coded sequence  $c_k$  at time  $(t - \Delta_k)$  and the channel transmission delay is  $d_k$  (for  $k = 1..N$ ). Sequences of the  $N$  cooperative nodes do not arrive at the reception node at the same moment as shown in Fig.4.1. The received signal is

$$r(t) = \sum_{l=-\infty}^{\infty} \sum_{k=1}^N \alpha_k c_k[l] p(t - lT_s - \Delta_k - d_k) + \eta(t) \quad (4.1)$$

where  $\alpha_k$  is the channel coefficient,  $c_k[l]$  is the  $l^{th}$  symbol of sequence  $c_k$ ,  $T_s$  is the symbol period,  $\eta(t)$  the white Gaussian noise and  $p(t)$  is the raised cosine pulse shape with a roll-off factor 0.25.

Let us define the transmission synchronization errors of the  $k^{th}$  cooperative node  $\delta_k = \Delta_k + d_k$ , for  $k = 1 \dots N$ . The received signal is then

$$r(t) = \sum_{l=-\infty}^{\infty} \sum_{k=1}^N \alpha_k c_k[l] p(t - lT_s - \delta_k) + \eta(t) \quad (4.2)$$

The effect of the transmission synchronization error is the superposition of the pulses from each node shifted by the corresponding  $\delta_k$  at the receiver. After the synchronization and the signal sampling process, an ISI between the unsynchronized sequences appears and the space-time sequences from the different nodes are no longer orthogonal. The orthogonal combination of space time codes can not be performed, which lead to the amplitude decrease of the desired signal and generates more interferences in final estimated symbols [74] [47].

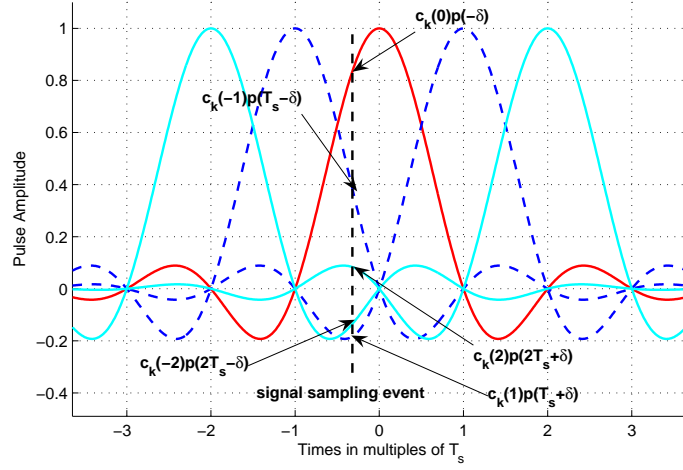
The receiver is considered to be perfectly synchronized to the desired space-time coded sequences for an independent evaluation of the cooperative transmission synchronization error impact and the proposed combination technique performance. In this thesis, for the simulation evaluation purpose, the transmission synchronization error  $\delta_k$  is considered having a Gaussian distribution  $N(0, \sigma^2)$  and varying from one frame to the other. As in a Gaussian distribution, 95% of the random variables are in the range  $[-2\sigma, 2\sigma]$ ,  $\Delta T_{syn} = 4\sigma$  is considered as the transmission synchronization error range in the simulation. The FER performance of cooperative MISO systems are investigated with different error ranges  $\Delta T_{syn}$  (as a function of the symbol duration  $T_s$ ).

We consider that the clock reference node is not in the cooperative MIMO transmission group (the real case of a typical wireless distributed network), which means that the different delays between these cooperative transmission nodes ( $\delta_i - \delta_j$ ) are random variables with a Gaussian distribution  $N(0, 2\sigma^2)$  (transmission delays between cooperative nodes is Gaussian distributed in  $[-\Delta T_{syn}, \Delta T_{syn}]$ ).

Let us consider the case of two cooperative transmit nodes using Alamouti codes with  $s_1$  and  $s_2$  two transmitted symbols in one block. The received signal is considered synchronized to transmission node 1 which has the most reliable channel. The two sampled values of the received signal are

$$\begin{aligned} r_1[1] &= r(t = T_s + \delta_1) = \alpha_1 c_1[1] + \alpha_2 c_2[1] p(\delta_1 - \delta_2) + \alpha_2 ISI_2^1(\delta_1 - \delta_2) + \eta_1[1] \\ r_1[2] &= r(t = 2T_s + \delta_1) = \alpha_1 c_1[2] + \alpha_2 c_2[2] p(\delta_1 - \delta_2) + \alpha_2 ISI_2^2(\delta_1 - \delta_2) + \eta_1[2] \end{aligned} \quad (4.3)$$

where  $ISI_k^i(\delta_l - \delta_k)$  is the ISI at  $i^{th}$  symbol of space time transmission sequence  $k$  with the time error offset  $(\delta_l - \delta_k)$  and  $\eta_k[i] = \eta(t = iT_s + \delta_k)$ . For simplicity, we consider that the ISI is just created by the four nearest neighbor symbols like in Fig. 4.2. In this case,


 Figure 4.2: ISI of un-synchronized sequence with the synchronization error  $\delta$ 

the inter symbol interference terms are

$$\begin{aligned}
 ISI_2^1(\delta_1 - \delta_2) &= c_2[-1]p(2T_s + \delta_1 - \delta_2) + c_2[0]p(T_s + \delta_1 - \delta_2) \\
 &\quad + c_2[2]p(T_s - \delta_1 + \delta_2) + c_2[3]p(2T_s - \delta_1 + \delta_2) \\
 ISI_2^2(\delta_1 - \delta_2) &= c_2[0]p(2T_s + \delta_1 - \delta_2) + c_2[1]p(T_s + \delta_1 - \delta_2) \\
 &\quad + c_2[3]p(T_s - \delta_1 + \delta_2) + c_2[4]p(2T_s - \delta_1 + \delta_2)
 \end{aligned} \tag{4.4}$$

with Alamouti space-time coded sequences  $\mathbf{C}_2 = \begin{bmatrix} \mathbf{c}_1 & \mathbf{c}_2 \end{bmatrix} = \begin{bmatrix} s_1 & -s_2^* \\ s_2 & s_1^* \end{bmatrix}$ . After the traditional space time combination, we have the two estimated symbols

$$\begin{aligned}
 \tilde{s}_1 &= \alpha_1^* r_1[1] + \alpha_2 r_1^*[2] = \underbrace{(|\alpha_1|^2 + |\alpha_2|^2 p(\delta_1 - \delta_2)) s_1}_{\text{desired signal}} + \underbrace{\alpha_1^* \alpha_2 (1 - p(\delta_1 - \delta_2)) s_2}_{\text{non-desired signal}} \\
 &\quad + \underbrace{\alpha_1^* (\alpha_2 ISI_2^1(\delta_1 - \delta_2) + \eta_1[1]) + \alpha_2 (\alpha_2 ISI_2^2(\delta_1 - \delta_2) + \eta_1[2])^*}_{\text{ISI and noise terms}} \\
 \tilde{s}_2 &= \alpha_2^* r_1[1] - \alpha_1 r_1^*[2] = (|\alpha_1|^2 + |\alpha_2|^2 p(-\delta_2)) s_2 + \alpha_1 \alpha_2^* (1 - p(-\delta_2)) s_1 \\
 &\quad + \alpha_2^* (\alpha_2 ISI_2^1(\delta_1 - \delta_2) + \eta_1[1]) - \alpha_1 (\alpha_2 ISI_2^2(\delta_1 - \delta_2) + \eta_1[2])^*
 \end{aligned} \tag{4.5}$$

In formula (4.5), if the synchronization error  $(\delta_1 - \delta_2) = 0$  (i.e. we have perfect transmission synchronization), the *non - desired signal* terms will be 0, and the orthogonal combination of the traditional Alamouti system is achieved. Otherwise, with the presence of synchronization error  $(\delta_1 - \delta_2)$ , the desired symbol amplitude decreases and an interference between  $s_1$  and  $s_2$  (*non - desired signal* terms) appears after the space-time combination. The system performance is affected depending on the level of synchronization error range.

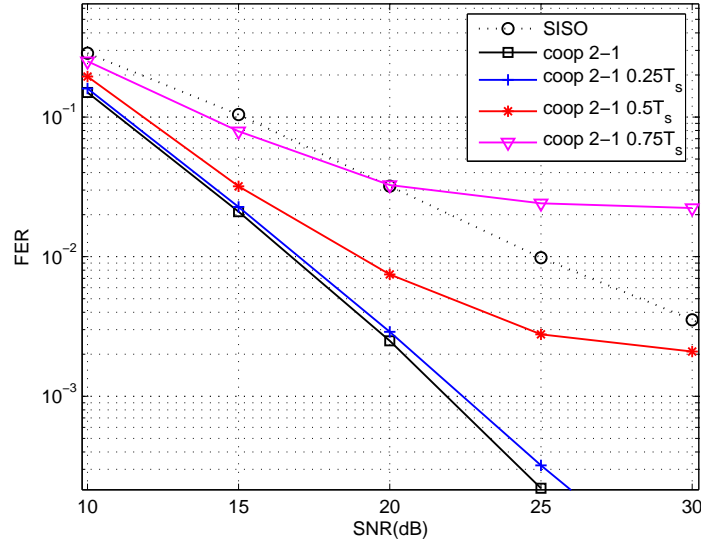


Figure 4.3: Effect of the transmission synchronization error on the performance of cooperative MISO systems with two transmit nodes  $N = 2$ , Alamouti STBC over a Rayleigh fading channel.

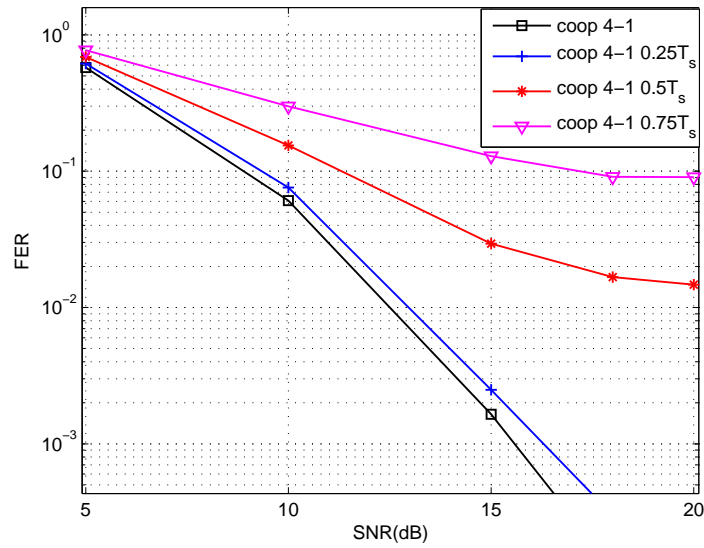


Figure 4.4: Effect of transmission synchronization error on the performance of cooperative MISO systems with four transmit nodes  $N = 4$ , Tarokh STBC over a Rayleigh fading channel.

In Fig. 4.3 and 4.4, simulation results of cooperative MISO 2-1 and MISO 4-1 system with two and four transmit nodes (coop 2-1, coop 4-1) are presented for the synchronization error ranges  $\Delta T_{syn} = 0.25T_s, 0.5T_s$  and  $0.75T_s$ . It can be seen that, for the case of synchronization error range  $\Delta T_{syn} = 0.25T_s$ , the cooperative MISO system is rather tolerant. However, when the error range increases, the FER performance decreases quickly.

In the case of a cooperative MISO system with four transmission nodes, due to more transmission space time sequences at the same time and more symbols in one space-time block, there are more ISI from un-synchronized sequences at the receiver and more *non-desired* terms after the space time combination. The effect of transmission synchronization error is thus more significant.

Some other space-time codes in [70] [91] or techniques using a joint equalizer and space time combination like [62] are proposed for a better tolerance to the ISI, but they result in data rate loss, larger transmission delay and an increase in the complexity of the equalizer and the combination technique.

#### 4.2.2 Channel Estimation Error

In order to estimate the Rayleigh fading channel, at the beginning of each frame (fading block) of antenna  $i$ , a training sequence  $\mathbf{w}_i$  is inserted ( $i = 1..N$ ). The  $\mathbf{w}_i$  sequences have a length of  $L$  symbols and are orthogonal from each other:

$$\mathbf{w}_i \otimes \mathbf{w}_k = \sum_{l=1}^L \mathbf{w}_i[l] \mathbf{w}_k[l] = 0, i \neq k. \quad (4.6)$$

Considering all training sequences  $\mathbf{w}_k$  known by the receiver, the received sequence  $\mathbf{r}^j$  at antenna  $j$  is

$$\mathbf{r}^j = \sum_{k=1}^N \alpha_{j,k} \mathbf{w}_k + \boldsymbol{\eta}^j, \quad (4.7)$$

where  $\boldsymbol{\eta}^j$  is the AGWN vector at antenna  $j$ . The channel coefficients  $\alpha_{j,k}$  can be estimated by [96] :

$$\tilde{\alpha}_{j,k} = \frac{\mathbf{r}^j \otimes \mathbf{w}_k}{\mathbf{w}_k \otimes \mathbf{w}_k} = \alpha_{j,k} + \frac{\boldsymbol{\eta}^j \otimes \mathbf{w}_k}{\mathbf{w}_k \otimes \mathbf{w}_k} = \alpha_{j,k} + \beta_{j,k}. \quad (4.8)$$

The estimation error  $\beta_{j,k}$  has a Gaussian distribution  $N(0, \frac{N_0}{2L.E_s})$  with a variance depending on  $L$  and the received SNR  $E_s/N_0$ . In the case of cooperative MISO, due to the synchronization error, the received training sequences from each antenna are no longer orthogonal, and are

$$\mathbf{r}^j = \sum_{k=1}^N \alpha_{j,k} \mathbf{w}'_k + \boldsymbol{\eta}^j \quad (4.9)$$

where  $\mathbf{w}'_k$  is the sequence  $\mathbf{w}_k$  delayed by  $\delta_k$ .

The estimated channel coefficients  $\tilde{\alpha}_{j,k}$  are affected not only by the Gaussian noise but also by the ISI and the correlated interference  $\mathcal{R}_{i,k}(t)$  of the other training sequences:

$$\tilde{\alpha}_{j,k} = \frac{\mathbf{r}^j \otimes \mathbf{w}_k}{\mathbf{w}_k \otimes \mathbf{w}_k} = \frac{\alpha_{j,k} \mathcal{R}_{k,k}(\delta_k)}{\mathcal{R}_{k,k}(0)} + \sum_{i=1, i \neq k}^N \frac{\alpha_{j,i} \mathcal{R}_{i,k}(\delta_k - \delta_i)}{\mathcal{R}_{k,k}(0)} + \frac{\boldsymbol{\eta}^j \otimes \mathbf{w}_k}{\mathcal{R}_{k,k}(0)} \quad (4.10)$$

The precision of CSI estimation is reduced depending on the synchronization error range and affects the total performance of cooperative MISO systems.

In the presence of cooperative synchronization error, the error rate will increase due to the ISI, the non-orthogonal combination and the less precise channel estimation. Therefore, more transmission energy (more energy for signal amplification power) must be used for the same FER requirement which will lead to a higher total energy consumption.

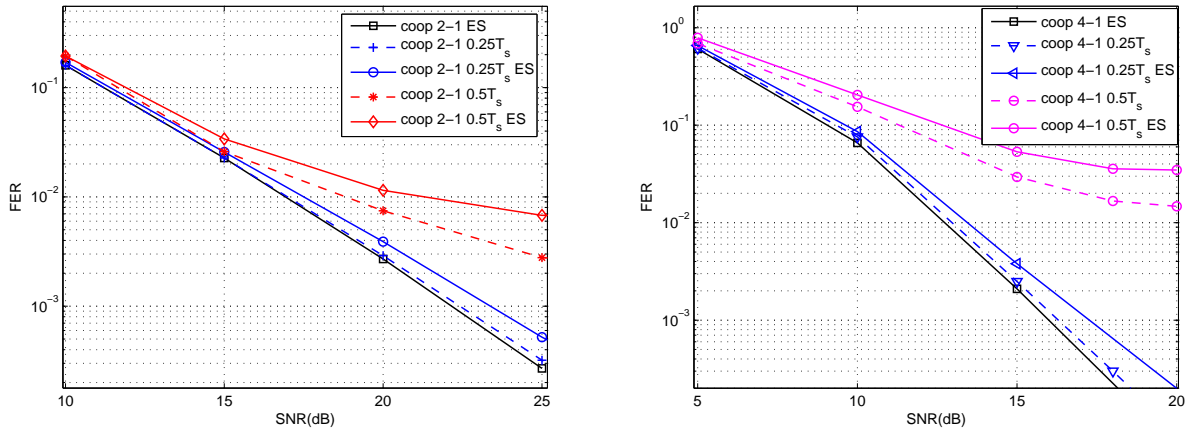


Figure 4.5: Effect of transmission synchronization and channel estimation errors on the performance of cooperative MISO systems with two and four transmit nodes  $N = 2$  and  $N = 4$ , Alamouti and Tarokh STBCs over a Rayleigh fading channel.

In Fig. 4.5, simulation results of cooperative MISO 2-1 and MISO 4-1 systems with two and four transmit nodes (coop 2-1, coop 4-1) are presented for the synchronization error ranges  $\Delta T_{syn} = 0.25T_s$  to  $0.5T_s$ , with (legend *ES*) and with-out the presence of channel estimation error at the receiver.

The cooperative MISO system is rather tolerant for the synchronization error range  $\Delta T_{syn} = 0.25T_s$ . The performance degradation is increased with the number of cooperative transmit antennas. Moreover, with  $\Delta T_{syn}$  as large as  $0.5T_s$ , some performance saturation of cooperative MISO is appearing for large SNR range due to the ISI generated by the synchronization error, the non-orthogonal combination and channel estimation errors.

### 4.3 Effect of Cooperative Reception Techniques

The cooperative reception technique presented in [16] considers that the cooperative node quantizes one received symbol to  $N_{sb} = 10$  bits and then forwards the bit sequences to the destination node  $D$ . For short range SISO transmission, the circuit energy dominates the total system consumption. The strategy of quantizing one symbol to  $N_{sb}$  bits will increase the transmission data, the transmission time and the circuit consumption, which significantly increases the total energy consumption of the cooperative reception phase and affects the energy efficiency of the cooperative reception.

Decode-and-Forward and Amplify-and-Forward techniques used in [75] for cooperative relay transmission can be applied at the reception in the cooperative MIMO system for a better energy efficient cooperative reception. Because of the small received SNR in each cooperative reception node, it is better to transmit (amplify and forward or combine, amplify and forward) the analog symbol values than to transmit the decoded digital bits to the destination node  $D$ .

#### 4.3.1 Proposed Strategies for Cooperative Reception

In order to reduce the energy consumption of the cooperative reception phase, we propose in this thesis two cooperative reception techniques: Forward-and-Combine and Combine-and-Forward. The two proposed techniques, based on the relaying principle, help to significantly reduce the circuit energy consumption which dominates the total energy consumption of the cooperative reception phases.

##### Forward-and-Combine Technique

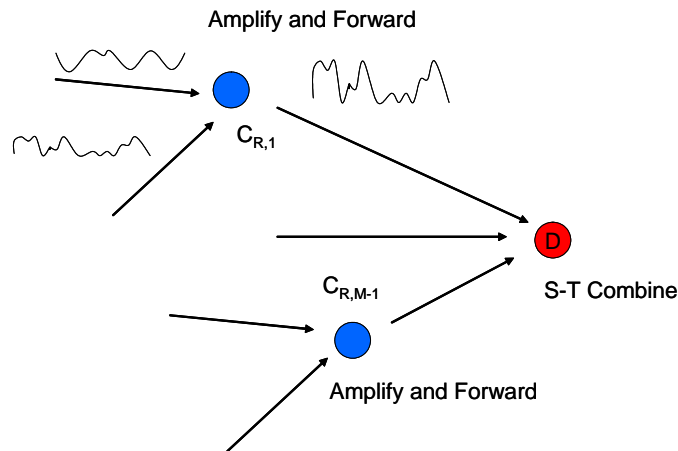


Figure 4.6: Forward-and-Combine cooperative reception technique principle.

In Forward-and-Combine (F-C) cooperative reception technique, illustrated in Fig. 4.6, each cooperative node amplifies its space time received symbols and then forwards respectively its analog sequence to the destination D (the short distance channel between two cooperative nodes is considered AWGN) like the Amplify-and-Forward principle of the relay technique. Then, the space-time combination is performed at the destination node D.

Considering the case of two transmit nodes using Alamouti STBC, the space time received symbols at each cooperative node  $j$  are:

$$\mathbf{r}^j = [r^j[1] \ r^j[2]] = [\alpha_{j,1}s_1 + \alpha_{j,2}s_2 \quad -\alpha_{j,1}s_2^* + \alpha_{j,2}s_1^*] + [\eta^j[1] \ \eta^j[2]] \quad (4.11)$$

In order to reduce the effect of the thermal noise, the amplification process ensures the amplification factor  $K_c$  of the received signal  $\mathbf{r}'^j$  at destination node D.

$$\mathbf{r}'^j = K_c[r_1^j \ r_2^j] + [n_1'^j \ n_2'^j] \Rightarrow \tilde{\mathbf{r}}^j = [r_1^j \ r_2^j] + [n_1'^j \ n_2'^j]/K_c, \quad (4.12)$$

for  $j = 2..M$ . Let us define the effective Gaussian noise  $n_{eff}^j = n_i^j + (n_i'^j/K_c)$  with  $i = 1, 2$ . After the space time combination, we have the estimated symbols:

$$\begin{aligned} \tilde{s}_1 &= \sum_{j=1}^M (|\alpha_{j,1}|^2 + |\alpha_{j,2}|^2) s_1 + \sum_{j=1}^M (\alpha_{j,1}^* n_{eff}^j + \alpha_{j,2} n_{eff}^{j*}) \\ \tilde{s}_2 &= \sum_{j=1}^M (|\alpha_{j,1}|^2 + |\alpha_{j,2}|^2) s_2 + \sum_{j=1}^M (\alpha_{j,2}^* n_{eff}^j - \alpha_{j,1} n_{eff}^{j*}) \end{aligned} \quad (4.13)$$

### Combine-and-Forward Technique

In Combine-and-Forward (C-F) cooperative reception technique, illustrated in Fig. 4.7, the space time combination is done at each cooperative node. Then, each cooperative node amplifies its combined symbols value, amplifies and forwards it to destination node D.

The space time combined symbols at each cooperative node  $j$  are:

$$\begin{aligned} \tilde{s}_1^j &= (|\alpha_{j,1}|^2 + |\alpha_{j,2}|^2) s_1 + \alpha_{j,1}^* n_1^j + \alpha_{j,2} n_2^{j*} \\ \tilde{s}_2^j &= (|\alpha_{j,1}|^2 + |\alpha_{j,2}|^2) s_2 + \alpha_{j,2}^* n_1^j - \alpha_{j,1} n_2^{j*} \end{aligned} \quad (4.14)$$

Then each cooperative node amplifies its combined symbol value and forwards it respectively to the destination node D. In order to reduce the effect of the thermal noise, the amplification process ensures the amplification factor  $K_c$  of the received signal:

$$\mathbf{r}'^j = K_c[\tilde{s}_1^j \ \tilde{s}_2^j] + [n_1'^j \ n_2'^j] \Rightarrow \tilde{\mathbf{r}}^j = [\tilde{s}_1^j \ \tilde{s}_2^j] + [n_1'^j \ n_2'^j]/K_c \quad (4.15)$$

The final space time combined symbols are the addition of all  $M$  received  $\tilde{\mathbf{R}}^j$ :

$$[\tilde{s}_1 \ \tilde{s}_2] = \sum_{j=1}^M \tilde{\mathbf{r}}^j = \sum_{j=1}^M [\tilde{s}_1^j \ \tilde{s}_2^j] + \sum_{j=2}^M [n_1'^j \ n_2'^j]/K_c \quad (4.16)$$



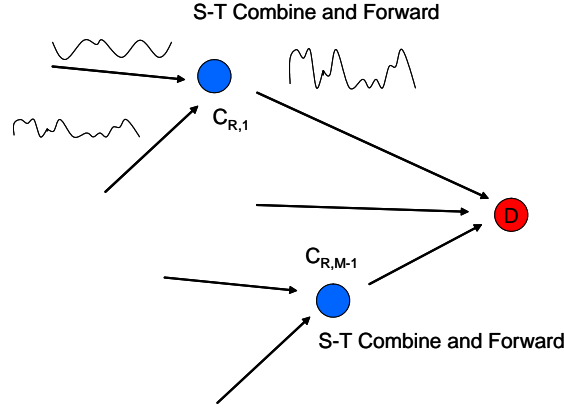


Figure 4.7: Combine-and-Forward cooperative reception technique principle.

Finally, the estimated symbols are

$$\begin{aligned}\tilde{s}_1 &= \sum_{j=1}^M (||\alpha_{j,1}||^2 + ||\alpha_{j,2}||^2) s_1 + \sum_{j=1}^M (\alpha_{j,1}^* n_1^j + \alpha_{j,2} n_2^{j*} + n_1'^j / K_c) \\ \tilde{s}_2 &= \sum_{j=1}^M (||\alpha_{j,1}||^2 + ||\alpha_{j,2}||^2) s_2 + \sum_{j=1}^M (\alpha_{j,2}^* n_1^j - \alpha_{j,1} n_2^{j*} + n_2'^j / K_c)\end{aligned}\quad (4.17)$$

From (4.13) and (4.17), it can be observed that the effective noise due to the cooperative reception techniques depends on the number of cooperative reception nodes  $M$  and the amplification factor  $K_c$ .

By using the two proposed cooperative reception techniques rather than the quantization technique, the transmission time can be reduced to  $N_{sb}/M_m$  where  $M_m$  is the number of bits/symbol of modulation technique used in the cooperative reception transmission in [16]. The reduced cooperative reception consumption will lead to a more energy efficient cooperative MIMO system.

### 4.3.2 Proposed Cooperative Reception Techniques Performance

For the trade-off of performance and energy consumption of cooperative reception technique, let us consider the amplification factors of the two cooperative reception technique  $K_c = \sqrt{4}$  and  $K_c = \sqrt{8}$  (6dB and 9dB energy amplification) for the performance simulation.

The performance of cooperative MIMO systems, using the two proposed cooperative reception techniques, in the presence of the transmission synchronization error with error range  $\Delta T_{syn} = 0.25T_s$  is presented in Fig. 4.8.

The performance degradation of cooperative MIMO systems using the cooperation strategy Forward-and-Combine (legend F-C in Fig. 4.8) with two and four cooperative

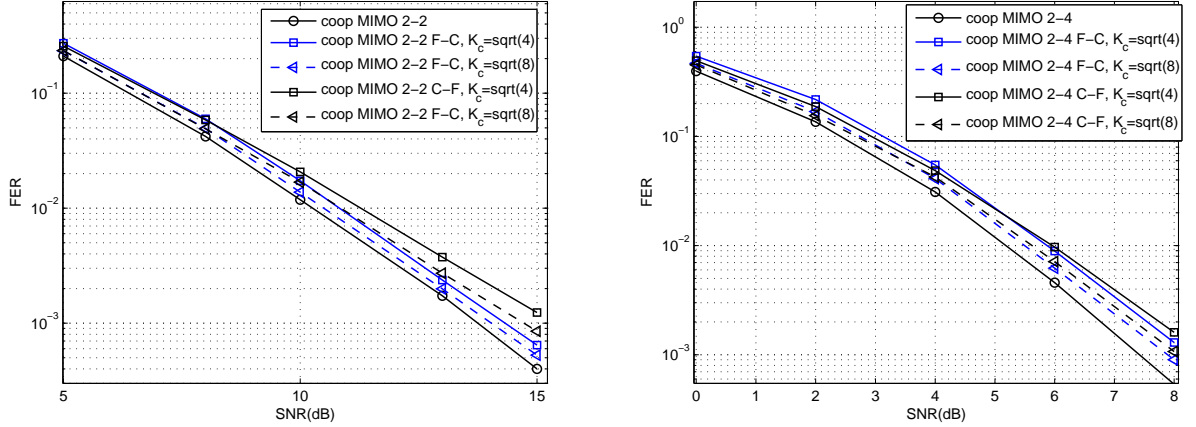


Figure 4.8: Performance of the proposed cooperative reception techniques, Alamouti STBC over a Rayleigh fading channel, transmission synchronization error  $\Delta T_{syn} = 0.25T_s$

reception nodes is acceptable for the amplification factor  $K_c = \sqrt{4}$  and  $K_c = \sqrt{8}$ . The performance degradation increases when the number of cooperative reception nodes increases or the amplification factor decreases.

For an amplification factor  $K_c = \sqrt{8}$  and the  $FER = 10^{-3}$  requirement, we lost  $0.3dB$  or  $1dB$  by using cooperative reception F-C technique or the C-F technique in cooperative MIMO 2-2 systems. And in a cooperative MIMO 2-4 system, we lost  $0.5dB$  or  $0.8dB$  by using cooperative reception strategy F-C or C-F.

The FER performance of cooperative reception strategy F-C is better than strategy C-F because of the smaller effective Gaussian noise. However in the C-F technique, most of the signal processing and combination calculations are distributed among the cooperative nodes. For some ad-hoc WSN applications, it is better than the strategy F-C where all calculations are centralized in the destination node D and the energy consumption of D will be higher than other cooperative reception nodes.

Moreover, if the number of cooperative transmission nodes is three or four, the OSTBC with the transmission rate  $3/4$  must be used for the complex symbol modulation. Therefore, the C-F technique have  $4/3$  times less analog symbols to be transmitted than the F-C technique. That helps to reduce the C-F circuit energy consumption, which dominates the total energy consumption in cooperative reception phase, by  $4/3$  times in comparison with the circuit energy of the F-C technique.

#### 4.4 Cooperative MIMO Energy Consumption

In spite of synchronization error at the cooperative transmission side and additive noise at the cooperative reception side, the cooperative MIMO performance is much better than

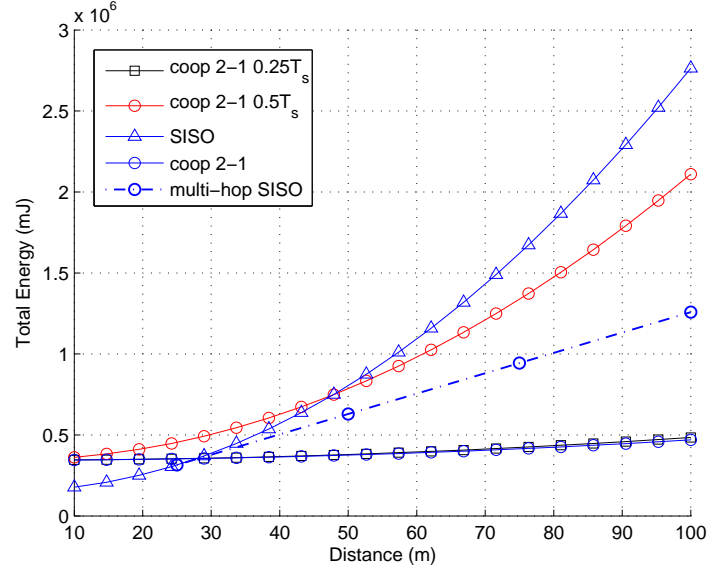


Figure 4.9: Total energy consumption of cooperative MISO vs. SISO and multi-hop SISO systems,  $FER = 10^{-3}$  requirement, power path-loss factor  $K = 2$ .

SISO performance for the synchronization range smaller as  $0.25T_s$  and amplification factor as great as  $K_c = \sqrt{4}$ . Therefore, we still have the transmission energy-efficiency advantage of cooperative MIMO technique over SISO technique or multi-hop SISO technique, like results in chapter 3, for the middle and long range transmission in WSN. The energy calculations were performed using the same energy consumption model presented in chapter 3 (based on the energy consumption parameters of [15]).

Fig. 4.9 shows the energy consumption comparison between the SISO, multi-hop SISO and cooperative MISO systems in the presence of transmission synchronization errors  $\Delta T_s = 0.25T_s$  and  $0.5T_s$ . It can be seen that the energy consumption of the cooperative MISO with the error range  $\Delta T_s = 0.25T_s$  (legend coop 2-1  $0.25T_s$ ) is as small as the perfect cooperative MISO 2-1 with the synchronization error  $\Delta T_s = 0$  (legend coop 2-1), and much better than the SISO and multi-hop SISO techniques. At the distance  $d = 100\text{m}$ , 80% or 60% energy is saved by using the cooperative MISO 2-1 (legend coop 2-1  $0.25T_s$ ) instead of SISO or multi-hop SISO techniques, respectively.

However, the performance of the cooperative MISO is not good enough to retain the energy consumption advantage over the multi-hop SISO with the synchronization error  $\Delta T_s = 0.5T_s$  and error rate requirement  $FER = 10^{-3}$ .

Fig. 4.10 shows the energy consumption comparison with the error rate requirement  $FER = 10^{-2}$ . With the lower required error rate, the energy consumption of the cooperative MISO in the presence of transmission error  $\Delta T_s = 0.5T_s$  is smaller than that of the

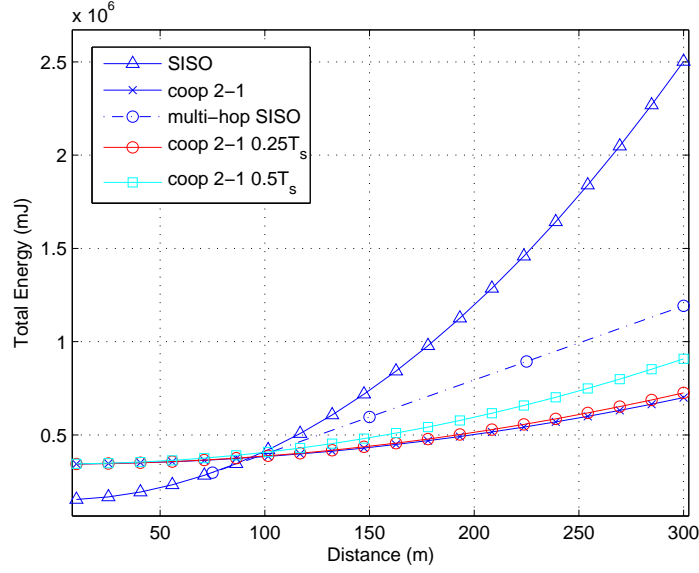


Figure 4.10: Total energy consumption of cooperative MISO vs. SISO and multi-hop SISO systems,  $FER = 10^{-2}$  requirement, power path-loss factor  $K = 2$ .

SISO and multi-hop SISO.

In comparison with the quantization technique used in [16], the two proposed strategies can reduce significantly the transmission time in cooperative reception, which reduces the cooperative energy consumption and the total energy consumption. Fig. 4.11 shows the energy consumption comparison between the two proposed cooperative reception techniques and the quantization technique (including the energy consumption of cooperative MISO 3-1 and 4-1). The transmission synchronization error range  $\Delta T_s = 0.25T_s$  at the transmission side and the amplification factor  $K_c = \sqrt{4}$  at the cooperative reception side are considered.

The energy consumption of the cooperative MIMO 2-2 using cooperative reception technique F-C is always smaller than the cooperative MISO 4-1 consumption, and smaller than cooperative MISO 3-1 consumption for distances  $d > 100m$ . At  $d = 500m$ , 25% energy is saved by using the cooperative MIMO 2-2 technique instead of the cooperative MISO 4-1 technique. In comparison with energy consumptions result in Fig. 3.9, it is obvious that the energy efficiency of the cooperative MIMO systems increases significantly by using the two proposed cooperative techniques.

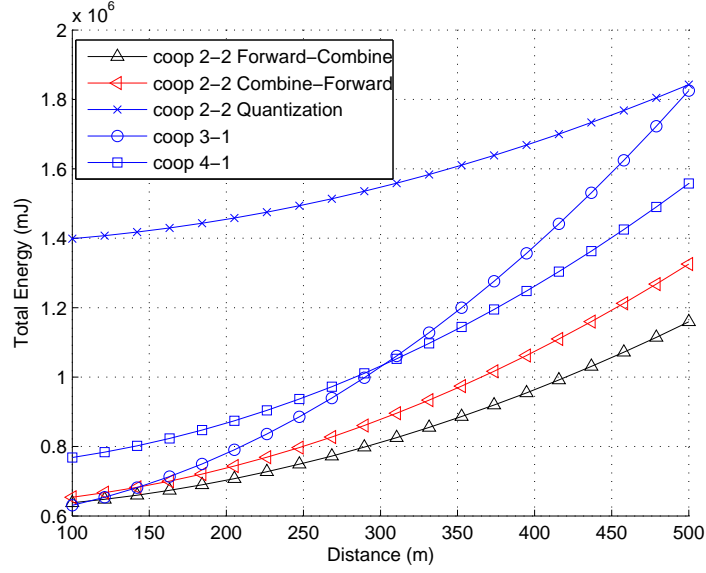


Figure 4.11: Total energy consumption of cooperative MIMO with different reception techniques vs. cooperative MISO,  $\Delta T_{syn} = 0.25T_s$ ,  $FER = 10^{-3}$  requirement, power path-loss factor  $K = 2$ .

### Optimal cooperative MIMO selection scheme

In the condition that the cooperative reception technique Forward-and-Combine (with the power amplification factor  $K_c = \sqrt{4}$ ) is used and the range of transmission synchronization errors  $\Delta T_{syn}$  equals to  $0.25T_s$ , the required  $SNR$  of the cooperative MIMO system for ensuring the error rate  $FER = 10^{-3}$  is presented in Tab. 4.1

$SNR$	$N = 1$	$N = 2$	$N = 3$	$N = 4$
$M = 1$	35.2 dB	22.5 dB	18.3 dB	16.5 dB
$M = 2$	20.6 dB	14.2 dB	12 dB	10.9 dB
$M = 3$	13.6 dB	10.4 dB	9.3 dB	8.6 dB
$M = 4$	11.1 dB	8.1 dB	7.3 dB	7 dB

Table 4.1:  $SNR$  requirement of cooperative MIMO system for  $FER = 10^{-3}$ , transmission synchronization error  $\Delta T_{syn} = 0.25T_s$ , Forward-and-Combine cooperative reception with  $K_c = \sqrt{4}$ , Rayleigh fading channel

Based on this required  $SNR$  values, the energy consumption optimal selection of transmit-receive nodes number in a function of transmission distances and the energy consumption lower bound of the cooperative MIMO system can be performed. Fig. 4.12 and 4.13 show the new optimal selection scheme and the new energy consumption lower bound, in comparison with the old lower bound (in Fig. 3.11).

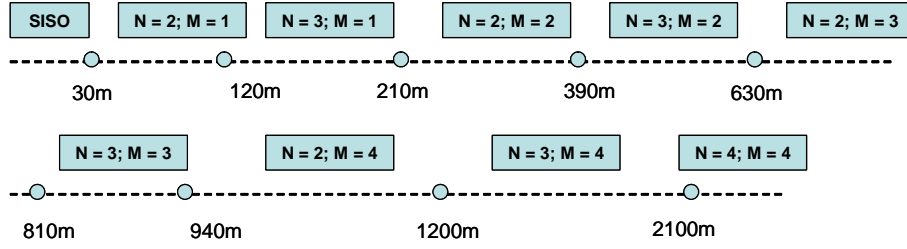


Figure 4.12: Optimal  $N - M$  transmit and receive antennas set selection as a function of transmission distance,  $FER = 10^{-3}$  requirement, Rayleigh fading channel with power path-loss factor  $K = 2$ .

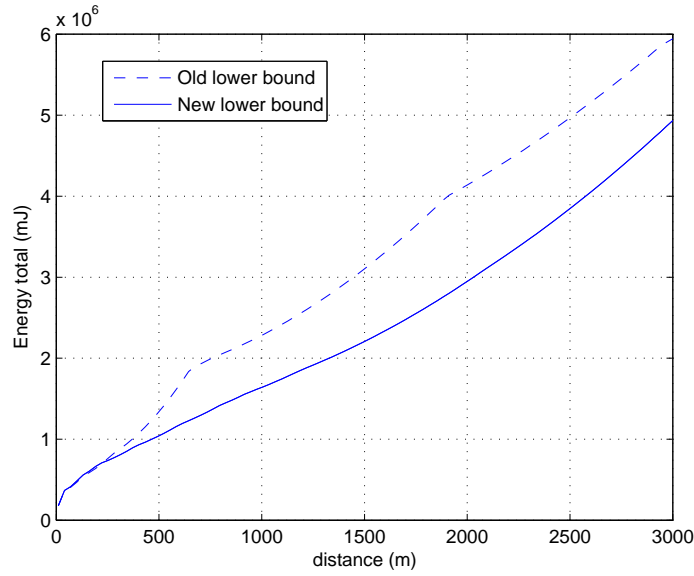


Figure 4.13: Energy consumption lower bound of cooperative MIMO systems,  $FER = 10^{-3}$  requirement, Rayleigh fading channel with power path-loss factor  $K = 2$ .

It can be seen that, the new bound is lower than the old one due to the cooperation energy saved by using the proposed Forward-and-Combine technique instead of the quantization reception technique.

## 4.5 Conclusion

The effects of transmission synchronization error, channel estimation error and cooperative reception techniques on the performance of cooperative MIMO were investigated in this chapter. The performance degradation increases with the transmission synchronization error range and the number of cooperative transmission and reception nodes. However, the cooperative MIMO system is rather tolerant for small range of transmission synchronization error and the degradation is negligible for synchronization error range as small as  $0.25T_s$  (and small for error range as small as  $0.5T_s$ ). This error range is reasonable for a low speed transmission in WSN, where the symbols duration is approximated as 20 to  $200\mu s$  (for a transmission rate from 10 to 100kbps using un-coded QPSK modulation) with the delay profile distribution of the channel and the precision level of clock synchronization process in WSN are around several to  $10\mu s$  [60], [26], [76], [30].

Two cooperative reception techniques were also proposed for a better energy-efficiency than the previous cooperative reception technique. The first consists in performing the whole space-time combination at the destination node, and in the second signal processing and space time combination are done independently at each cooperative node.

For small transmission synchronization errors, the performance degradation is small enough to keep the energy efficiency advantage of cooperative MISO system over SISO and multi-hop SISO techniques. Moreover, by using the two proposed cooperative reception techniques, the new cooperative MIMO system is much more energy-efficient and easily outperforms the cooperative MISO technique for long range transmission.

However, the performance degradation is significant for transmission synchronization errors as large as  $0.75T_s$ . Therefore, a new space-time combination technique, which has a better performance and low complexity, is proposed in chapter 5.

## Chapter 5

# MSOC Combination for Un-synchronized Cooperative MIMO Transmissions

### 5.1 Introduction

In wireless distributed networks, transmission synchronization errors lead to performance degradation of STBC in a cooperative MIMO system and affects the energy efficiency advantage of cooperative MIMO system over SISO system [74] [47].

In chapter 4, the analysis of the transmission synchronization error effect for two cooperative transmission nodes using Alamouti codes has been investigated. For small range of transmission synchronization error, the performance degradation is negligible and the cooperative MISO system performance is rather tolerant. However, for large ranges of error, the performance decreases quickly and the degradation is significant. Fine synchronization techniques [90] can be used to obtain a better time synchronization precision, but at the cost of energy and processing time.

In this chapter, a new efficient space time combination technique is proposed for the un-synchronized transmission cooperative MISO systems. The principle of the Multiple Sampling Orthogonal Combination (MSOC) technique is proposed. The multiple sampling of the received signal and the combination from different sampled sequences enable to reconstruct the space time orthogonal combination of STBC in the presence of transmission synchronization error. The proposed technique has a low complexity algorithm as the traditional combination technique and has a better performance. In this chapter, the efficiency of this technique is demonstrated for the case of two, three and four cooperative transmission nodes using Alamouti and max-SNR STBC. Otherwise, this principle can be extended to an arbitrary Orthogonal STBC which satisfies a required coding matrix



condition.

Some other space-time codes like time-reversal block codes have also a good tolerance towards the transmission synchronization errors [91, 66], but have some drawbacks such as a reduced data rate and a more complex combination algorithm. With this new proposed combination technique, we retain not only the full data rate for the case of two transmission nodes (or the 3/4 data rate for the case of three and four transmission nodes), but also the low complexity algorithm of traditional STBC codes. Our approach is also different from distributed space time coding from [33] where the delay must be a multiple of the symbol duration.

The rest of this chapter is organized as follows. The transmission synchronization error effect on the performance of cooperative MISO systems using the max-SNR STBC is presented in Section 5.2. In Section 5.3, the synchronization processes and the new modified space-time combination technique for two, three and four transmission nodes are proposed. The performance of the new space time combination technique is proved by simulation results.

## 5.2 Effect of Transmission Synchronization Error on the performance of the max-SNR OSTBC

In chapter 4, the analysis of the transmission synchronization error effect for two cooperative transmission nodes using Alamouti codes has been investigated. In the case of a cooperative MISO system with three and four transmission nodes using other OSTBC, due to more transmission space-time sequences in the same time and more symbols in one space-time block, there are more ISI from un-synchronized sequences at the receiver and more *non – desired* terms after the space time combination. The effect of transmission synchronization error is thus more significant. Instead of using the Tarokh STBC for the case of three and four transmission nodes (like in chapter 4), cooperative MIMO system can use other STBC with the same performance like max-SNR STBC [31]. The coding matrices of the max-SNR STBC are

$$\mathbf{C}_{m3} = \begin{bmatrix} s_1 & s_2 & s_3 \\ -s_2^* & s_1^* & 0 \\ -s_3^* & 0 & s_1^* \\ 0 & -s_3^* & s_2^* \end{bmatrix}, \mathbf{C}_{m4} = \begin{bmatrix} s_1 & s_2 & s_3 & 0 \\ -s_2^* & s_1^* & 0 & s_3 \\ -s_3^* & 0 & s_1^* & -s_2 \\ 0 & -s_3^* & s_2^* & s_1 \end{bmatrix} \quad (5.1)$$

In the max-SNR coding matrix, the positions of the zero symbols avoid the ISI to the other neighbour symbols in the presence of synchronization errors. In this case, less ISI

is generated, so that the performance of max SNR is expected to be better than the full-diversity Tarokh STBC in the unsynchronized transmission cooperative MIMO systems.

Let us consider a cooperative transmission with four cooperative transmission nodes using STBC  $\mathbf{C}_{m4}$ , where the receiver is synchronized to transmission node 1 which is considered to have the most reliable channel. The four received symbols are

$$r_1[i] = r(t = iT_s + \delta_1) = \alpha_1 c_1[i] + n(iT_s + \delta_1) + \sum_{m=2}^4 (\alpha_m c_m[i] p(\delta_1 - \delta_m) + ISI_m^i(\delta_1 - \delta_m)), i = 1..4. \quad (5.2)$$

By using the traditional combination technique, the estimated symbol  $\tilde{s}_1$  is

$$\begin{aligned} \tilde{s}_1 &= \alpha_1^* r_1[1] + \alpha_2^* r_1[2] + \alpha_3^* r_1[3] + \alpha_4^* r_1[4] \\ &= \alpha_1^* [\alpha_1 s_1 + \alpha_2 (s_2 p(\delta_1 - \delta_2) + ISI_2^1(\delta_1 - \delta_2)) + \alpha_3 (s_3 p(\delta_1 - \delta_3) + ISI_3^1(\delta_1 - \delta_3)) \\ &\quad + \alpha_4 ISI_4^1(\delta_1 - \delta_4) + n_1[1]] \\ &\quad + \alpha_2 [-\alpha_1^* s_2 + \alpha_2^* (s_1 p(\delta_1 - \delta_2) + ISI_2^2(\delta_1 - \delta_2)^* + \alpha_3^* ISI_3^2(\delta_1 - \delta_3)^* + \alpha_4^* (s_3^* p(\delta_1 - \delta_4) \\ &\quad + ISI_4^2(\delta_1 - \delta_4)^*) + n_1^*[2])] \\ &\quad + \alpha_3 [-\alpha_1^* s_3 + \alpha_2^* ISI_2^3(\delta_1 - \delta_2)^* + \alpha_3^* (s_1 p(\delta_1 - \delta_3) + ISI_3^3(\delta_1 - \delta_3)^*) + \alpha_4^* (-s_2^* p(\delta_1 - \delta_4) \\ &\quad + ISI_4^3(\delta_1 - \delta_4)^*) + n_1^*[3]] \\ &\quad + \alpha_4^* [0 + \alpha_2 (-s_3^* p(\delta_1 - \delta_2) + ISI_2^4(\delta_1 - \delta_2)) + \alpha_3 (s_2^* p(\delta_1 - \delta_3) + ISI_3^4(\delta_1 - \delta_3)) \\ &\quad + \alpha_4 (s_1 p(\delta_1 - \delta_4) + ISI_4^4(\delta_1 - \delta_4)) + n_1[4]] \\ &= \underbrace{(|\alpha_1|^2 + |\alpha_2|^2 p(\delta_1 - \delta_2) + |\alpha_3|^2 p(\delta_1 - \delta_3) + |\alpha_4|^2 p(\delta_1 - \delta_4)) s_1}_{\text{desired signal}} \\ &\quad + \underbrace{\alpha_1^* \alpha_2 s_2 (p(\delta_1 - \delta_2) - 1) + \alpha_3 \alpha_4^* s_2^* (p(\delta_1 - \delta_2) - p(\delta_1 - \delta_2)) + \alpha_1^* \alpha_3 s_3 (p(\delta_1 - \delta_3) - 1) + \alpha_2 \alpha_4^* s_3^* (p(\delta_1 - \delta_4) - p(\delta_1 - \delta_2))}_{\text{non-desired signals}} \\ &\quad + \underbrace{\alpha_1^* (\alpha_2 ISI_2^1(\delta_1 - \delta_2) + \alpha_3 ISI_3^1(\delta_1 - \delta_3) + \alpha_4 ISI_4^1(\delta_1 - \delta_4) + n_1[1]) + \dots}_{\text{ISI and noise terms}} \end{aligned} \quad (5.3)$$

A similar result is obtained for estimated values of symbols  $s_2$  and  $s_3$  (presented in appendix A), the desired symbol amplitude decreases and an interference (*non-desired signals* terms) of  $s_1$  and  $s_3$  (or  $s_1$  and  $s_2$ ) appears after the space-time combination.

In the presence of transmission synchronization error, the orthogonality of STBC can not be obtained by using the traditional space time combination technique. This leads to the performance degradation of max-SNR STBC in cooperative MIMO system. The performance is affected depending on the level of synchronization error range and the number of cooperative transmission nodes. More transmission energy consumption is

therefore needed to ensure the same error rate requirement, affecting the energy efficiency advantage of cooperative MIMO system over SISO and multi-hop SISO systems.

Fig. 5.1 shows the *FER* simulation results of the non-cooperative MISO system using Tarokh STBC (legend *MISO 4-1*) and the cooperative MISO system using Tarokh and max-SNR STBC with the transmission nodes  $N = 4$  and the transmission synchronization error ranges  $\Delta T_{syn} = 0.25T_s, 0.5T_s$  and  $0.75T_s$ .

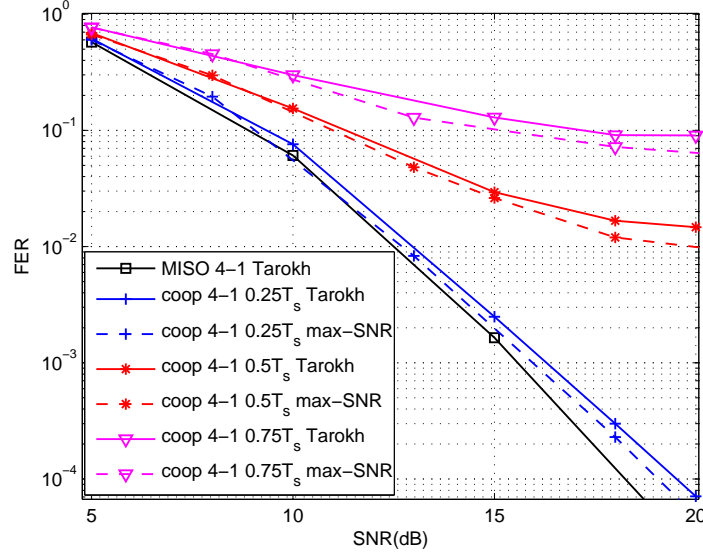


Figure 5.1: Effect of transmission synchronization error on the performance of cooperative MISO systems with four transmit nodes  $N = 4$ , using Tarokh and max-SNR STBC over a Rayleigh fading channel.

For a small synchronization error range  $\Delta T_{syn} = 0.25T_s$ , the performance degradation of the cooperative MISO 4-1 is negligible. However, the system performance decreases and saturates quickly when the error range increases. We can also observe that the performance of max-SNR STBC is better than Tarokh STBC in the presence of transmission synchronization error due to the less occurred ISI.

### 5.3 Multiple Sampling Orthogonal Combination Technique

In formulas (4.5) and (5.3), besides the ISI generated after the synchronization and sampling processes, the performance degradation is caused mainly by the non-orthogonal space-time combination of the received symbols values. By using a modified synchronization and combination process, we can re-construct the orthogonal space-time combination in order to increase the performance of cooperative MISO systems in the presence of transmission synchronization error.

### 5.3.1 Synchronization Technique

Let us consider that the receiver can determine the time offset to synchronize perfectly the sequences from different cooperative transmission nodes. For example, each cooperative node uses a different known preamble  $Pr_k$  for the signal synchronization purpose (the preamble sequences  $Pr_k$ ,  $k = 1..N$ , are orthogonal to each other). After the over sampling process (in the preamble part of the received signal), the receiver can perform the multiple correlations between the received signal and the known preamble of each cooperative node in order to determine the peak of correlation and the time offset corresponding to each arriving sequence, as illustrated in Fig. 5.2

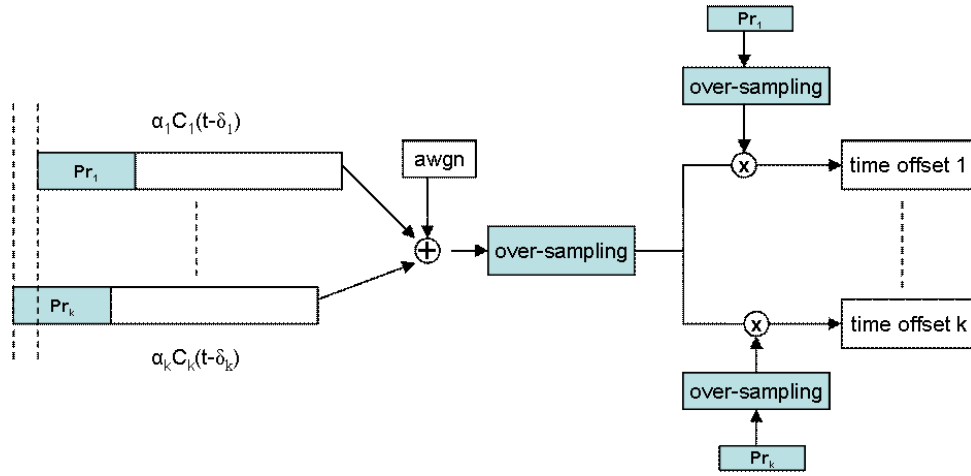


Figure 5.2: Signal synchronization process of the MSOC combination technique

The received signal is then sampled sequentially with  $N$  time offsets, and the  $N$  different sampled sequences corresponding to  $N$  sequences arriving from  $N$  cooperative nodes are obtained. The  $i^{th}$  symbol value of sampled sequence  $k$  can be expressed as

$$\begin{aligned}
 r_k[i] &= r(t = iT_s + \delta_k) = \alpha_k c_k[i] + n(iT_s + \delta_k) \\
 &+ \sum_{m=1, m \neq k}^N (\alpha_m c_m[i] p(\delta_k - \delta_m) + ISI_m^i(\delta_k - \delta_m))
 \end{aligned} \tag{5.4}$$

Then, the  $N$  sampled sequences are registered to  $N$  different memory banks for the space time combination in the next step.

In the case that the received signal is over-sampled both in preamble and information parts, the receiver just takes a sampled sequence that corresponds to the time offset  $i$  of the cooperative node  $i$ .

### 5.3.2 Space-time Combination Technique

#### Two cooperative transmission nodes

The principle of the MSOC combination technique, for two transmit nodes, is illustrated in Fig.5.3. For one Alamouti block of two transmitted symbols, instead of registering two sampled values, the receiver needs to register four values from two sampled sequences  $r_1$  and  $r_2$ .

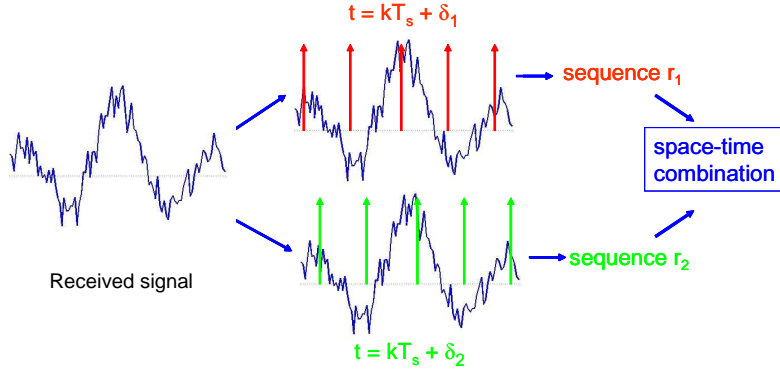


Figure 5.3: MSOC space-time combination technique

Considering that the receiver can synchronize (i.e. determine the time offsets) perfectly to the two sequences from cooperative transmission nodes, the two sampled values corresponding to node 1 are:

$$\begin{aligned} r_1[1] &= r(t = T_s + \delta_1) = \alpha_1 c_1[1] + \alpha_2 c_2[1]p(\delta_1 - \delta_2) + \alpha_2 ISI_2^1(\delta_1 - \delta_2) + n_1[1] \\ r_1[2] &= r(t = 2T_s + \delta_1) = \alpha_1 c_1[2] + \alpha_2 c_2[2]p(\delta_1 - \delta_2) + \alpha_2 ISI_2^2(\delta_1 - \delta_2) + n_1[2] \end{aligned} \quad (5.5)$$

and the two sampled values corresponding to node 2 are:

$$\begin{aligned} r_2[1] &= r(t = T_s + \delta_2) = \alpha_1 c_1[1]p(\delta_2 - \delta_1) + \alpha_1 ISI_1^1(\delta_2 - \delta_1) + \alpha_2 c_2[1] + n_2[1] \\ r_2[2] &= r(t = 2T_s + \delta_2) = \alpha_1 c_1[2]p(\delta_2 - \delta_1) + \alpha_1 ISI_1^2(\delta_2 - \delta_1) + \alpha_2 c_2[2] + n_2[2] \end{aligned} \quad (5.6)$$

The space-time combination technique of Alamouti codes can be modified in order to re-construct the orthogonal space-time combination from the two sampled sequences  $r_1$  and  $r_2$ . Taking into account the symmetry property of the raised cosine pulse shape  $p(\delta_1 - \delta_2) = p(\delta_2 - \delta_1)$ , the two sampled sequences  $r_1$  and  $r_2$  are space-time combined and

the two estimated symbols are given by

$$\begin{aligned}
 \tilde{s}_1 &= \alpha_1^* r_1[1] + \alpha_2 r_2^*[2] = \|\alpha_1\|^2 s_1 + \alpha_1^* \alpha_2 s_2 p(\delta_1 - \delta_2) + \alpha_1^* (\alpha_2 ISI_2^1(\delta_1 - \delta_2) \\
 &\quad + n_1[1]) - \alpha_1^* \alpha_2 s_2 p(\delta_2 - \delta_1) + \|\alpha_2\|^2 s_1 + \alpha_2 (\alpha_1 ISI_1^2(\delta_2 - \delta_1) + n_2[2])^* \\
 &= \underbrace{(\|\alpha_1\|^2 + \|\alpha_2\|^2) s_1}_{\text{desired signal}} + \underbrace{\alpha_1^* (\alpha_2 ISI_2^1(\delta_1 - \delta_2) + n_1[1]) + \alpha_2 (\alpha_1 ISI_1^2(\delta_2 - \delta_1) + n_2[2])^*}_{\text{ISI and noise terms}} \\
 \tilde{s}_2 &= \alpha_2^* r_2[1] - \alpha_1 r_1^*[2] = \alpha_1 \alpha_2^* s_1 p(\delta_1 - \delta_2) + \alpha_2^* (\alpha_1 ISI_1^1(\delta_2 - \delta_1) \\
 &\quad + n_2[1]) + \|\alpha_2\|^2 s_2 + \|\alpha_1\|^2 s_2 - \alpha_1 \alpha_2^* s_1 p(\delta_2 - \delta_1) - \alpha_1 (\alpha_2 ISI_2^2(\delta_1 - \delta_2) + n_1[2])^* \\
 &= \underbrace{(\|\alpha_1\|^2 + \|\alpha_2\|^2) s_2}_{\text{desired signal}} + \underbrace{\alpha_2^* (\alpha_1 ISI_1^1(\delta_2 - \delta_1) + n_2[1]) - \alpha_1 (\alpha_2 ISI_2^2(\delta_1 - \delta_2) + n_1[2])^*}_{\text{ISI and noise terms}}
 \end{aligned} \tag{5.7}$$

In comparison with the estimated symbols in formula (4.5), the amplitude of the desired symbol in formula (5.7) does not decrease and the interference between two symbols  $s_1$  and  $s_2$  (non-desired signal) does not appear after space-time combination. The orthogonal space-time combination is achieved and the signal to interference noise ratio (SINR) increases. Therefore, the performance of the proposed combination technique will be better than the traditional combination in the presence of transmission synchronization error.

### Three and four cooperative transmission nodes

Due to the nature of the proposed combination technique, the condition of the orthogonal space-time coding matrix must be  $\mathbf{C}_{ij} = -\mathbf{C}_{ji}^*$  (with  $i \neq j$ ) in order to reconstruct the orthogonality in the presence of transmission synchronization error. Not all orthogonal STBCs can satisfy this condition. For the case of 3 and 4 transmission nodes using Tarokh STBC for complex symbol modulation [94], we can not perform the orthogonal reconstruction combination. However, the max-SNR orthogonal STBC (non-full diversity) in [31] satisfies the required condition  $\mathbf{C}_{ij} = -\mathbf{C}_{ji}^*$ . Therefore, the proposed MSOC combination technique can be used to obtain better performance in the presence of transmission synchronization error.

For the case of four cooperative transmission nodes using max-SNR STBC  $C_4$ , after performing the four different bit synchronization and sampling processes corresponding to the delays of the four different cooperative transmission nodes, the receiver combines the symbol values of the four different sampled sequences,  $r_k$  with  $k = 1..4$ , to reconstruct the orthogonal combination. The space-time combination algorithm and the estimated symbol  $\tilde{s}_1$  are given as follow:

$$\begin{aligned}
 \tilde{s}_1 &= \alpha_1^* r_1[1] + \alpha_2 r_2^*[2] + \alpha_3 r_3^*[3] + \alpha_4^* r_4[4] \\
 &= \alpha_1^* [\alpha_1 s_1 + \alpha_2 (s_2 p(\delta_1 - \delta_2) + ISI_2^1(\delta_1 - \delta_2)) + \alpha_3 (s_3 p(\delta_1 - \delta_3) + ISI_3^1(\delta_1 - \delta_3)) \\
 &\quad + \alpha_4 ISI_4^1(\delta_1 - \delta_4) + n_1[1]] \\
 &\quad + \alpha_2 [-\alpha_1^* (s_2 p(\delta_2 - \delta_1) + ISI_1^2(\delta_2 - \delta_1)^*) + \alpha_2^* s_1 + \alpha_3^* ISI_3^2(\delta_2 - \delta_3)^* + \alpha_4^* (s_3^* p(\delta_2 - \delta_4) \\
 &\quad + ISI_4^2(\delta_2 - \delta_4)^*) + n_2^*[2]] \\
 &\quad + \alpha_3 [-\alpha_1^* (s_3 p(\delta_3 - \delta_1) + ISI_1^3(\delta_3 - \delta_1)^*) + \alpha_2^* ISI_2^3(\delta_3 - \delta_2)^* + \alpha_3^* s_1 + \alpha_4^* (-s_2^* p(\delta_3 - \delta_4) \\
 &\quad + ISI_4^3(\delta_3 - \delta_4)^*) + n_3^*[3]] \\
 &\quad + \alpha_4^* [\alpha_1 (ISI_1^4(\delta_4 - \delta_1)) + \alpha_2 (-s_3^* p(\delta_4 - \delta_2) + ISI_2^4(\delta_4 - \delta_2)) + \alpha_3 (s_2^* p(\delta_4 - \delta_3) \\
 &\quad + ISI_3^4(\delta_4 - \delta_3)) + \alpha_4 s_1 + n_4[4]] \\
 &= \underbrace{(|\alpha_1|^2 + |\alpha_2|^2 + |\alpha_3|^2 + |\alpha_4|^2) s_1}_{\text{desired signal}} \\
 &\quad + \underbrace{\alpha_1^* (\alpha_2 ISI_2^1(\delta_1 - \delta_2) + \alpha_3 ISI_3^1(\delta_1 - \delta_3) + \alpha_4 ISI_4^1(\delta_1 - \delta_4) + n_1[1]) + \dots}_{\text{ISI and noise terms}} \tag{5.8}
 \end{aligned}$$

Thanks to the structure of the max-SNR STBC matrix and the MSOC combination technique, the space time orthogonal combination is achieved in formula (5.8). In comparison with the combination result in formula (5.3), the desired signal amplitude does not decrease and the non-desired interferences between the symbols  $s_1, s_2, s_3$  do not appear. Like in the case of two cooperative transmission nodes, the performance of the proposed combination technique is only affected by the *ISI* terms and will be much better than the performance of traditional combination technique in the presence of transmission synchronization errors. The combination algorithm and estimated values of symbols  $\tilde{s}_2$  and  $\tilde{s}_3$  are presented in appendix B.

For the case of three transmission nodes, the combination algorithm and estimated results are the same as the case of four nodes without the presence of the fourth STBC sequence and  $\alpha_4$  channel value terms. This efficient combination principle can be extended to other cooperative MIMO systems with an arbitrary number of transmission nodes and other orthogonal STBCs which satisfy the required coding matrix condition  $\mathbf{C}_{ij} = -\mathbf{C}_{ji}^*$  (with  $i \neq j$ ) (e.g. cooperative MIMO systems using the Tarokh STBC for real signal modulation in [94] with the number of cooperative transmission nodes from 2 to 8).

### 5.3.3 Performance of the MSOC Technique

Fig. 5.4 shows the *FER* simulation results of the cooperative MISO 2-1 system with a perfect transmission synchronization (legend *MISO 2-1*) and the cooperative MISO 2-1 system with the proposed MSOC space-time combination technique (legend *MSOC coop 2-1*) versus the traditional Alamouti combination technique (legend *coop 2-1*) in the presence

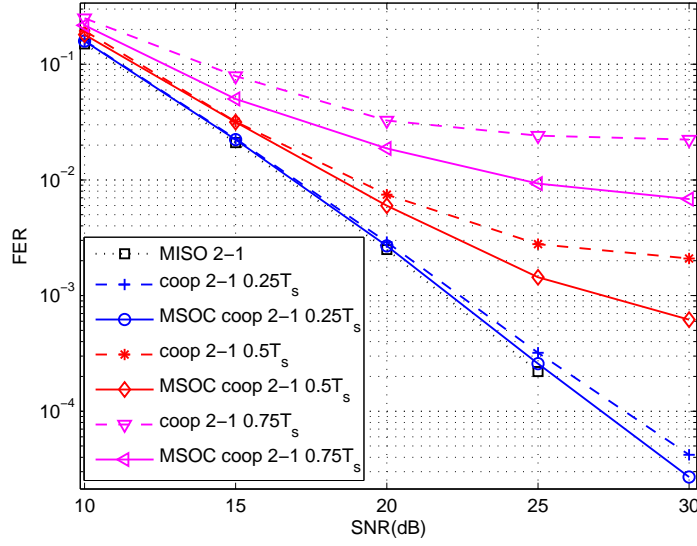


Figure 5.4: FER of MSOC technique vs. traditional combination technique with two transmission nodes, QPSK modulation over a Rayleigh channel

of transmission synchronization errors  $\Delta T_{syn} = 0.25T_s, 0.5T_s$  and  $0.75T_s$ .

For a small synchronization error range  $\Delta T_{syn} = 0.25T_s$ , the performance degradation of the cooperative MISO 2-1 is negligible and the performance of the MSOC technique is better than the traditional combination technique. For  $\Delta T_{syn} = 0.5T_s$  and  $FER = 2 \cdot 10^{-3}$  requirement, a gain of 6dB can be obtained by using the proposed MSOC combination technique.

Fig. 5.5 and Fig. 5.6 show the  $FER$  simulation results of the non-cooperative MISO 3-1 and MISO 4-1 system using max-SNR STBC (legend *MISO 3-1* and *MISO 4-1*) and the corresponding cooperative MISO systems with the proposed MSOC space-time combination technique (legend *MSOC coop 3-1* and *MSOC coop 4-1*) versus the traditional combination technique (legend *coop 3-1* and *coop 4-1*) in the presence of transmission synchronization error ranges  $\Delta T_{syn} = 0.25T_s, 0.5T_s$  and  $0.75T_s$ .

As in the case of cooperative MISO 2-1 system, the performance degradation of cooperative MISO system is rather small for a transmission synchronization error as small as  $0.25T_s$ . For a synchronization error  $\Delta T_{syn}$  larger than  $0.25T_s$ , the performance of the traditional combination technique decreases and saturates quickly, but the performance of the new combination technique remains acceptable until  $\Delta T_{syn} = 0.5T_s$ .

For the case of three cooperative transmission nodes shown in Fig. 5.5, with error range  $\Delta T_{syn} = 0.5T_s$ , a gain of 4dB can be achieved at  $FER = 10^{-2}$  by using the new MSOC technique. And for the case of four cooperative transmission nodes shown in Fig. 5.6, with



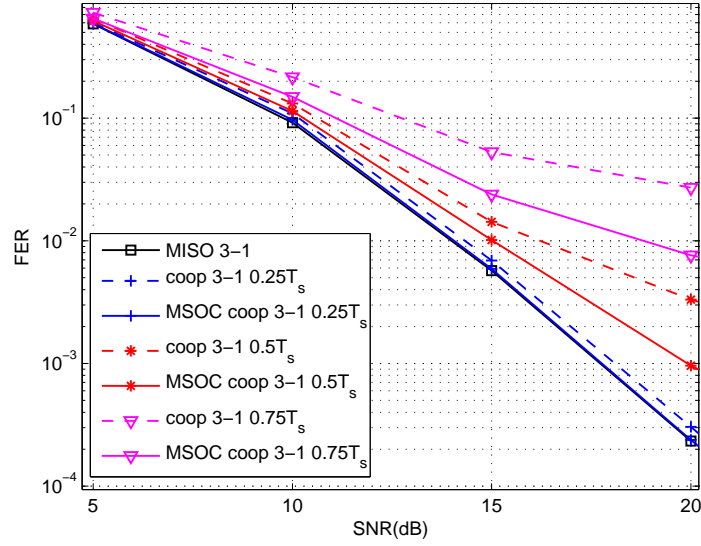


Figure 5.5: FER of MSOC technique vs. traditional combination technique with three transmission nodes, QPSK modulation over a Rayleigh channel

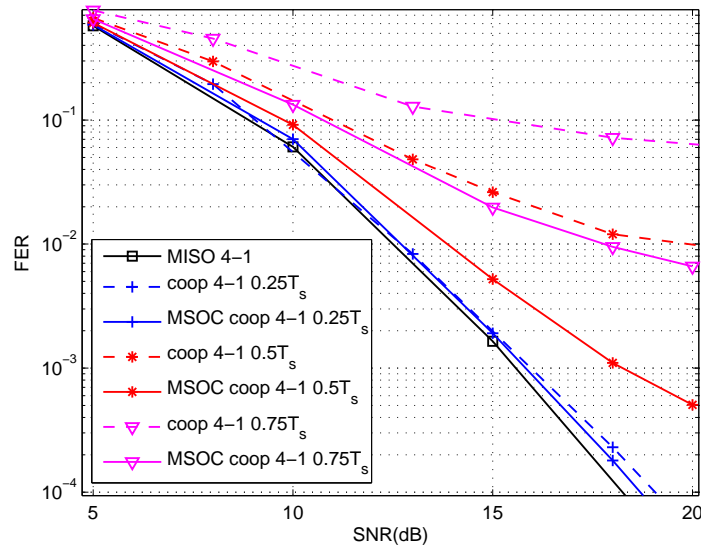


Figure 5.6: FER of MSOC technique vs. traditional combination technique with four transmission nodes, QPSK modulation over a Rayleigh channel

error range  $\Delta T_{syn} = 0.5T_s$ , a gain of more than 6dB can be achieved at  $FER = 10^{-2}$  by using the new MSOC technique.

## 5.4 Energy consumption of MSOC Technique

For small range of transmission synchronization error  $\Delta T_{syn} \leq 0.25T_s$ , the performance difference between the two combination techniques is small, and therefore the energy consumption difference is negligible. However, as the synchronization error increases, the performance gap between the two combination techniques increases quickly which leads to a lower energy consumption of the MSOC technique.

Fig. 5.7 shows the energy consumption of a cooperative MISO 2-1 system using the MSOC technique and traditional combination technique for the error rate requirement  $FER = 10^{-3}$  and the synchronization error range  $\Delta T_{syn} = 0.5T_s$ . It can be seen that the cooperative MISO with the traditional combination technique (legend *coop 2-1 0.5T<sub>s</sub>*) is less efficient than the multi-hop SISO technique. At  $d = 100m$ , the new combination technique (legend *coop 2-1 0.5T<sub>s</sub> MSOC*) can save 66% the total energy consumption of the traditional combination technique.

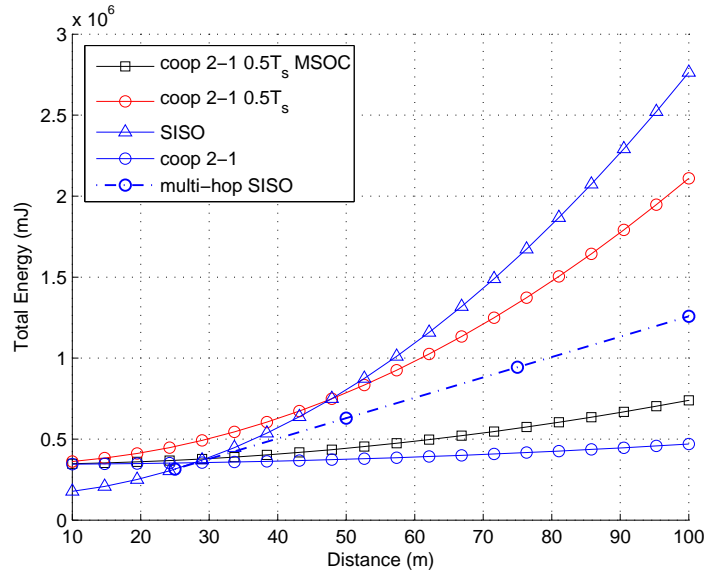


Figure 5.7: Energy consumption of new combination and traditional combination,  $N=2$ ,  $M=1$ ,  $FER = 10^{-3}$

Fig. 5.8 shows the energy consumption of the cooperative MISO systems (with three and four transmit nodes) using the proposed MSOC technique and the traditional combination technique for an error rate requirement  $FER = 10^{-2}$  (the traditional combination

technique can not support the error rate as low as  $FER = 10^{-3}$ , shown in Fig. 5.5 and 5.6) in the presence of the synchronization error with  $\Delta T_{syn} = 0.5T_s$ .

At  $d = 500m$ , the cooperative MISO with three transmit nodes using the new combination technique (legend *MSOC coop 3-1 0.5T<sub>s</sub>*) can save 20% the total energy consumption of the cooperative MISO 3-1 using the traditional combination technique (legend *coop 3-1 0.5T<sub>s</sub>*). The cooperative MISO with four transmit nodes using the new combination technique (legend *MSOC coop 4-1 0.5T<sub>s</sub>*) can save 40% the total energy consumption of the cooperative MISO 4-1 using the traditional combination technique. When the error rate requirement increases (e.g.  $FER = 10^{-3}$ ), the energy consumption advantage of the new MSOC combination will increase.

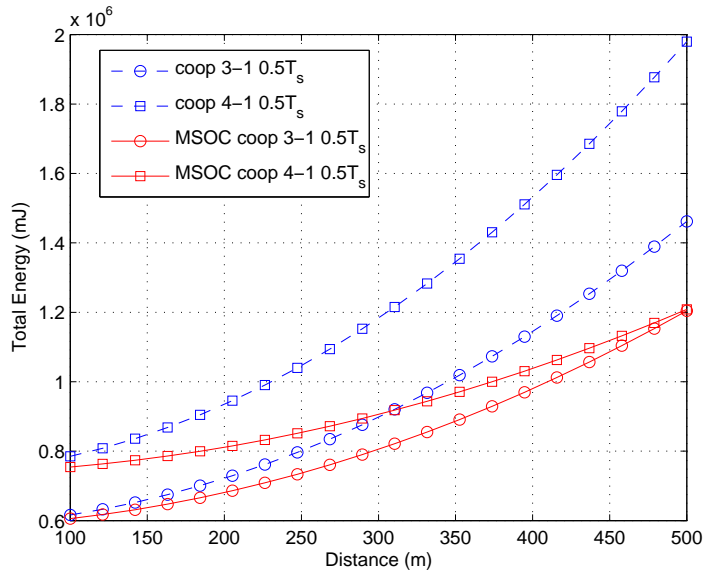


Figure 5.8: Energy consumption of new combination and traditional combination,  $N=3$  and  $4$ ,  $M=1$ ,  $FER = 10^{-2}$

## 5.5 Conclusion and Discussion

In the context of cooperative MIMO system where system performances are affected by a non-desired unsynchronized MISO transmission, a new efficient space-time combination technique MSOC (Multiple Sampling Orthogonal Combination) for unsynchronized cooperative MISO transmission was proposed. Since the proposed MSOC technique can reconstruct the orthogonal combination of STBC in the presence of transmission synchronization errors, it has much better performance than the traditional combination technique, especially for large transmission synchronization error ranges.

By using this new technique, a better performance can be achieved and the tolerance

to the transmission synchronization error of cooperative MISO systems increases. Consequently, less transmission energy is needed for cooperative MISO (or cooperative MIMO) systems.

Although results in this chapter were performed with cooperative MISO systems using Alamouti and max-SNR STBCs for complex symbol modulations, the proposed MSOC principle can also be extended to other cooperative MIMO systems with an arbitrary number of transmission nodes with an orthogonal STBC which satisfies the required coding matrix condition (e.g. the cooperative MIMO system using Tarokh STBCs for real signal modulation in [94] with the number of cooperative transmission nodes from 2 to 8).

This new proposed combination technique retains not only the full data rate transmission for the case of two transmit nodes (or the 3/4 rate for the case of three and four transmit nodes), but also the low complexity algorithm of the traditional STBC codes.

For the MSOC technique implementation, the traditional combination receiver just needs a small modification in synchronization and sampling processes of the base-band signal. The only drawback of the new combination technique is that the receiver has to synchronize  $N$  times the received signal and register  $N$  times the sampled values, but the extra processing time and the memory resource cost are reasonable.

## Chapter 6

# Cooperative MIMO and Relay Association Strategy

### 6.1 Introduction

In wireless distributed networks where multiple antennas can not be installed in one wireless node, cooperative relay techniques can be used to exploit the spatial and temporal diversity gain. Relay techniques have been known as a simple and energy efficient technique to extend the transmission range due to their simplicity and their performance for wireless transmissions over fading channels [58], [85] and [57]. In a relay cooperative network, the received signals coming from different independent fading channels are combined, so that the probability of deep fading is minimized. The result is that the system performance is improved [75], [43] or less transmission energy consumption is needed for the same performance.

In chapter 2, relay and cooperative MIMO techniques are proposed as cooperative solutions which help to increase the performance or reduce the energy consumption in WSNs. The performance and the energy consumption of these two cooperative techniques are investigated in this chapter. The detailed comparison between relay and cooperative MIMO techniques in terms of performances and energy consumption shows that cooperative MIMO techniques have some advantages over relay techniques. But under certain conditions, the relay is better than cooperative MIMO techniques (e.g. in the presence of large transmission synchronization error).

The best choice between these two cooperative techniques for WSN depends on the particular network structure or on the application, i.e. the position and number of cooperative (or relay) wireless nodes, the power path loss factor, the transmission synchronization process. In this context, an association strategy of these two techniques is proposed, in this chapter, in order to exploit simultaneously the advantages of these two techniques.

The principle of this association strategy is that a cooperative MIMO technique is employed at multiple relay nodes to retransmit the signal by using a MIMO transmission in one transmission phase instead of multiple transmission phases of the traditional parallel relay technique. This technique follows the same idea as the Space-Time Relaying techniques or Distributed Space Time Coding for relay networks referred in [59], [38], [51], [83], [105] and [55]. The proposed association technique has an equal performance and much less transmission delay than the relay technique, and its energy consumption is also better than that of the cooperative MIMO technique in certain conditions.

The rest of the chapter is organized as follows. The performance comparison of cooperative MIMO and relay techniques and the energy consumption of both cooperative techniques are presented in Section 6.2 and 6.3. In Section 6.4, the association strategy of the two techniques is proposed and its energy consumption and transmission delay are investigated.

The performance and the energy consumption of these two techniques are illustrated by simulation results through this chapter. The relay techniques using Amplify-Forward and Decode-Forward techniques and the cooperative MISO systems using Alamouti codes for two cooperative transmit nodes and max-SNR STBC for three and four nodes, are considered. We ensure the same transmit power and total received SNR for each technique (the total received SNR of relay technique is the sum of the SNRs of multiple received signals). In this condition, the received SNR at the relay node is greater than the received SNR at the destination node and depends on the source-relay distance.

## 6.2 Cooperative MIMO and Relay Techniques Performance Comparison

In relay cooperative networks, the received signal comes from different independent fading channels, so that the probability of deep fading is minimized. After the combination process, the receiver can exploit the diversity gain to decrease the error rate or the transmission power for the same required error rate, therefore reducing the transmission energy consumption.

The Decode-and-Forward technique can eliminate the noise amplification drawback of the Amplify-and-Forward technique. If the signal at the relay node is decoded perfectly, the total performance at the destination node is better. However, if the detection at the relay node is not reliable, this will affect the performance of the MRC combination at the destination node D. The choice between two relay techniques depends on the quality of the source-relay channel. In the general case, if the relay node is near the source node, the Decode-and-Forward technique is selected, and if the relay node is far from the source node, the Amplify-and-Forward technique is better [75].

The performance of relay techniques is limited by the decoding (or signal processing) process at the relay nodes. The error bit (or noise amplification) occurring at the relay node can not be always corrected at the destination node. Although with the same diversity gain, the performance of relay is always lower than MISO space time coding techniques.

### 6.2.1 Case of Two Cooperation Transmission Nodes

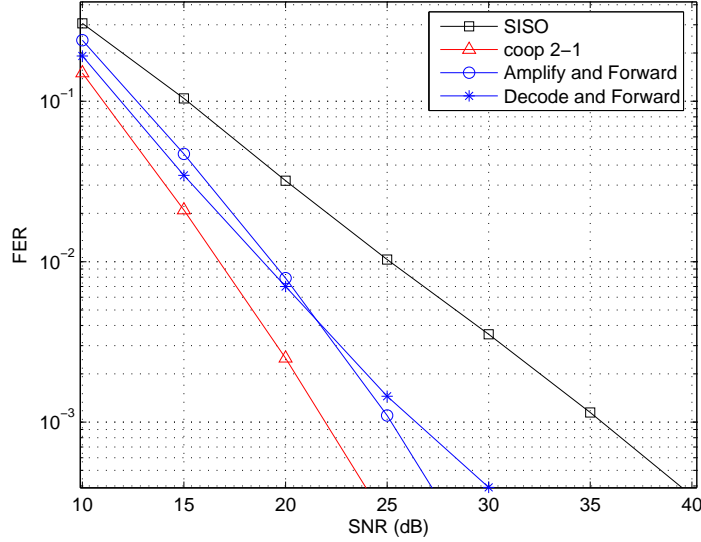


Figure 6.1: FER of relay technique vs. cooperative MIMO technique with two transmission nodes, non-coded QPSK modulation over a Rayleigh channel, 120 bits/frame, source-relay distance  $d_1 = d/3$ , and power path-loss factor  $K=2$ .

Fig. 6.1 represents the Frame Error Rate (FER) performance comparison of the relay techniques (Amplify-and-Forward and Decode-and-Forward techniques) with the cooperative MISO technique for two transmit antennas. Due to the noise amplification or the error occurred at the relay node, the performance of Amplify-and-Forward and Decode-and-Forward relay techniques are  $3dB$  and  $4.5dB$  less than the cooperative MISO at the  $FER = 10^{-3}$ , respectively.

For example, when the SNR at the destination node is  $22dB$ , the received SNR at the relay node is  $22 + 10 \log(\frac{d}{d_1})^K = 31.5dB$  with  $d_1 = d/3$  and power loss factor  $K = 2$ . With  $SNR = 31.5dB$ , the FER at the relay node after signal decoding is approximately  $FER = 3 \cdot 10^{-3}$ . The relay node retransmits the messages with this FER, so that the error rate at the destination node can not be equal to the one of traditional MISO technique ( $FER = 10^{-3}$  at  $SNR = 22dB$ ).

The final performance of relay techniques depends on the performance at the relay

node. So that for the relay technique that uses Decode-Forward, if the relay node is closer to the source node, the performance will be better due to the better received SNR at the relay node. For example: if the distance between source and relay nodes is  $d_1 = d/5$ , the received SNR will be greater than the case that the distance between source and relay nodes  $d_1 = d/3$ . Less error bits occur at the relay node which leads to a better performance.

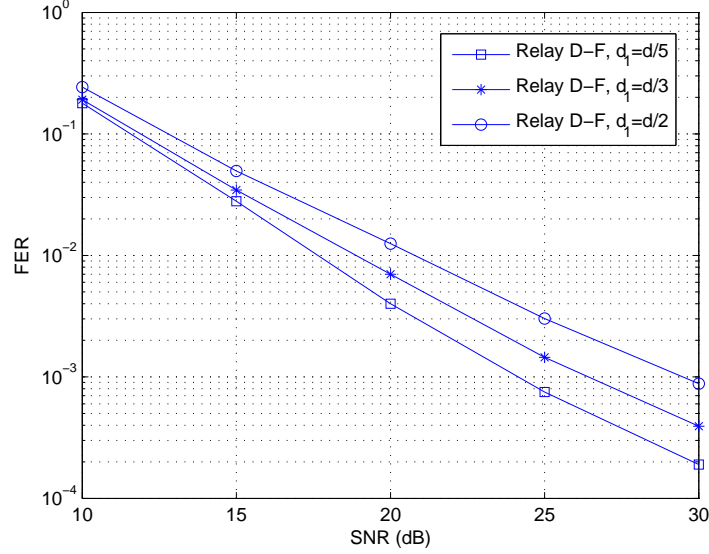


Figure 6.2: FER of relay techniques with different source-relay distances, non-coded QPSK modulation over a Rayleigh channel, 120 bits/frame and the power path-loss factor  $K=2$ .

This effect is illustrated by Fig. 6.2 with the source-relay transmission distance  $d_1 = d/5$ ,  $d/3$  and  $d/2$ .

### 6.2.2 Case of Multiple Cooperation Transmission Nodes

In parallel relay networks, the diversity gain increases with the number of independent fading received signals (i.e. the number of relay nodes). In perfect conditions, the diversity gain of these parallel relays system with  $N$  transmit nodes is equal to MRC technique with  $N$  reception nodes and one transmit node. However, the performance of parallel relays also suffers from the noise amplification or the error bits that occurred at the multiple relay nodes.

In Fig. 6.3, the performance comparison of parallel relay technique with two and three relay nodes using Decode-and-Forward technique with the cooperative MISO technique is shown. The source-relay distance  $d_1 = d/3$  and the number of transmit nodes is three (i.e. two relay nodes, legend *Relay N = 3*) and four (i.e. three relay nodes, legend



Relay  $N = 4$ ).

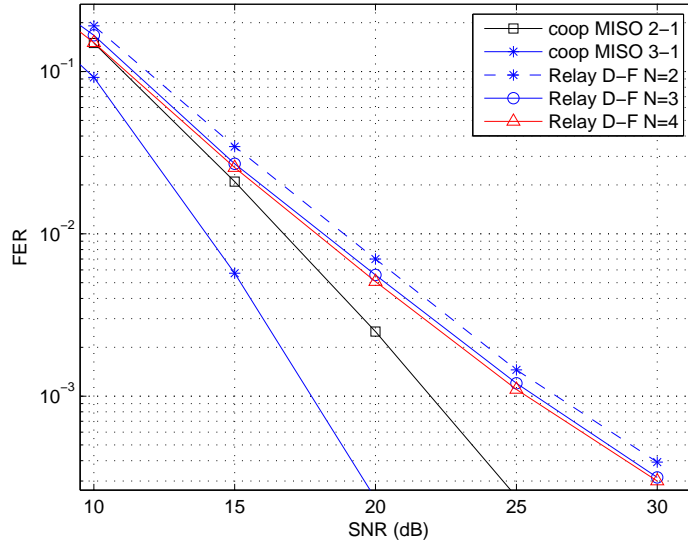


Figure 6.3: FER performance of relay techniques vs. cooperative MIMO techniques with three and four transmission nodes, non-coded QPSK modulation over a Rayleigh channel, source-relay distance  $d_1 = d/3$ .

It can be observed that when the number of relay node increases, the performance increases. However, the performance gain is not as much as the cooperative MISO technique due to the error rate occurring at the relay nodes. At error rate requirement  $FER = 10^{-3}$ , relay techniques with two and three relays nodes have  $2dB$  and  $3dB$  less performance than cooperative MISO techniques with two and three transmit nodes, respectively.

In order to increase the performance of parallel relay technique, adaptive cooperative protocols, where the relays autonomously decide whether or not to retransmit, or the selected combination techniques could be employed [57], [68].

### 6.2.3 Effect of Transmission Synchronization Error

The performance of cooperative MISO technique is affected by the un-synchronized transmission of cooperative distributed networks. For small transmission synchronization error ranges, the degradation is negligible but it becomes significant for large error range. The advantage of relay techniques over cooperative MIMO techniques is that these techniques do not need the synchronous transmission of relay nodes, and so relay techniques do not suffer from the transmission synchronization error problem.

Fig. 6.4 shows the performance comparison of these two techniques with transmission

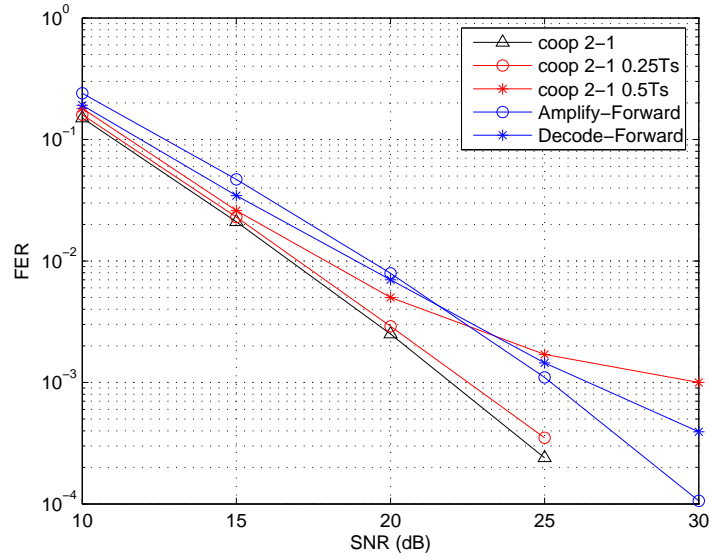


Figure 6.4: Performance of relay technique vs. cooperative MIMO technique with transmission synchronization error  $\Delta T_{syn} = 0.25T_s$  and  $0.5T_s$ , source-relay distance  $d_1 = d/3$ .

synchronization errors  $\Delta T_{syn} = 0.25T_s$  and  $0.5T_s$ . Although the performance of cooperative MIMO techniques decreases in the presence of transmission synchronization error, it still outperforms the relay techniques with a synchronization error range as large as  $0.25T_s$ . But with a larger error range  $\Delta T_{syn} = 0.5T_s$ , the relay technique is better than the cooperative MISO at  $FER = 10^{-3}$ .

As a consequence, if the wireless distributed network can not ensure the timer synchronization error as small as  $0.5T_s$  (e.g. under conditions of high speed transmission rate or less precise synchronization process), relay techniques are a better solution than cooperative MISO for cooperative transmission.

#### 6.2.4 Effects of Power Path-loss Factor and Error Control Coding

The received SNR at the relay node depends on the ratio of source-relay and source-destination transmission distance  $d_1/d$  and the channel power path loss factor  $K$ . If the received SNR at destination node D is fixed and the path loss factor  $K$  increases, the received SNR at relay nodes is higher than this one in the case of the power path-loss factor  $K = 2$ . That leads to the less error bits occurrence (or less noise amplification) at relay nodes. Therefore, with the same received SNR at destination node, the error rate of the relay technique decreases.

Fig. 6.5 shows the performance comparison of the cooperative MISO 2-1 and relay techniques with the path loss factors  $K = 2$  and  $K = 3$ . It can be seen that the

performance difference between the cooperative MISO technique and the relay technique becomes smaller in the case  $K = 3$ .

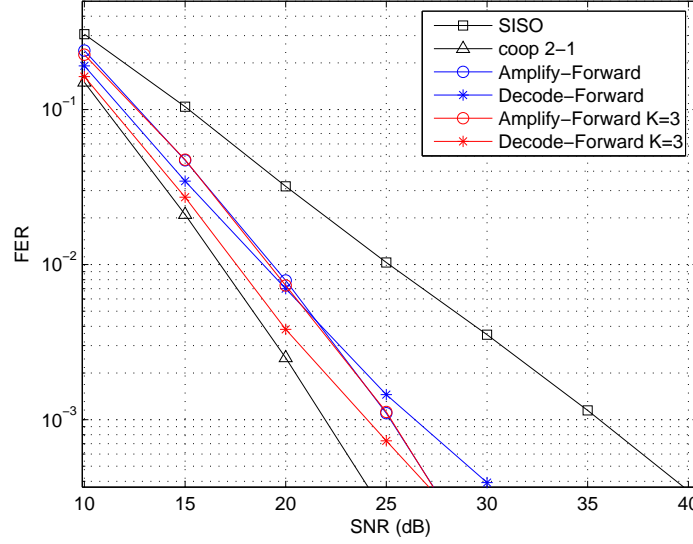


Figure 6.5: FER performance of relay technique vs. cooperative MIMO technique, non-coded QPSK modulation over a Rayleigh channel, power path-loss factor  $K = 3$ , source-relay distance  $d_1 = d/3$ .

The performance of relay techniques is limited by the error rate at relay nodes. So if channel coding is employed, the error rate at the relay node will decrease, leading to a better performance.

Fig. 6.6 shows the performance of relay techniques and cooperative MIMO techniques which use rate 1/2 Convolution Coding CONV [4, 15, 17] with the constraint length equal to four. Due to less error bits at the relay node, the performance gap between the MIMO technique and the relay technique is  $2.7dB$ , which represents a small decrease in comparison with the  $3dB$  gap of non-coding performance result in Fig. 6.1.

### 6.3 Cooperative MISO and Relay Techniques Energy Consumption Comparison

It has been shown that the performance of the relay technique, with the same diversity gain order (i.e. same transmit node number), is less than the MISO technique for the same received SNR due to the error rate limited at relay nodes in section 6.2.1 and 6.2.2. However, due to the shorter distance between the relay and destination nodes, less transmission energy than the MISO technique is needed for ensuring the same received SNR.

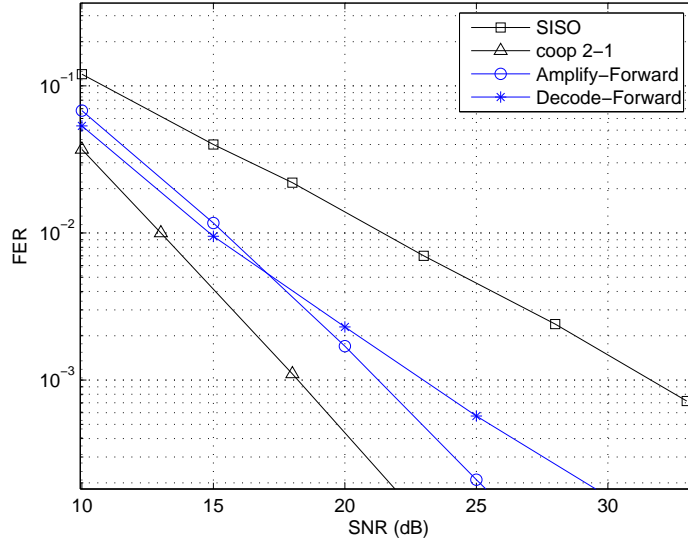


Figure 6.6: FER of relay technique vs. cooperative MIMO technique, with convolution Codes [4, 15, 17], QPSK modulation over a Rayleigh channel, power path-loss factor  $K = 2$ , source-relay distance  $d_1 = d/3$

Moreover, relay techniques do not need a dedicated phase for transmitting signal to the relay node (i.e. phase one of cooperative MISO technique). In certain situation, that may help relay techniques to reduce the transmission energy consumption although the needed SNR is greater than for the cooperative MISO.

However, as the destination node must work in several time slots ( $N$  time slots), the circuit consumption of the relay technique will be higher than the corresponding cooperative MISO. Moreover, the relay needs a higher transmission energy from source node to destination node because of the higher SNR needed at the destination for the same FER requirement. Therefore, in many cases, the total energy consumption of the relay technique is higher than the cooperative MISO technique.

### 6.3.1 Energy Consumption Analysis

Let us consider cooperative MISO and relay systems with  $N$  transmit nodes and one receive node. The energy consumption of relay technique can be divided into  $N$  SISO transmissions of  $N$  communication phases (see chapter 2).

- The transmission energy consumption of phase 1:  $E_{pa,S}$
- The circuit energy consumption of phase 1:  $E_{c,Tx,R} + NE_{c,Rx,R}$
- The transmission energy consumption of phases 2 to  $N$ :  $(N - 1)E_{pa,R}$

- The circuit energy consumption of phases 2 to  $N$ :  $(N - 1)(E_{c,Tx,R} + E_{c,Rx,R})$

The total energy consumption of the relay techniques is

$$\begin{aligned} E_{relay} &= E_{pa,S} + E_{c,Tx,R} + NE_{c,Rx,R} + (N - 1)E_{pa,R} + (N - 1)(E_{c,Tx,R} + E_{c,Rx,R}) \\ &= E_{pa,S} + NE_{c,Tx,R} + (2N - 1)E_{c,Rx,R} + (N - 1)E_{pa,R} \end{aligned} \quad (6.1)$$

where  $E_{pa,S}$  and  $E_{pa,R}$  are the transmission energy of the source node and one relay node, ( $E_{c,Tx,R}$  and  $E_{c,Rx,R}$ ) are the circuit energy of one transmit and one receive node. Because the relay-destination nodes distance is smaller than the source-destination nodes distance, the transmission consumption of one relaying phase  $E_{pa,R}$  is smaller than the transmission consumption of phase one  $E_{pa,S}$ .

The energy consumption of the cooperative MISO technique with  $N$  cooperative transmit nodes is composed of:

- The transmission energy consumption of phase 1:  $E_{pa,coop}$
- The circuit energy consumption of phase 1:  $E_{c,Tx,coop} + (N - 1)E_{c,Rx,coop}$
- The transmission energy consumption of phase 2:  $NE_{pa,M}$
- The circuit energy consumption of phase 2:  $NE_{c,Tx,M} + E_{c,Rx,M}$

The total energy consumption of the cooperative MISO is

$$E_{coopMISO} = E_{pa,coop} + E_{c,Tx,coop} + (N - 1)E_{c,Rx,coop} + NE_{pa,M} + NE_{c,Tx,M} + E_{c,Rx,M} \quad (6.2)$$

where  $E_{pa,coop}$  and  $E_{pa,M}$  are the transmission energy of one node in the data exchange phase 1 and the MISO transmission phase 2,  $E_{c,Tx,coop}$  (or  $E_{c,Rx,coop}$ ) and  $E_{c,Tx,M}$  (or  $E_{c,Rx,M}$ ) are the circuit energy of one transmit (or receive) node in the data exchange phase 1 and the MISO transmission phase 2.

For the same transmission time, the circuit consumption of cooperative MISO and relay technique is the same (neglecting the difference in signal processing energy consumption), i.e.  $E_{c,Tx,R} \approx E_{c,Tx,M}$  and  $E_{c,Rx,R} \approx E_{c,Rx,M}$ . And for the same received SNR, the transmission energy consumption  $E_{pa,M}$  of the cooperative MIMO technique are the same as the transmission energy consumption of the phase one of the relay technique  $E_{pa,S}$ , i.e.  $E_{pa,M} = E_{pa,S}$ .

In the data exchange of phase one, cooperative MISO techniques use high-speed transmission to reduce the circuit consumption. For example, if a 16-QAM modulation is used, the transmission time can be reduced twice in comparison with a QPSK modulation. In this condition, the circuit energy consumptions in phase one of cooperative MISO  $E_{c,Tx,coop}$  and  $E_{c,Rx,coop}$  are approximated as  $E_{c,Tx,m}/2$  and  $E_{c,Rx,M}/2$ . The transmission

energy  $E_{pa,coop}$  is also much smaller than the circuit energy  $E_{c,Tx,coop}$  and  $E_{c,Rx,coop}$  for short distance transmission (as shown in Fig. 3.3).

The energy consumption difference between cooperative MISO and relay techniques with  $N$  cooperative transmit nodes is:

$$\begin{aligned}
 E_{coopMISO} - E_{relay} &= [E_{pa,coop} + E_{c,Tx,coop} + (N-1)E_{c,Rx,coop} + NE_{pa,M} + NE_{c,Tx,M} + E_{c,Rx,M}] \\
 &\quad - [E_{pa,S} + NE_{c,Tx,R} + (2N-1)E_{c,Rx,R} + (N-1)E_{pa,R}] \\
 &\approx [NE_{pa,M} + (N+1/2)E_{c,Tx,M} + \frac{N+1}{2}E_{c,Rx,M}] \\
 &\quad - [E_{pa,S} + NE_{c,Tx,R} + (2N-1)E_{c,Rx,R} + (N-1)E_{pa,R}] \\
 &\approx [(N-1)E_{pa,M} + \frac{1}{2}E_{c,Tx,M}] - [\frac{3(N-1)}{2}E_{c,Tx,R} + (N-1)E_{pa,R}]
 \end{aligned} \tag{6.3}$$

It can be seen that the circuit energy consumption of relay technique is bigger than cooperative MIMO, because relay needs multi-phase transmissions from multiple relay nodes to the destination node. For the same received SNR at the destination, the transmission energy  $E_{pa,M}$  is greater than  $E_{pa,R}$  (because  $E_{pa,R} < E_{pa,S}$  and  $E_{pa,S} = E_{pa,M}$ ). However, as the performance of cooperative MIMO is better, this technique needs less required SNR (so less transmission energy for the same error rate requirement as the relay technique. For example, at the same FER requirement ( $FER = 10^{-3}$ ), cooperative MIMO has a gain of 3dB over relay technique (as shown in Fig.6.1). Therefore, the needed transmission energy consumption is 3dB less than relay, which means  $E_{pa,M} \approx \frac{1}{\sqrt{2}}E_{pa,R} \approx 0.7E_{pa,R}$  with a power path loss factor  $K = 2$ . That is the reason why the transmission energy consumption of cooperative MIMO is smaller than relay technique for the same error rate performance.

Fig. 6.7 shows the energy consumption of relay technique in comparison with SISO technique and cooperative MISO 2-1 technique, using MSOC technique and the transmission synchronization error range  $\Delta T_{syn} = 0.25T_s$ . It is obvious that the energy consumption of relay technique is lower than SISO technique (and multi-hop SISO technique), but still higher than the cooperative MISO technique. For a lower FER constraint (e.g.  $FER = 10^{-2}$ ), the energy consumption advantage of cooperative MIMO over relay techniques is reduced.

The performance of the relay technique does not increase quickly like the cooperative MIMO technique when the number of transmit nodes increases (as shown in Fig. 6.3). Although parallel relay technique can save transmission energy consumption at relay nodes (relay-destination distances are smaller than source-destination distance), the needed transmission energy of relay is still greater than cooperative MISO with the same cooperative transmit nodes due to the higher required SNR (as shown in Fig. 6.3).

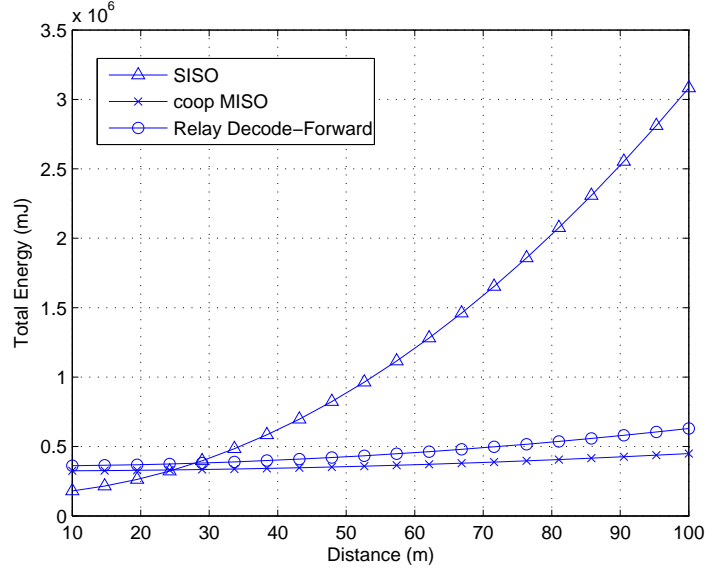


Figure 6.7: Energy Consumption of relay technique vs. cooperative MIMO technique with two transmission nodes, power path-loss factor  $K = 2$ , source-relay distance  $d_1 = d/3$ .

In Fig. 6.8, the energy consumption comparison of cooperative MISO and parallel relay techniques with a number of transmission nodes  $N = 2$  and  $N = 3$  is shown. It is obvious that the total energy consumption of cooperative MISO is smaller due to the fact that cooperative MISO needs less transmission energy (less required SNR) than parallel relay for the same error rate requirement. At distance  $d = 300m$ , 75% energy consumption can be saved by using the cooperative MISO 3 – 1 technique rather than the parallel relay  $N = 3$  technique.

### Effect of the power path loss and transmission synchronization error

When the channel path loss factor increases, more transmission energy consumption can be saved by using the relay technique because the relay-destination distance is smaller than the source-destination distance. Therefore, the fact that transmission energy consumption of one cooperative MISO node  $E_{pa,M}$  can be smaller than the transmission energy consumption of one relay node  $E_{pa,R}$  is no longer justified. Fig. 6.9 shows the energy consumption comparison of the cooperative MISO 2-1 and the relay technique with a power path loss factor  $K = 3$ . The total energy consumption of the relay technique is better than that of the cooperative MISO technique.

In the presence of transmission errors, the performance of cooperative MISO technique decreases. For a small synchronization error, the degradation is negligible but it becomes significant for a large error range, which leads to more required transmission energy. Fig.

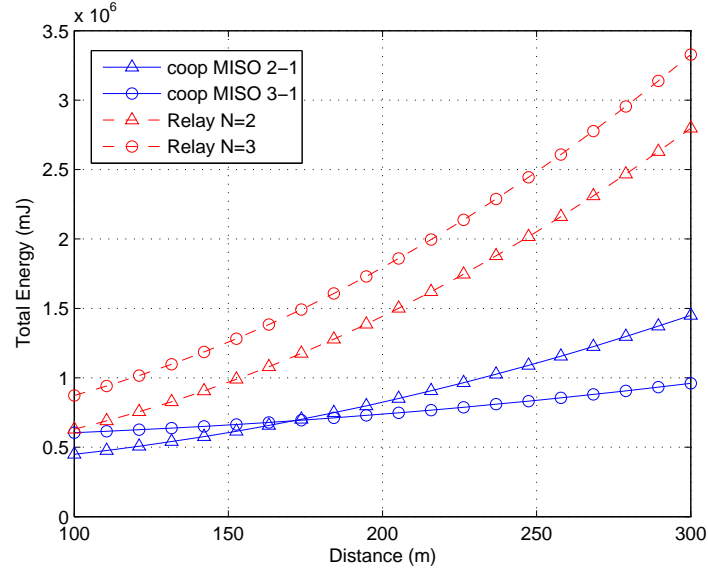


Figure 6.8: Energy consumption of relay technique vs. cooperative MIMO technique with two and three transmission nodes, power path-loss factor  $K = 2$ , source-relay distance  $d_1 = 1/3d$ .

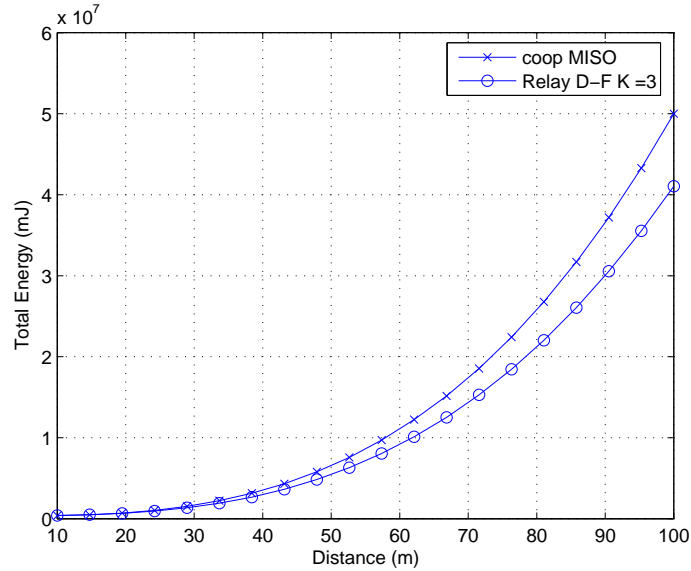


Figure 6.9: Energy consumption of relay technique vs. cooperative MISO technique with two transmission nodes  $N = 2$ , power path-loss factor  $K = 3$ , error rate  $FER = 10^{-2}$  and source-relay distance  $d_1 = d/3$



6.10 shows the energy consumption comparison of cooperative 2-1 and relay techniques with the path loss factor  $K = 3$  and the transmission synchronization error  $\Delta T_{syn} = 0.5T_s$ . In this condition, the relay is clearly better than the cooperative MISO in terms of energy consumption.

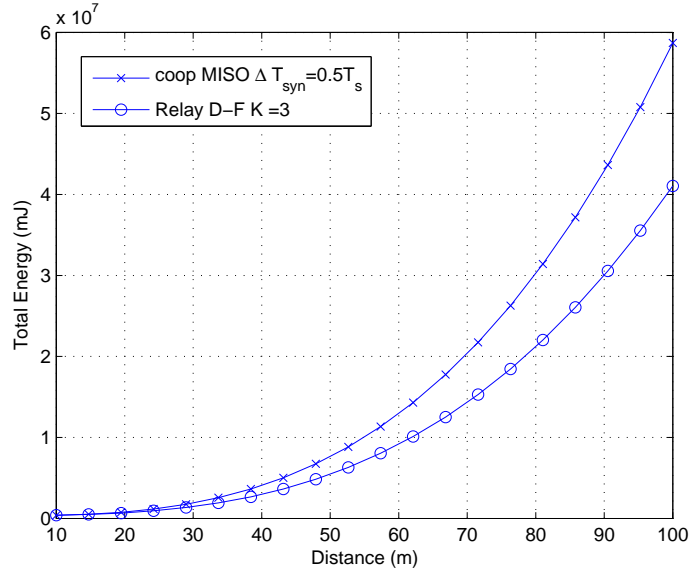


Figure 6.10: Energy consumption of relay technique vs. cooperative MISO technique with two transmission nodes  $N = 2$ , power path-loss factor  $K = 3$ , error rate  $FER = 10^{-2}$ , transmission synchronization error range  $\Delta T_{syn} = 0.5T_s$  and source-relay distance  $d_1 = d/3$ .

### 6.3.2 Transmission Delay Comparison

For a parallel relay network with  $N$  transmit nodes, the system needs typically  $N$  transmission phases to transmit all signals from  $N - 1$  relay nodes to the destination node (if orthogonal frequency channels are not considered). And for a cooperative MISO network with  $N$  transmit nodes, the system needs typically 2 transmission phases (data exchange and MISO transmission phases).

The time needed for one transmission phase depends typically on the number of transmit symbols in this phase. For the same data rate (case  $N = 2$ ), the time needed for one transmission phase of relay techniques can be approximated as the time needed for MISO transmission phase (phase two) of MISO techniques. For three or four transmit node (rate 3/4 STBCs are used), the time needed for phase two of MISO techniques is approximated as 4/3 the time needed for one transmission phase of relay techniques. Due to the fact that high-speed transmission can be employed in the phase one of cooperative MISO (16-QAM modulation instead of QPSK modulation), the time needed of phase one is approximated

as a half of the time needed of phase two for the case of  $N = 2$ , and less than a half for the case of  $N = 3$  and  $N = 4$ .

Therefore, for the case of two transmit nodes, the total time needed of cooperative MISO is smaller than the relay technique. And when the number of transmit nodes increases, the cooperative MISO has a great advantage over relay in terms of delay because the cooperative MISO needs just two transmission phases instead of the  $N$  transmission phases of the parallel relay.

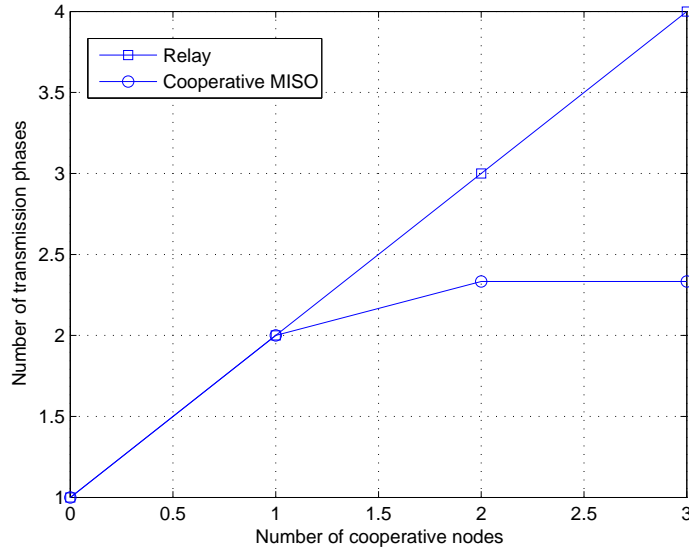


Figure 6.11: Delay Comparison of Relay technique vs. Cooperative MISO technique with different number of cooperative (or relay) nodes.

Consider the time needed of one transmission phase of relay technique as a reference, Fig. 6.11 shows the delay comparison (number of needed phases) of cooperative MISO and relay techniques as a function of transmit node number ( $N = 2, 3$  and  $4$ ).

In this simple scenario comparison, the transmission delay of cooperative MISO is obviously better than in the case of relay. However, the delay depends also on the higher layer protocols (e.g. MAC, LLC, Routing layer protocols). Therefore, taking account of the more complex protocols needed to deploy a cooperative MISO transmission [106, 2], the delay advantage of cooperative MISO may be smaller.

## 6.4 Cooperative MISO and Relay Association Strategies

The efficiency of relay techniques is very useful when cooperative MISO techniques can not be employed (depending on the network topology) or when cooperative MISO is less

efficient than relay (e.g. in presence of large transmission synchronization errors). However, the transmission delay of parallel relay techniques is a big draw-back in comparison with cooperative MISO techniques.

In order to reduce the transmission delay, a strategy associating the cooperative MISO and relay techniques is proposed. The principle of this association strategy is that STBC is employed at multiple relay nodes to perform a MISO transmission in one transmission phase instead of multiple transmission phases of relay nodes. This proposed association technique has the same performance as the relay, and has less transmission delay than both relay and cooperative MISO technique with a number of transmit nodes greater than two.

#### 6.4.1 Association Schemes

Fig. 6.12 represents the principle of the association strategy with  $N$  transmit nodes. There are two phases of transmission.

- Phase one: source node  $S$  transmits the information to destination node  $D$  and  $N - 1$  relay nodes.
- Phase two:  $N - 1$  relay nodes decode the received signal, encode using MIMO STBC, and then transmit the space-time encoded signals, at the same time, to the destination node  $D$ .

At the destination, node  $D$  uses space-time combination technique to combine the signal from  $N - 1$  relay nodes, and then performs the MRC combining with the direct signal from source node  $S$ .

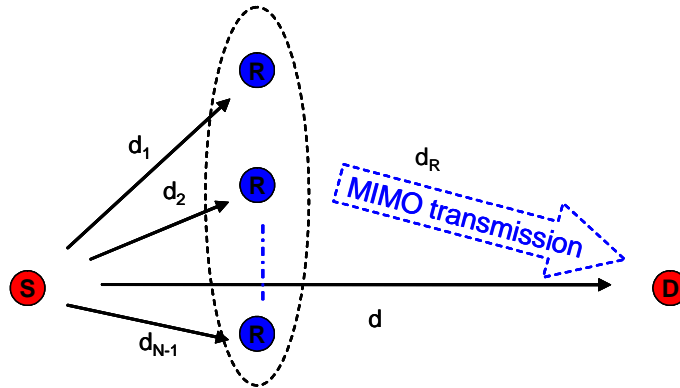


Figure 6.12: Association scheme of cooperative MIMO and relay techniques

Consider the case of two relay nodes, the diversity gain of this association technique is equal to the cooperative MISO with three transmit antennas. This technique has a full

rate transmission in phase two, which is better than the  $3/4$  rate of the cooperative MISO technique in phase two ( $N = 3$ ). It means that the new association strategy has a less transmission delay than a cooperative MISO with three nodes. Moreover, this association strategy needs just two transmission phases which is less than three transmission phases of a typical parallel relay technique with two relay nodes.

This technique has also the advantage of relay techniques, which helps to reduce the transmission energy consumption of relay nodes (particularly when the power path loss factor is greater than 2). However, as this strategy is an association scheme, it has the performance limitation of the relay and suffers from the transmission synchronization error effect of the cooperative MISO. For a number of relay nodes greater than two, the full rate transmission from relay nodes to the destination node can not be achieved because of the limitation of OSTBC. A number of relay nodes less than four seems to be practical for WSN applications, and using two relay nodes for this association strategy is the optimal solution in terms of transmission delay (as illustrated in Fig. 6.15).

#### 6.4.2 Performance and Energy Consumption of the Association Scheme

Fig. 6.13 shows the performance of this association strategy with two and three relay nodes, using Alamouti and max-SNR OSTBC for MIMO relaying (legend MIMO Relay). The performance of the association strategy is lower than the performance of the cooperative MISO 3-1, and approximated as the performance of D-F relay technique. However, the advantages of this association strategy are the delay over the relay technique and the energy consumption over the cooperative technique.

Fig. 6.14 and Fig. 6.15 show the energy consumption and the transmission delay approximation of the association strategy (legend Cooperation K=3 and Cooperation Strategy respectively) using Alamouti and max-SNR OSTBC, in comparison with the cooperative MISO and relay techniques. It can be seen that the association technique has a lowest transmission delay (in Fig. 6.15), and has also the lower energy consumption than the cooperative MISO 3 – 1 when the power path-loss factor  $K = 3$  (in Fig. 6.14).

Therefore, in the conditions that the parallel relay outperforms the cooperative MISO in terms of energy consumption or the cooperative MISO can not be deployed, the association scheme can be employed instead of the parallel relay technique in order to save the transmission delay.

## 6.5 Conclusion

Cooperative relay techniques provide attractive benefits for wireless distributed systems when the temporal and spatial diversity can be exploited to reduce the transmission energy consumption. Relay techniques is more efficient than the SISO technique, but still less

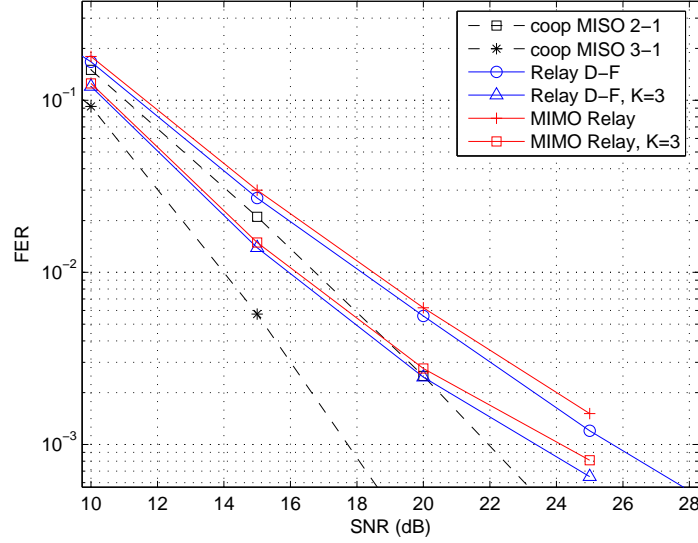


Figure 6.13: FER performance of the association strategy vs. relay technique vs. cooperative MIMO technique, number of transmission nodes  $N = 3$ , non-coded QPSK modulation over a Rayleigh channel, power path-loss factor  $K = 2$ , source-relay distance  $d_1 = d/3$ .

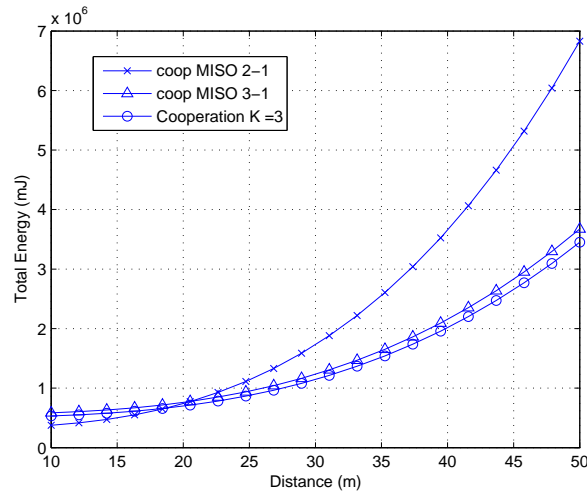


Figure 6.14: Energy Consumption of the Association Strategy vs. Relay technique vs. Cooperative MIMO technique, number of transmission nodes  $N = 3$ , non-coded QPSK modulation over a Rayleigh channel, power path-loss factor  $K = 3$ , source-relay distance  $d_1 = 1/3d$ .

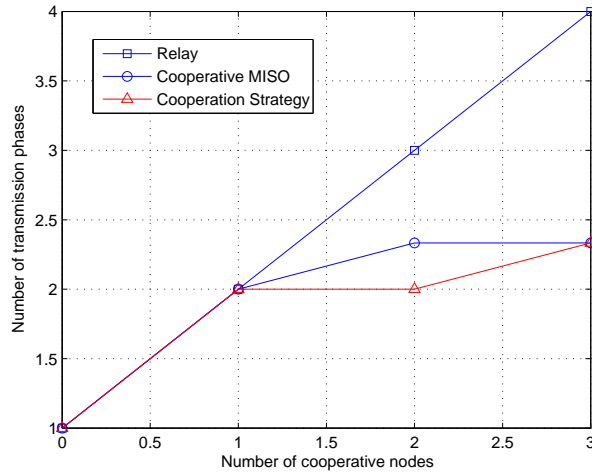


Figure 6.15: Transmission delay comparison of the Association Strategy vs. Relay technique vs. Cooperative MIMO technique, with the number of cooperative (or relay) nodes = 1, 2 and 3.

efficient than cooperative MISO techniques in terms of energy consumption.

Performance of relay techniques is not as good as cooperative MISO techniques for the same SNR. However, relay techniques are not affected by the un-synchronized transmission scheme. When the transmission synchronization error becomes significant, the performance of relay is better than the performance of cooperative MISO, leading to a better energy efficiency.

The significant drawback of parallel relay techniques is the transmission delay of multiple relaying phases. In this condition, an association strategy that associates the cooperative MISO transmission and relay techniques is proposed in order to reduce significantly the transmission delay, and to exploit simultaneously the advantages of both two cooperative techniques. The proposed technique has a performance which is equivalent to the relay technique but with much less transmission delay.

## Chapter 7

# Conclusion and Future Works

The thesis has investigated cooperative MIMO strategies for wireless sensor networks. In this thesis, we have proved that, over a Rayleigh block fading channel, the cooperative MIMO technique can exploit the diversity gain of space-time coding transmission to increase the performance or to reduce efficiently the energy consumption in the distributed WSN where multiple antennas can not be integrated in a single wireless node. The energy efficiency of the cooperative MIMO techniques was shown and compared with the SISO, multi-hop SISO and relay techniques. Some cooperative strategies based on the cooperative MIMO technique have been proposed for energy efficient transmissions in CAPTIV, an intelligent transport system project, where the energy consumption is an important design criterion.

In chapter 3, the cooperative MIMO systems, using the OSTBC, were investigated. By using the energy consumption reference model for a multiple antenna RF system, we have shown that the total energy consumption of the cooperative MISO is lower than SISO and traditional multi-hop SISO techniques for a transmission distance greater than 30m (or 50m in the case of coded systems). The cooperative MIMO helps to reduce the transmission energy consumption, therefore it is practical for medium to long range transmission distances where the transmission consumption dominates the total energy consumption. An optimal cooperative MIMO scheme selection is presented in order to find the best transmit-receive antennas number configuration for a given transmission distance. A multi-hop cooperative MIMO technique based on the cooperative MIMO 2-2 transmission for each hop is also proposed in this chapter.

In chapter 4, drawbacks of cooperative MIMO techniques, the unsynchronized transmission and the wireless cooperative reception noise, in wireless distributed networks have been investigated. The performance of the cooperative MIMO decreases in the presence of transmission synchronization errors and the degradation depends on the error range and the number of cooperative transmission nodes. However, the cooperative MIMO system is rather tolerant for a small range of transmission synchronization error and the degradation

is negligible for synchronization error range as small as  $0.25T_s$ , reasonable for a low speed transmission WSN. As the cooperative reception technique used in chapter 3 is not efficient enough, two cooperative reception techniques, Combine-and-Forward and Forward-and-Combine, based on the principle of the Amplify-and-Forward relay technique, were also proposed. We have shown that these two techniques are much more energy-efficient than the quantization cooperative reception technique. Using the two proposed cooperative reception techniques, a cooperative MIMO 2-2 system is more energy-efficient than a cooperative MISO 4-1 system for a transmission distance longer than 140m.

In chapter 5, a new efficient space-time combination technique MSOC (Multiple Sampling Orthogonal Combination) has been proposed in order to increase the performance of cooperative MIMO in the presence of transmission synchronization errors. The proposed MSOC technique can reconstruct the orthogonality of STBC even with an unsynchronized cooperative MISO transmission, and has a much better performance than the traditional combination technique, especially for large transmission synchronization error range. Consequently, less transmission energy is needed for cooperative MISO systems by using the MSOC technique. This new combination technique retains not only the full data rate for the case of two transmission nodes (or the 3/4 data rate for three and four transmission nodes), but also the low complexity combination of the traditional STBC codes. The proposed MSOC principle can also be extended to other cooperative MIMO systems with an arbitrary number of transmission nodes.

In chapter 6, the performance and the energy consumption of the cooperative MIMO and the cooperative relay techniques were investigated. We have shown that the performance of relay is not as good as that of cooperative MISO, but when transmission synchronization error is large, the robustness of the relay technique leads to a better energy efficiency than the cooperative MISO technique. The advantages of the cooperative MISO technique over the relay technique is small for a short range transmission (using two transmit nodes), but significant for a long distance transmission, where the transmit nodes number is usually greater than two for the optimal energy consumption. If the advantage of the relay technique is that it is not affected by the transmission synchronization error, a significant drawback of multiple relay techniques, in comparison with the cooperative MISO, is the transmission delays of multiple relaying phases when the number of relay nodes is greater than two. In this condition, a new cooperation strategy that associates the cooperative MISO transmission and relay techniques is proposed in order to exploit simultaneously the advantages of both techniques. The principle of the proposed technique is that the space-time MIMO transmission is employed at multiple relay nodes in order to transmit the signal at the same time and reduce the transmission delay. We have shown that the proposed technique has a performance which is equivalent to the relay technique but with much less transmission delay.



## Discussions

In this thesis, we investigated the energy consumption for medium to long range transmissions in WSN applications as required by the CAPTIV project. For short range applications where the transmission distance is less than 10m or 20m, the transmission energy consumption is less important than the circuit energy consumption. As cooperative MISO can efficiently increase the number of transmit bits/symbol to reduce the transmission time and the circuit consumption [17, 22], it can be slightly better than the SISO technique in terms of energy consumption. It has been mentioned in chapter 3 that convolution codes can help to reduce the transmission energy consumption, which is important for long range transmission. For a short distance, high-speed codes like Trellis Code Modulation (TCM) can be employed, in concatenation with the space-time codes [7, 64, 81, 35], to increasing the data rate and reducing the circuit energy consumption but the complexity drawback is prohibitive. Furthermore, for the case of two transmit nodes, the performance difference between the cooperative MISO and relay is small. For a short range application, the cooperative relay technique is as efficient as the cooperative MIMO and the relay technique can be a better solution due to its low complexity, the absence of transmission synchronization effect and an easier interface with higher layer protocol.

Transmission synchronization errors affect the performance of cooperative MIMO systems. The synchronization process must ensure a clock synchronization precision less than half of the symbol duration ( $0.5T_s$ ) in order to retain the gain of cooperative MIMO transmissions. As the precision synchronization process costs some energy consumption, the trade-off between the precision and the complexity of the clock synchronization [76, 93]) must be considered for the energy optimization purpose.

To deploy a MIMO transmission, cooperative nodes need a "rendez-vous" frame in order to determine the precise moment for the synchronous space-time transmission [106, 2, 13]. This procedure costs some delay and an extra energy consumption. A more detailed study in energy consumption and transmission delay between cooperative MIMO and relay techniques with the constraints of higher layer is needed for a global evaluation of this two cooperative techniques. Indeed, an energy efficient WSN requires a cross layer optimization, with the constraints of the other design criterion like transmission delay, reliability, mobility...[18, 106, 11, 23, 107]

The cooperative MIMO system needs a precise synchronization, but in varying WSN applications, wireless nodes are not synchronized all the time in order to reduce the active energy consumption. A modified version of the MAC layer protocol that takes into account the clock synchronization procedure or the temporal synchronization procedure to perform a synchronous MIMO transmission must be envisaged. For low density, long range transmission or clustered WSN applications, cooperative MIMO is easy to deploy.

As cooperative MIMO performs a long range transmission, it can transmit the signal over plenty of intermediate nodes. Therefore, in a high density distributed WSN, this may cause collisions and needs well designed MAC and routing algorithms to exploit the energy efficiency of the cooperative MIMO.

## Future works

Un-synchronized transmission affects the performance of cooperative MIMO systems. For a typical low speed transmission from 10 to 100kbps using QPSK modulation, where the symbols duration is around 20 to 200 $\mu s$ , the effect is not significant as the synchronization error range is usually less than a quarter of symbol duration ( $0.25T_s$ ). Since the transmission rate will increase for future WSN applications, this impact of transmission synchronization error becomes more significant. Therefore, other efficient techniques to deal with the unsynchronized transmission are important for cooperative MIMO systems. The study of time-reversal STBC [91, 66] and distributed space-time codes [62, 51, 70, 101, 72, 84], which is more tolerant to transmission synchronization errors, is envisaged in order to find a good trade-off between the performance, the complexity and the transmission delay.

Higher layer energy constrained design for cooperative MIMO transmission, consulting existing protocols for cooperative MIMO in WSN, or cooperative relay and virtual antennas array in telephone mobile networks, can be envisaged. This would help to evaluate the other extra energy consumption of cooperative MIMO and to perform a cross layer evaluation and comparison with the multi-hop SISO technique, the relay technique in terms of energy consumption and transmission delay. Working on MAC and routing protocols for cooperative MIMO in WSN applications [65, 13, 2] will be envisaged in order to deploy a real prototype in the future.

Since low cost commercial transceivers for WSN (Zigbee, IEEE 802.15.4 or UHF 800-900Mhz transceivers) in the market do not support the analog signal level access, the cooperative MIMO implementation needs a customized chip or demands a software radio implementation on low-consumption FPGAs or DSPs. The cooperative MIMO hardware implementation will help to investigate the real effect of the distributed scheme (like the transmission synchronization error, the cooperative reception impact...) on the performance of cooperative MIMO. As the symbol duration in low-speed data transmission in WSN is long enough to neglect the multi-path effect, the complexity of wireless channel transmission is still difficult to determine. An implementation will help to estimate the wireless channel delay profile, in order to evaluate the impact of the transmission synchronization error. The effect of RF transmission channel, antenna characteristic in the interested frequency band is also envisaged.

# Appendix A

## Estimated values of the traditional combination technique

In the presence of transmission synchronization errors, the estimated symbols  $s_2$  and  $s_3$  of the cooperative MISO system, using the max-SNR STBC for four transmit nodes, are:

$$\begin{aligned}
 \tilde{s}_2 &= \alpha_1^* r_1[1] + \alpha_2 r_1^*[2] + \alpha_3 r_1^*[3] + \alpha_4^* r_1[4] \\
 &= \alpha_1^* (\alpha_1 s_1 + \alpha_2 (s_2 p(\delta_1 - \delta_2) + ISI_2^1(\delta_1 - \delta_2)) + \alpha_3 (s_3 p(\delta_1 - \delta_3) + ISI_3^1(\delta_1 - \delta_3)) + \alpha_4 ISI_4^1(\delta_1 - \delta_4) + n_1[1]) \\
 &\quad + \alpha_2 (-\alpha_1^* s_2 + \alpha_2^* (s_1 p(\delta_1 - \delta_2) + ISI_2^2(\delta_1 - \delta_2))^* + \alpha_3^* ISI_3^2(\delta_1 - \delta_3)^* + \alpha_4^* (s_3^* p(\delta_1 - \delta_4) + ISI_4^2(\delta_1 - \delta_4)^*) + n_1^*[2]) \\
 &\quad + \alpha_3 (-\alpha_1^* s_3 + \alpha_2^* ISI_2^3(\delta_1 - \delta_2)^* + \alpha_3^* (s_1 p(\delta_1 - \delta_3) + ISI_3^3(\delta_1 - \delta_3)^*) + \alpha_4^* (-s_2^* p(\delta_1 - \delta_4) + ISI_4^3(\delta_1 - \delta_4)^*) + n_1^*[3]) \\
 &\quad + \alpha_4^* (0 + \alpha_2 (-s_3^* p(\delta_1 - \delta_2) + ISI_2^4(\delta_1 - \delta_2)) + \alpha_3 (s_2^* p(\delta_1 - \delta_3) + ISI_3^4(\delta_1 - \delta_3)) + \alpha_4 (s_1 p(\delta_1 - \delta_4) + ISI_4^4(\delta_1 - \delta_4)) + n_1[4]) \\
 &= \underbrace{(|\alpha_1|^2 + |\alpha_2|^2 p(\delta_1 - \delta_2) + |\alpha_3|^2 p(\delta_1 - \delta_3) + |\alpha_4|^2 p(\delta_1 - \delta_4)) s_1}_{\text{desired signal}} \\
 &\quad + \underbrace{(\alpha_1^* \alpha_2 s_2 (p(\delta_1 - \delta_2) - 1) + \alpha_3 \alpha_4^* s_2^* (p(\delta_1 - \delta_2) - p(\delta_1 - \delta_2)) + \alpha_1^* \alpha_3 s_3 (p(\delta_1 - \delta_3) - 1) + \alpha_2 \alpha_4^* s_3^* (p(\delta_1 - \delta_4) - p(\delta_1 - \delta_2)))}_{\text{non-desired signals}} \\
 &\quad + \underbrace{\alpha_1^* (\alpha_2 ISI_2^1(\delta_1 - \delta_2) + \alpha_3 ISI_3^1(\delta_1 - \delta_3) + \alpha_4 ISI_4^1(\delta_1 - \delta_4) + n_1[1]) + \dots}_{\text{ISI and noise terms}}
 \end{aligned} \tag{7.1}$$

$$\begin{aligned}
 \tilde{s}_3 &= \alpha_1^* r_1[1] + \alpha_2 r_1^*[2] + \alpha_3 r_1^*[3] + \alpha_4^* r_1[4] \\
 &= \alpha_1^* (\alpha_1 s_1 + \alpha_2 (s_2 p(\delta_1 - \delta_2) + ISI_2^1(\delta_1 - \delta_2)) + \alpha_3 (s_3 p(\delta_1 - \delta_3) + ISI_3^1(\delta_1 - \delta_3)) + \alpha_4 ISI_4^1(\delta_1 - \delta_4) + n_1[1]) \\
 &\quad + \alpha_2 (-\alpha_1^* s_2 + \alpha_2^* (s_1 p(\delta_1 - \delta_2) + ISI_2^2(\delta_1 - \delta_2))^* + \alpha_3^* ISI_3^2(\delta_1 - \delta_3)^* + \alpha_4^* (s_3^* p(\delta_1 - \delta_4) + ISI_4^2(\delta_1 - \delta_4)^*) + n_1^*[2]) \\
 &\quad + \alpha_3 (-\alpha_1^* s_3 + \alpha_2^* ISI_2^3(\delta_1 - \delta_2)^* + \alpha_3^* (s_1 p(\delta_1 - \delta_3) + ISI_3^3(\delta_1 - \delta_3)^*) + \alpha_4^* (-s_2^* p(\delta_1 - \delta_4) + ISI_4^3(\delta_1 - \delta_4)^*) + n_1^*[3]) \\
 &\quad + \alpha_4^* (0 + \alpha_2 (-s_3^* p(\delta_1 - \delta_2) + ISI_2^4(\delta_1 - \delta_2)) + \alpha_3 (s_2^* p(\delta_1 - \delta_3) + ISI_3^4(\delta_1 - \delta_3)) + \alpha_4 (s_1 p(\delta_1 - \delta_4) + ISI_4^4(\delta_1 - \delta_4)) + n_1[4]) \\
 &= \underbrace{(|\alpha_1|^2 + |\alpha_2|^2 p(\delta_1 - \delta_2) + |\alpha_3|^2 p(\delta_1 - \delta_3) + |\alpha_4|^2 p(\delta_1 - \delta_4)) s_1}_{\text{desired signal}} \\
 &\quad + \underbrace{(\alpha_1^* \alpha_2 s_2 (p(\delta_1 - \delta_2) - 1) + \alpha_3 \alpha_4^* s_2^* (p(\delta_1 - \delta_2) - p(\delta_1 - \delta_2)) + \alpha_1^* \alpha_3 s_3 (p(\delta_1 - \delta_3) - 1) + \alpha_2 \alpha_4^* s_3^* (p(\delta_1 - \delta_4) - p(\delta_1 - \delta_2)))}_{\text{non-desired signals}} \\
 &\quad + \underbrace{\alpha_1^* (\alpha_2 ISI_2^1(\delta_1 - \delta_2) + \alpha_3 ISI_3^1(\delta_1 - \delta_3) + \alpha_4 ISI_4^1(\delta_1 - \delta_4) + n_1[1]) + \dots}_{\text{ISI and noise terms}}
 \end{aligned} \tag{7.2}$$

# Appendix B

## Estimated values of the MSOC combination technique

By using the proposed MSOC combination, the the estimated symbols  $s_2$  and  $s_3$  of the cooperative MISO system, using the max-SNR STBC for four transmit nodes, are:

$$\begin{aligned}
 \tilde{s}_2 &= \alpha_2^* r_2[1] - \alpha_1 r_1^*[2] - \alpha_4^* r_4[3] + \alpha_3 r_3^*[4] \\
 &= \alpha_2^* (\alpha_1 (s_1 p(\delta_2 - \delta_1) + ISI_1^1(\delta_2 - \delta_1)) + \alpha_2 s_2 + \alpha_3 (s_3 p(\delta_2 - \delta_3) + ISI_3^1(\delta_2 - \delta_3)) + \alpha_4 (ISI_4^1(\delta_2 - \delta_4))) + n_2[1] \\
 &\quad - \alpha_1 (-\alpha_1^* s_2 + \alpha_2^* (s_1 p(\delta_1 - \delta_2) + ISI_2^2(\delta_1 - \delta_2)^*) + \alpha_3^* ISI_3^2(\delta_1 - \delta_3)^* + \alpha_4^* (s_3^* p(\delta_1 - \delta_4) + ISI_4^2(\delta_1 - \delta_4)^*) + n_1^*[2]) \\
 &\quad - \alpha_4^* (-\alpha_1 (s_3^* p(\delta_4 - \delta_1) + ISI_1^3(\delta_4 - \delta_1)) + \alpha_2 ISI_2^3(\delta_4 - \delta_2) + \alpha_3 (s_1^* p(\delta_4 - \delta_3) + ISI_3^3(\delta_4 - \delta_3)) + n_4[3]) \\
 &\quad + \alpha_3 (\alpha_1^* ISI_1^4(\delta_3 - \delta_1)^* - \alpha_2^* (s_3 p(\delta_3 - \delta_2) + ISI_2^4(\delta_3 - \delta_2)^*) + \alpha_3^* s_2 + \alpha_4^* (s_1^* p(\delta_3 - \delta_4) + ISI_4^4(\delta_3 - \delta_4)^*) + n_3^*[4]) \\
 &= \underbrace{(|\alpha_1|^2 + |\alpha_2|^2 + |\alpha_3|^2 + |\alpha_4|^2) s_2}_{\text{desired signal}} + \underbrace{\alpha_2^* (\alpha_1 ISI_1^1(\delta_2 - \delta_1) + \alpha_3 ISI_3^1(\delta_2 - \delta_3) + \alpha_4 ISI_4^1(\delta_2 - \delta_4) + n_2[1]) + \dots}_{\text{ISI and noise terms}}
 \end{aligned} \tag{7.3}$$

$$\begin{aligned}
 \tilde{s}_3 &= \alpha_3^* r_3[1] + \alpha_4^* r_4[2] - \alpha_1 r_1^*[3] - \alpha_2 r_2^*[4] \\
 &= \alpha_3^* (\alpha_1 (s_1 p(\delta_3 - \delta_1) + ISI_1^1(\delta_3 - \delta_1)) + \alpha_2 (s_2 p(\delta_3 - \delta_2) + ISI_2^1(\delta_3 - \delta_2)) + \alpha_3 s_3 + \alpha_4 ISI_4^1(\delta_3 - \delta_4) + n_3[1]) \\
 &\quad + \alpha_4^* (-\alpha_1 (s_2^* p(\delta_4 - \delta_1) + ISI_1^2(\delta_4 - \delta_1)) + \alpha_2 (s_1^* p(\delta_4 - \delta_2) + ISI_2^2(\delta_4 - \delta_2)) + \alpha_3 ISI_3^2(\delta_4 - \delta_3) + \alpha_4 s_3 + n_4[2]) \\
 &\quad - \alpha_1 (-\alpha_1^* s_3 + \alpha_2^* ISI_2^3(\delta_1 - \delta_2)^* + \alpha_3^* (s_1 p(\delta_1 - \delta_3) + ISI_3^3(\delta_1 - \delta_3)^*) - \alpha_4^* (s_2^* p(\delta_1 - \delta_4) + ISI_4^3(\delta_1 - \delta_4)^*) + n_1^*[3]) \\
 &\quad - \alpha_2 (\alpha_1^* ISI_1^4(\delta_2 - \delta_1)^* - \alpha_2^* s_3 + \alpha_3^* (s_2 p(\delta_2 - \delta_3) + ISI_3^4(\delta_2 - \delta_3)^*) + \alpha_4^* (s_1^* p(\delta_2 - \delta_4) + ISI_4^4(\delta_2 - \delta_4)^*) + n_2^*[4]) \\
 &= \underbrace{(|\alpha_1|^2 + |\alpha_2|^2 + |\alpha_3|^2 + |\alpha_4|^2) s_3}_{\text{desired signal}} + \underbrace{\alpha_3^* (\alpha_1 ISI_1^1(\delta_3 - \delta_1) + \alpha_2 ISI_2^1(\delta_3 - \delta_2) + \alpha_4 ISI_4^1(\delta_3 - \delta_4) + n_3[1]) + \dots}_{\text{ISI and noise terms}}
 \end{aligned} \tag{7.4}$$

# Bibliography

- [1] E. Agrell, T. Eriksson, A. Vardy, and K. Zeger, "Closest point search in lattices," *IEEE Transactions on Information Theory*, vol. 48, no. 8, pp. 2201–2214, 2002.
- [2] M. Ahmad, E. Dutkiewicz, and X. Huang, "MAC Protocol for Cooperative MIMO Transmissions in Asynchronous Wireless Sensor Networks," in *International Symposium on Communications and Information Technologies*, 2008, pp. 580–585.
- [3] D. Aktas and M. Fitz, "Distance spectrum analysis of space-time trellis-coded Modulations in quasi-static Rayleigh-fading channels," *IEEE Transactions on Information Theory*, vol. 49, no. 12, pp. 3335–3344, 2003.
- [4] S. Alamouti, "A simple transmit diversity technique for wireless communications," *IEEE Journal on Selected Areas in Communications*, vol. 16, no. 8, pp. 1451–1458, 1998.
- [5] G. Andrieux, J. Diouris, and Y. Wang, "A comparison between spatial and polarisation diversity for transmit beamforming techniques," in *The European Conference on Wireless Technology, 2005*, 2005, pp. 161–164.
- [6] P. Balaban and J. Salz, "Dual diversity combining and equalization in digital cellular mobile radio," *IEEE Transactions on Vehicular Technology*, vol. 40, no. 2, pp. 342–354, 1991.
- [7] G. Bauch, "Concatenation of space-time block codes and turbo-TCM," in *IEEE International Conference on Communications, ICC'99*, vol. 2, 1999.
- [8] G. Bauch and J. Hagenauer, "Analytical evaluation of space-time transmit diversity with FEC-coding," in *IEEE Global Communications Conference*, 2001, pp. 435–439.
- [9] F. Bond, C. Cahn, and H. Meyer, "Interference and Channel Allocation Problems Associated with Orbiting Satellite Communication Relays," *Proceedings of the IRE*, vol. 48, no. 1, pp. 608–612, 1960.

- [10] M. Borran, M. Memarzadeh, and B. Aazhang, "Design of coded modulation schemes for orthogonal transmit diversity," in *IEEE International Symposium on Information Theory*, 2001, pp. 339–339.
- [11] G. Bravos and A. Kanatas, "Energy efficiency comparison of MIMO-based and multi-hop sensor networks," *EURASIP Journal on Wireless Communications and Networking*, vol. 8, no. 3, 2008.
- [12] S. Brown and S. G.F., "Project SCORE," *Proceedings of the IRE*, vol. 48, no. 1, pp. 624–630, 1960.
- [13] W. Chen, Y. Yuan, C. Xu, K. Liu, and Z. Yang, "Virtual MIMO protocol based on clustering for wireless sensor network," in *10th IEEE Symposium on Computers and Communications*, 2005, pp. 335–340.
- [14] T. Cover and A. Gamal, "Capacity theorems for the relay channel," *IEEE Transactions on Information Theory*, vol. 25, no. 5, pp. 572–584, 1979.
- [15] S. Cui, A. J. Goldsmith, and A. Bahai, "Modulation optimization under energy constraints," in *IEEE International Conference on Communications*, Anchorage, AK, USA, May 2003, pp. 2805 – 2811.
- [16] —, "Energy-efficiency of MIMO and cooperative MIMO techniques in sensor networks," *IEEE Jour. on Selected Areas in Communications*, vol. 22, no. 6, pp. 1089 – 1098, August 2004.
- [17] S. Cui, A. Goldsmith, and A. Bahai, "Energy-efficiency of MIMO and cooperative MIMO techniques in sensor networks," *IEEE Journal on Selected Areas in Communications*, vol. 22, no. 6, pp. 1089–1098, 2004.
- [18] S. Cui, R. Madan, A. Goldsmith, and S. Lall, "Joint routing, MAC, and link layer optimization in sensor networks with energy constraints," in *2005 IEEE International Conference on Communications, 2005. ICC 2005*, vol. 2, 2005.
- [19] H. C.W., "Radio-relay-systems Development by the Radio Corporation of America," *Proceedings of the IRE*, vol. 33, pp. 156–168, 1945.
- [20] M. Dohler, "Wireless sensor networks: the biggest cross-community design exercise to-date," *Bentham Recent Patents on Computer Science*, vol. 1, pp. 9–25, 2008.
- [21] M. Dohler and H. Aghvami, "Information outage probability of distributed STBCs over Nakagami fading channels," *IEEE Communications Letters*, vol. 8, no. 7, pp. 437–439, 2004.

- [22] M. Dohler, A. Gkelias, A. Aghvami, and F. Meylan, “Capacity of distributed PHY-layer sensor networks,” *IEEE Transactions on Vehicular Technology*, vol. 55, no. 2, pp. 622–639, 2006.
- [23] M. Dohler, A. Gkelias, and H. Aghvami, “A resource allocation strategy for distributed MIMO multi-hop communication systems,” *IEEE Communications Letters*, vol. 8, no. 2, pp. 99–101, 2004.
- [24] M. Dohler, E. Lefranc, and H. Aghvami, “Space-time block codes for virtual antenna arrays,” in *The 13th IEEE International Symposium on Personal, Indoor and Mobile Radio Communications*, vol. 1, 2002.
- [25] M. Dohler, Y. Li, B. Vucetic, A. Aghvami, M. Arndt, and D. Barthel, “Performance Analysis of Distributed Space-Time Block-Encoded Sensor Networks,” *IEEE Transactions on Vehicular Technology*, vol. 55, no. 6, pp. 1776–1789, 2006.
- [26] J. Elson, L. Girod, and D. Estrin, “Fine-grained network time synchronization using reference broadcasts,” *ACM SIGOPS Operating Systems Review*, vol. 36, pp. 147–163, 2002.
- [27] G. Foschini, “Layered space-time architecture for wireless communication in a fading environment when using multiple antennas,” *Bell Labs Technical Journal*, vol. 1, no. 2, pp. 41–59, 1996.
- [28] G. Foschini, D. Chizhik, M. Gans, C. Papadias, and R. Valenzuela, “Analysis and performance of some basic space-time architectures,” *IEEE Journal on Selected Areas in Communications*, vol. 21, no. 3, pp. 303–320, 2003.
- [29] G. Foschini and M. Gans, “On Limits of Wireless Communications in a Fading Environment when Using Multiple Antennas,” *Wireless Personal Communications*, vol. 6, no. 3, pp. 311–335, 1998.
- [30] S. Ganeriwal, R. Kumar, and M. Srivastava, “Timing-sync protocol for sensor networks,” in *International conference on Embedded networked sensor systems*. ACM New York, USA, 2003, pp. 138–149.
- [31] G. Ganesan and P. Stoica, “Space-time block codes: a maximum SNR approach,” *IEEE Transactions on Information Theory*, vol. 47, no. 4, pp. 1650–1656, 2001.
- [32] —, “Space-Time Diversity Using Orthogonal and Amicable Orthogonal Designs,” *Wireless Personal Communications*, vol. 18, no. 2, pp. 165–178, 2001.
- [33] D. Goeckel and Y. Hao, “Space-time coding for distributed antenna arrays,” *IEEE International Conference on Communications, ICC 2004*, vol. 2, pp. 747–751, 2004.

- [34] A. Goldsmith and S. Wicker, "Design challenges for energy-constrained ad hoc wireless networks," *IEEE wireless communications*, vol. 9, no. 4, pp. 8–27, 2002.
- [35] Y. Gong and B. Letaief, "Concatenated space-time block coding with trellis coded modulation in fading channels," *IEEE Transactions on Wireless Communications*, vol. 1, no. 4, pp. 580–590, 2002.
- [36] J. Guey, M. Fitz, M. Bell, and W. Kuo, "Signal design for transmitter diversity wireless communication systems over Rayleigh fading channels," *IEEE Transactions on Communications*, vol. 47, no. 4, pp. 527–537, 1999.
- [37] L. X. H. Dai and Q. Zhou, "Energy efficiency of mimo transmission strategies in wireless sensor networks," in *International Conference on Computing, Communications and Control Technologies (CCCT)*, Austin, TX, USA, August 2004.
- [38] I. Hammerstroem, M. Kuhn, B. Rankov, and A. Wittneben, "Space-time processing for cooperative relay networks," in *IEEE 58th Vehicular Technology Conference, VTC 2003-Fall*, vol. 1, 2003.
- [39] M. Handelsman and G. Base, "Performance Equations for a" Stationary" Passive Satellite Relay (22,000-Mile Altitude) for Communication," *IRE Transactions on Communications Systems*, vol. 7, pp. 31–37, 1959.
- [40] K. He and G. Cauwenberghs, "An area-efficient analog VLSI architecture for state-parallel Viterbi decoding," in *IEEE International Symposium on Circuits and Systems, ISCAS'99*, vol. 2, 1999.
- [41] B. H.H., "The New York-Philadelphia ultra-high-frequency facsimile relay system," *RCA Review*, vol. 1, pp. 15–31, 1936.
- [42] R. Horn and C. Johnson, *Matrix Analysis*. Cambridge University Press, 1985.
- [43] T. Hunter and A. Nosratinia, "Diversity through coded cooperation," *IEEE Transactions on Wireless Communications*, vol. 5, no. 2, pp. 283–289, 2006.
- [44] H. Jafarkhani, "A quasi-orthogonal space-time block code," *IEEE Transactions on Communications*, vol. 49, no. 1, pp. 1–4, 2001.
- [45] H. Jafarkhani and N. Hassanpour, "Super-quasi-orthogonal space-time trellis codes for four transmit antennas," *Wireless Communications, IEEE Transactions on*, vol. 4, no. 1, pp. 215–227, 2005.
- [46] H. Jafarkhani and N. Seshadri, "Super-orthogonal space-time trellis codes," *IEEE Transactions on Information Theory*, vol. 49, no. 4, pp. 937–950, 2003.



- 
- [47] S. Jagannathan, H. Aghajan, and A. Goldsmith, "The effect of time synchronization errors on the performance of cooperative MISO systems," in *IEEE Global Telecommunications Conference Workshops, GlobeCom Workshops 2004*, 2004, pp. 102 – 107.
  - [48] S. K. Jayaweera, "Energy analysis of mimo techniques in wireless sensor networks," in *38th Annual Conference on Information Sciences and Systems*, Princeton University, USA, March 2004.
  - [49] S. Jayaweera, "An energy-efficient virtual MIMO architecture based on V-BLAST processing for distributed wireless sensor networks," in *IEEE Conference on Sensor and Ad Hoc Communications and Networks*, 2004, pp. 299–308.
  - [50] —, "Virtual MIMO-based cooperative communication for energy-constrained wireless sensor networks," *IEEE Transactions on Wireless Communications*, vol. 5, no. 5, pp. 984–989, 2006.
  - [51] Y. Jing and B. Hassibi, "Distributed space-time codes in wireless relay networks," in *Sensor Array and Multichannel Signal Processing Workshop Proceedings, 2004*, 2004, pp. 249–253.
  - [52] J. Jootar, J. Diouris, and J. Zeidler, "Performance of polarization diversity in correlated Nakagami-m fading channels," *IEEE Transactions on Vehicular Technology*, vol. 55, no. 1, pp. 128–136, 2006.
  - [53] I. Kang, A. Willson Jr, Q. Inc, and C. San Diego, "Low-power Viterbi decoder for CDMA mobile terminals," *IEEE Journal of Solid-State Circuits*, vol. 33, no. 3, pp. 473–482, 1998.
  - [54] Kateyeva, "Performance Equations for a" Stationary" Passive Satellite Relay (22,000-Mile Altitude) for Communication," *Radio Technika (in Russian)*, vol. 14, p. 67, 1959.
  - [55] Y. Kim and H. Liu, "Infrastructure Relay Transmission With Cooperative MIMO," *IEEE Transactions on Vehicular Technology*, vol. 57, no. 4, pp. 2180–2188, 2008.
  - [56] S. Kubota, S. Kato, and T. Ishitani, "Novel Viterbi decoder VLSI implementation and its performance," *IEEE Transactions on Communications*, vol. 41, no. 8, pp. 1170–1178, 1993.
  - [57] J. Laneman, D. Tse, and G. Wornell, "Cooperative diversity in wireless networks: Efficient protocols and outage behavior," *IEEE Transactions on Information Theory*, vol. 50, no. 12, pp. 3062–3080, 2004.

- [58] J. Laneman and G. Wornell, “Energy-efficient antenna sharing and relaying for wireless networks,” in *IEEE Wireless Communications and Networking Conference, WCNC*, vol. 1, 2000.
- [59] —, “Distributed space-time-coded protocols for exploiting cooperative diversity in wireless networks,” *IEEE Transactions on Information Theory*, vol. 49, no. 10, pp. 2415–2425, 2003.
- [60] Q. Li and D. Rus, “Global clock synchronization in sensor networks,” *IEEE Transactions on Computers*, vol. 55, no. 2, pp. 214–226, 2006.
- [61] X. Li, “Energy efficient wireless sensor networks with transmission diversity,” *Electronics Letters*, vol. 39, p. 1753, 2003.
- [62] —, “Space-time coded multi-transmission among distributed transmitters without perfect synchronization,” *Signal Processing Letters, IEEE*, vol. 11, no. 12, pp. 948–951, 2004.
- [63] X. Li, M. Chen, and W. Liu, “Application of STBC-encoded cooperative transmissions in wireless sensor networks,” *IEEE Signal Processing Letters*, vol. 12, no. 2, pp. 134–137, 2005.
- [64] T. Liew, J. Pliquett, B. Yeap, L. Yang, and L. Hanzo, “Concatenated space-time block codes and TCM, turbo TCM, convolutional as well as turbo codes,” in *IEEE Global Telecommunications Conference, GLOBECOM’00*, vol. 3, 2000.
- [65] R. Lin and A. Petropulu, “A new wireless network medium access protocol based on cooperation,” *IEEE Transactions on Signal Processing*, vol. 53, no. 12, pp. 4675–4684, 2005.
- [66] E. Lindskog, D. Flore, A. Inc, and C. San Jose, “Time-reversal space-time block coding and transmit delay diversity-separate and combined,” *Conference Record of the Thirty-Fourth Asilomar Conference on Signals, Systems and Computers, 2000*, vol. 1, 2000.
- [67] N. Marechal, J. Pierrot, and J. Gorce, “Fine Synchronization for Wireless Sensor Networks Using Gossip Averaging Algorithms,” in *IEEE International Conference on Communications, ICC’08*, 2008, pp. 4963–4967.
- [68] I. Maric and R. Yates, “Forwarding strategies for Gaussian parallel-relay networks,” in *IEEE International Symposium on Information Theory, ISIT*, 2004.
- [69] M. Maróti, B. Kusy, G. Simon, and Á. Lédeczi, “The flooding time synchronization protocol,” *Proceedings of the 2nd international conference on Embedded networked sensor systems*, pp. 39–49, 2004.

- [70] Y. Mei, Y. Hua, A. Swami, and B. Daneshrad, “Combating synchronization errors in cooperative relays,” *Proceedings of IEEE International Conference on Acoustics, Speech, and Signal Processing, ICASSP’05*, vol. 3, 2005.
- [71] R. Min and A. Chandrakasan, “A framework for energy-scalable communication in high-density wireless networks,” in *Proceedings of the 2002 international symposium on Low power electronics and design*. ACM New York, NY, USA, 2002, pp. 36–41.
- [72] F. Ng, J. Hwu, M. Chen, and X. Li, “Asynchronous space-time cooperative communications in sensor and robotic networks,” in *IEEE International Conference Mechatronics and Automation*, vol. 3, 2005.
- [73] T. Nguyen, O. Berder, and O. Sentieys, “Cooperative MIMO schemes optimal selection for wireless sensor networks,” *IEEE 65th Vehicular Technology Conference, VTC-Spring 07*, pp. 85–89, 2007.
- [74] —, “Impact of Transmission Synchronization Error and Cooperative Reception Techniques on the Performance of Cooperative MIMO Systems,” *IEEE International Conference on Communications, ICC Beijing*, pp. 4601–4605, 2008.
- [75] A. Nosratinia, T. Hunter, and A. Hedayat, “Cooperative communication in wireless networks,” *IEEE Communications Magazine*, vol. 42, no. 10, pp. 1266 – 1273, 2004.
- [76] S. PalChaudhuri, A. Saha, and D. Johnson, “Adaptive clock synchronization in sensor networks,” in *Proceedings of the 3rd international symposium on Information processing in sensor networks*. ACM New York, NY, USA, 2004, pp. 340–348.
- [77] C. Papadias and G. Foschini, “Capacity-approaching space-time codes for systems employing four transmitter antennas,” *IEEE Transactions on Information Theory*, vol. 49, no. 3, pp. 726–732, 2003.
- [78] J. Proakis, *Digital communications*. McGraw-Hill, Fourth Edition, 2000.
- [79] G. Raleigh and J. Cioffi, “Spatio-temporal coding for wireless communication,” *IEEE Transactions on Communications*, vol. 46, no. 3, pp. 357–366, 1998.
- [80] T. Rappaport, *Wireless Communications: Principles and Practice*. IEEE Press Piscataway, NJ, USA, 1996.
- [81] S. Sandhu, R. Heath, and A. Paulraj, “Space-time block codes versus space-time trellis codes,” in *IEEE International Conference on Communications, ICC 2001*, vol. 4, 2001.
- [82] B. Schein and R. Gallager, “The Gaussian parallel relay network,” in *IEEE International Symposium on Information Theory, ISIT*, 2000.

- [83] G. Scutari and S. Barbarossa, "Distributed space-time coding for regenerative relay networks," *IEEE Transactions on Wireless Communications*, vol. 4, no. 5, pp. 2387–2399, 2005.
- [84] K. Seddik, A. Sadek, and K. Liu, "Protocol-aware design criteria and performance analysis for distributed space-time coding," in *IEEE Global Telecommunications Conference*, 2006, pp. 1–5.
- [85] A. Sendonaris, E. Erkip, and B. Aazhang, "User cooperation diversity. Part I. System description," *IEEE Transactions on Communications*, vol. 51, no. 11, pp. 1927–1938, 2003.
- [86] A. Sendonaris, E. Erkip, B. Aazhang, Q. Inc, and C. Campbell, "User cooperation diversity. Part II. Implementation aspects and performance analysis," *IEEE Transactions on Communications*, vol. 51, no. 11, pp. 1939–1948, 2003.
- [87] H. Shah, A. Hedayat, and A. Nosratinia, "Performance of concatenated channel codes and orthogonal space-time block codes," *IEEE Transactions on Wireless Communications*, vol. 5, no. 6, p. 1406, 2006.
- [88] C. Shannon, "A mathematical theory of communication," *ACM SIGMOBILE Mobile Computing and Communications Review*, vol. 5, no. 1, pp. 3–55, 2001.
- [89] N. Sharma and C. Papadias, "Improved quasi-orthogonal codes through constellation rotation," *IEEE Transactions on Communications*, vol. 51, no. 3, pp. 332–335, 2003.
- [90] M. Sichitiu and C. Veerarittiphan, "Simple, accurate time synchronization for wireless sensor networks," *IEEE Wireless Communications and Networking(WCNC)*, vol. 2, pp. 74 – 80, 2003.
- [91] P. Stoica and E. Lindskog, "Space-time block coding for channels with inter-symbol interference," *Digital Signal Processing*, vol. 12, no. 4, pp. 616–627, 2002.
- [92] W. Su and X. Xia, "Signal constellations for quasi-orthogonal space-time block codes with full diversity," *IEEE Transactions on Information Theory*, vol. 50, no. 10, pp. 2331–2347, 2004.
- [93] B. Sundararaman, U. Buy, and A. Kshemkalyani, "Clock synchronization for wireless sensor networks: a survey," *Ad Hoc Networks Journal*, vol. 3, no. 3, pp. 281–323, 2005.
- [94] V. Tarokh, H. Jafarkhani, and A. R. Calderbank, "Space-time block codes from orthogonal designs," *IEEE Transactions on Information Theory*, vol. 45, no. 5, pp. 1456–1467, July 1999.

- [95] V. Tarokh, H. Jafarkhani, and A. Calderbank, "Space-time block coding for wireless communications: performance results," *IEEE Journal on Selected Areas in Communications*, vol. 17, no. 3, pp. 451–460, 1999.
- [96] V. Tarokh, A. Naguib, N. Seshadri, and A. Calderbank, "Space-time codes for high data rate wireless communication: performance criteria in the presence of channel estimation errors, mobility, and multiple paths," *IEEE Transactions on Communications*, vol. 47, no. 2, pp. 199 – 207, 1999.
- [97] V. Tarokh, N. Seshadri, and A. Calderbank, "Space-time codes for high data rate wireless communication: performance criterion and code construction," *IEEE Transactions on Information Theory*, vol. 44, no. 2, pp. 744–765, 1998.
- [98] E. Telatar, "Capacity of multi-antenna Gaussian channels," *European transactions on telecommunications*, vol. 10, no. 6, pp. 585–595, 1999.
- [99] E. Viterbo and J. Boutros, "A universal lattice code decoder for fading channels," *IEEE Transactions on Information Theory*, vol. 45, no. 5, pp. 1639–1642, 1999.
- [100] H. W., "Communication by Polar-orbit Satellite Relay," *IRE Transactions on Communications Systems*, vol. 8, pp. 250–254, 1960.
- [101] S. Wei, D. Goeckel, and M. Valenti, "Asynchronous cooperative diversity," *IEEE Transactions on Wireless Communications*, vol. 5, no. 6, pp. 1547–1557, 2006.
- [102] M. Win and J. Winters, "Analysis of Hybrid Selection/Maximal-Ratio Combining in Rayleigh Fading," *IEEE Transactions on Communications*, vol. 47, no. 12, p. 1773, 1999.
- [103] J. Winters, J. Salz, and R. Gitlin, "The impact of antenna diversity on the capacity of wireless communication systems," *IEEE Transactions on Communications*, vol. 42, no. 2-4, pp. 1740–1751, 1994.
- [104] P. Wolniansky, G. Foschini, G. Golden, and R. Valenzuela, "V-BLAST: an architecture for realizing very high data rates over the rich-scattering wireless channel," in *International Symposium on Signals, Systems, and Electronics, ISSSE 1998*, pp. 295–300.
- [105] S. Yang and J. Belfiore, "Optimal space-time codes for the MIMO amplify-and-forward cooperative channel," *IEEE Transactions on Information Theory*, vol. 53, no. 2, pp. 647–663, 2007.
- [106] Y. Yuan, Z. He, and M. Chen, "Virtual MIMO-based cross-layer design for wireless sensor networks," *IEEE Transactions on Vehicular Technology*, vol. 55, no. 3, pp. 856–864, 2006.

- [107] R. Zhang and J. Gorce, “Optimal transmission range for minimum energy consumption in wireless sensor networks,” *IEEE Wireless Communications and Networking Conference, WCNC*, 2008.